

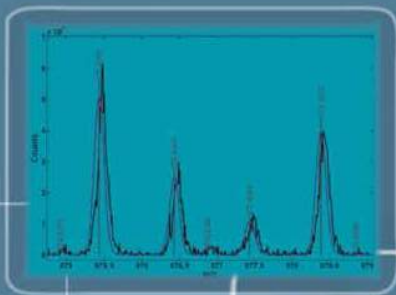


绿绵科技  
Lumiere Tech Ltd.

精准质量数测定

及分子式识别系统应用文集

( 第六期 )



# 前言

近年来，质谱技术日新月异，每年质谱厂家纷纷推出各种质谱创新技术，以满足不同领域的需求，主要集中在几个方面：更高灵敏度，更高分辨能力，更快分析速度，更高质量精度，对复杂基质有更好的分析能力和耐受力等。

质谱技术的出现，主要是为了对化合物分子量的测定，结构解析推测，以达到化合物定性的目的，随着法规和行业的要求，对一些低含量的，复杂基质的化合物定量分析，质谱技术已经成为首选工具，如三重四极杆串联质谱，是目前食品安全，药物代谢等领域必备的分析仪器。

质谱的种类分为：低分辨和高分辨。低分辨质谱，如大家熟知的单级四极杆质谱，三重四极杆串联质谱，被各个行业广泛使用，由于仪器本身只是单位质谱分辨，不能得到化合物的精确质量数，对未知物的定性分析，只能依靠谱库或标样来确定，定性能力受到限制，对于进一步的定性分析需求，则寄希望于高分辨质谱，如飞行时间质谱TOF，静电轨道阱质谱，甚至傅里叶回旋共振质谱。其特点是可以得到精确质量数，精度可以达到几个ppm，乃至1个ppm以内，目的就是要得到更为精确的质量数，以期候选的化合物尽可能的少，但仅仅依赖精确质量数，而不进行同位素峰形校正，并不能给出唯一的候选化合物分子式，与目标化合物质量数偏差最小的，并不一定是目标化合物。

美国Cerno Biosciences公司推出的2006年美国匹兹堡科学仪器博览会获奖产品——MassWorks在低分辨质谱和高分辨质谱之间架起了桥梁，利用其精确质量数测定和同位素峰形校正专利技术，让低分辨的质谱真正实现高分辨的功能，在低分辨的质谱上进行精确质量数测定，并且对候选化合物进行同位素峰形检索，确定最为可能的唯一化合物分子式，极大地拓展了低分辨质谱的功能；同时针对高分辨质谱，应用其同位素峰形自校正专利技术，有助于确定化合物唯一分子式。

MassWorks自推出以来，不断更新发展，加入新的功能。最近推出的V5.0版软件版本，集成了准确的质量校准和使用已知如NIST数据库进行未知物鉴定，因此所有的未知物鉴定任务能够通过一个MassWorks软件来完成。它还扩展了离子混合物分析的功能，包括5种不同类型的化学修饰，因此可以对一个复杂的离子混合物进行相对定量，而不需要分离多达5种不同类型的同位素标记物。例如，含有碳/氢/氮/氧/硫和所有可能的<sup>13</sup>C、<sup>2</sup>H、<sup>15</sup>N、<sup>18</sup>O、<sup>34</sup>S同位素标记物的混合物。我们相信随着新版本的推出，MassWokrs会给广大质谱用户带来更多的惊喜和新体验。

本应用文集收录了六篇MassWorks应用文章，希望能为广大质谱工作者提供一些有用的信息。更多资料可以从MassWorks技术专题下载：[http:// www.antpedia.com/special/ massworks.html](http://www.antpedia.com/special/massworks.html)。不足之处，请大家多提意见。

北京绿绵科技有限公司 市场部  
二零一八年四月

## 目 录

- Identification of low molecular weight organic acids by ion chromatography/hybrid quadrupole time-of-flight mass spectrometry during Uniblu-A ozonation  
.....Apollonia Amorisco, Vito Locaputo, Carlo Pastore and Giuseppe Mascolo (1)
- Spectral accuracy of a new hybrid quadrupole time-of-flight mass spectrometer: application to ranking small molecule elemental compositions  
..... Wei Jiang and John C. L. Erve (17)
- Characterization of sulfur compounds in whisky by full evaporation dynamic headspace and selectable one-dimensional/two-dimensional retention time locked gas chromatography–mass spectrometry with simultaneous element-specific detection  
..... Nobuo Ochiaia, Kikuo Sasamotoa, Kevin MacNamarab (26)
- Application of Spectral Accuracy to Improve the Identification of Organic Compounds in Environmental Analysis  
..... Emmanuel Eysseric, (35)  
Killian Barry, Francis Beaudry, Magali Houde, Christian Gagnon, and Pedro A. Segura
- 利用LC-MS 和二维色谱相关光谱技术识别HPLC 色谱图中杂质峰  
.....陈珍珍, 张斗胜, 王 楠, 冯 芳, 胡昌勤 (44)
- 天然同位素信息再多级质谱裂解规律解析中的应用——以磺胺类化合物为例  
.....张海燕, 刘鑫, 严华, 李建辉, 韩深, 张朝晖, 王金花, 许泓, 叶晓霞 (50)

Rapid Commun. Mass Spectrom. 2013, 27, 187–199  
(wileyonlinelibrary.com) DOI: 10.1002/rcm.6429

# Identification of low molecular weight organic acids by ion chromatography/hybrid quadrupole time-of-flight mass spectrometry during Uniblu-A ozonation

Apollonia Amorisco, Vito Locaputo, Carlo Pastore and Giuseppe Mascolo\*

Istituto di Ricerca Sulle Acque, Consiglio Nazionale delle Ricerche, Viale F. De Blasio 5, 70132 Bari, Italy

**RATIONALE:** The balance of organic nitrogen and sulfur during ozonation of organic pollutants often shows a lack of complete mineralization. It follows that polar and ionic by-products are likely to be present that are difficult to identify by liquid chromatography/mass spectrometry (LC/MS).

**METHODS:** The structural elucidation of low molecular weight organic acids arising from Uniblu-OH ozonation has been investigated by ion chromatography/electrospray tandem mass spectrometry (IC/ESI-MS/MS) employing a quadrupole time-of-flight mass spectrometer. Unequivocal elemental composition of the by-products was determined by a combination of mass accuracy and high spectral accuracy.

**RESULTS:** The employed identification strategy was demonstrated to be a powerful method of unequivocally assigning a single chemical composition to each identified compound. The exact mass measurements of  $[M-H]^-$  ions allowed the elemental formulae and related structures of eighteen by-products to be determined confidently. The main degradation pathways were found to be decarboxylation and oxidation. The experimental procedure allowed the identification of both nitrogen- and sulfur-containing organic acid by-products arising from Uniblu-OH ozonation.

**CONCLUSIONS:** The obtained results are of environmental relevance for the balance of organic nitrogen and sulfur during the ozonation of organic pollutants due to the lack of complete mineralization of the compounds containing these atoms. Copyright © 2012 John Wiley & Sons, Ltd.

It is known that the removal of organic pollutants during wastewater and drinking water treatment can be successfully achieved by powerful chemical methods, such as ozone treatment alone or ozone combined with UV or hydrogen peroxide.<sup>[1]</sup> The latter methods are known as advanced oxidation processes (AOPs) and are based on the generation of hydroxyl radicals ( $\cdot OH$ ), which, in turn, are able to oxidize contaminants in a non-selective manner.<sup>[2–7]</sup> AOPs are not employed at high dosages due to the high operational costs. This leads, in addition to the complete removal of parent organic pollutants, to the formation of several degradation products, which may be more toxic than the parent compounds.<sup>[8,9]</sup> It follows that the identification of the chemical structures of degradation products is a key issue for the environmental understanding of the investigated treatment process. As AOPs are oxidative processes, the resulting degradation by-products are more polar than the parent compounds, and liquid chromatography/electrospray ionization mass spectrometry (LC/ESI-MS), often employing accurate mass measurement, is a suitable technique for their analysis.<sup>[10,11]</sup> The degradation products formed in the early stage of AOPs are transient compounds

and they are further degraded, leading to the formation of low molecular weight carbonyl compounds which, in turn, are finally degraded to low molecular weight organic acids. Previous investigation showed that during the ozonation of dyestuffs, low molecular weight carbonyl compounds and organic acids identified only on the basis of authentic standards failed to account for the total organic carbon present in the ozonated aqueous solution.<sup>[12]</sup> It follows that other low molecular weight compounds are present that are not detectable in reversed-phase LC. Ion chromatography (IC) can, however, also be conveniently interfaced to ESI-MS and combined with accurate mass measurement, both in single and tandem MS, for the identification of unknown low molecular weight organic acids.

Such an approach was used herein to identify the final degradation product during the ozonation of hydrolyzed Uniblu-A (Uniblu-OH) at long contact times. Uniblu-A is a representative reactive dyestuff based on the anthraquinone structure used in cellulose fiber dyeing. Due to their fused aromatic structure these compounds are more resistant to biodegradation than azo-based ones.<sup>[13]</sup> The recovery of residual dye from spent baths is not possible because the fixation reaction onto fibers leads to the formation of the hydrolyzed dyestuff. As the fixation rate is usually below 90% the resulting spent waters are of no further use and they should be disposed of properly. Therefore, the efficient removal of residual hydrolyzed dye from wastewater is of environmental relevance.

\* Correspondence to: G. Mascolo, Istituto di Ricerca Sulle Acque, Consiglio Nazionale delle Ricerche, Viale F. De Blasio 5, 70132 Bari, Italy.  
E-mail: giuseppe.mascolo@ba.irsra.cnr.it

It was previously shown that ozonation of Uniblu-OH led to the formation of intermediate by-products more polar than the parent compound.<sup>[12]</sup> Their further degradation led to the formation of low molecular carbonyl compounds, aldehydes and ketones,<sup>[14]</sup> which, in turn, as a result of extensive oxidation of the Uniblu-OH, disappeared leading probably to hydroxylated organic acids.

Several methods, e.g. gas chromatography (GC),<sup>[15,16]</sup> capillary electrophoresis (CE),<sup>[17,18]</sup> LC,<sup>[19,20]</sup> and various kinds of ion chromatography, such as ion-exchange chromatography and ion-exclusion chromatography,<sup>[21,22]</sup> are suitable for the analysis of polyhydroxy organic acids. In particular, ion chromatography with conductivity detection (IC-CD) has been employed in many applications.<sup>[23–25]</sup>

The identification of final ozonation by-products should be possible by coupling an IC system, equipped with a membrane ion suppressor, and ESI-MS using accurate mass measurement, both in single and tandem MS, using quadrupole time-of-flight mass spectrometry (QqTOF-MS), although it is not always possible to differentiate isomers. In IC/ESI-MS a membrane ion suppressor is successfully used to minimize background spectral interferences and to enhance the  $[M-H]^-$  ion signal. Therefore, it is possible to combine the advantages of the unique selectivity offered by IC with the specificity and structural elucidation capability of MS.<sup>[26–29]</sup> IC/MS has previously been successfully used for the detection of inorganic and organic species at low detection limits.<sup>[30,31]</sup> However, only a few studies have focused on its use for the analysis of low molecular mass mono- and dicarboxylic acids.<sup>[32–34]</sup> Specifically, in IC/ESI-MS the use of a membrane ion suppressor has been proved to effectively remove sodium ions from the mobile phase that cause the formation in the MS interface of uncharged species (i.e. organic/inorganic anion with a sodium counter-ion). These neutral species reduce transfer efficiency from the atmospheric part of the interface to the vacuum region causing, in turn, a decrease in the MS detection sensitivity. Therefore, the ion suppressor makes it possible to combine the advantages of the unique selectivity offered by IC with the specificity and structural elucidation capability of MS.<sup>[31,35,36]</sup>

The objective of this investigation was the identification of low molecular weight aliphatic carboxylic acids, formed as end products during the ozonation of hydrolysed Uniblu-A (Uniblu-OH). The assignment of chemical structures was made possible by combining high-resolution mass spectrometry data, obtained in single and in tandem MS mode, with the information contained in high-resolution mass spectra about the isotopic distribution of ions, defined as spectral accuracy.<sup>[37,38]</sup> Several reports have focused on how isotope

pattern can be used as a tool to help identify unknowns on various mass spectrometer types. In this case the concept of spectral accuracy was employed to further enhance the formula determination using a high-resolution time-of-flight instrument.

## EXPERIMENTAL

### Chemicals

Uniblu-A (95% purity; Sigma-Aldrich, Milan, Italy) was used without further purification. Uniblu-OH was obtained by hydrolyzing an aqueous solution of Uniblu-A (500 mg/L) at pH 12 and 50 °C for 1 h (hydrolysis yield >90%),<sup>[14]</sup> as shown in Scheme 1.

Water used for ion chromatography as well as for preparing all standard aqueous solutions (18.2 MΩcm, organic carbon content ≤4 μg/L) was obtained from a Milli-Q Gradient A-10 system (Millipore, Billerica, MA, USA). NaOH used for IC was from J.T. Baker (Deventer, The Netherlands). All other reagents were analytical grade and purchased from VWR (Milan, Italy) or Carlo Erba (Milan, Italy).

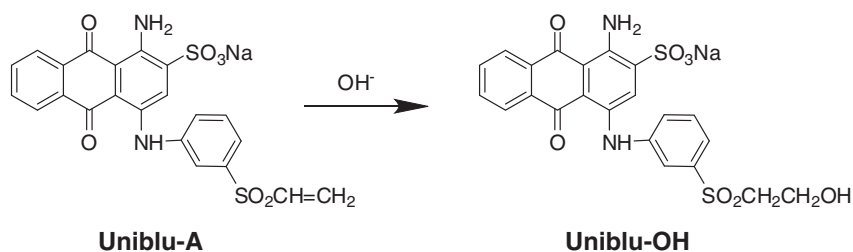
### Ozonation experiments

Uniblu-OH aqueous solution (500 mL), after adjusting the pH to 7 by the addition of HCl, was placed into a Normag reactor (Hofheim am Taunus, Germany). Ozone was produced by a 502 ozonator (Fisher, Meckenheim, Germany) fed with oxygen. The oxygen/ozone mixture (flow rate of 1 L/min, 16 mg/L) was split to allow only 0.1 L/min to be bubbled into the Normag reactor. The ozone output was monitored before each experiment by determining (by titration with sodium thiosulfate) the amount of free iodine liberated from a potassium iodide solution. Samples (10 mL) were withdrawn from the reaction mixtures at scheduled times and the residual ozone was stripped from them by purging with air.

### IC/ESI-QqTOFMS and IC/ESI-QqTOFMS/MS analysis

#### Data acquisition

Determinations were carried out by a GS50 chromatography system (Dionex-Thermo Fisher Scientific, Sunnyvale, CA, USA) equipped with an AS50 autosampler, an ED50 conductivity detector and an ASRS-ultra suppressor, operated at 100 mA in external water mode. Samples, injected via a 25 μL loop, were eluted at a flow rate of 0.5 mL/min through an analytical IonPac AS-11 column (250 mm × 2 mm; Dionex)



**Scheme 1.** Uniblu-A hydrolysis employed to obtain Uniblu-OH.



equipped with a IonPac AG-11 guard-column (50 mm × 2 mm) with the following gradient: from 10/0/90 (NaOH 5 mM/NaOH 100 mM/water), held for 2.5 min, to 100/0/0 in 3.5 min, then to 50/50/0 in 12 min, held for 5 min. The flow from the conductivity detector of the IC system was split 1:1, by means of a zero dead volume T-piece, to allow one-half to enter the interface of the mass spectrometer. The optimization of the ESI-MS interface was performed by using only the IonPac AG-11 guard column in isocratic mode (0/20/80 of NaOH 0.5 mM/NaOH 100 mM/water) at a flow rate of 0.5 mL/min. These analytical conditions were carefully chosen in order to elute all the organic acids within 2 min and, consequently, to run several injections during a MS acquisition for optimizing each ESI interface parameter. Ten  $\mu\text{L}$  of a standard solution of organic acids (1 mg/L) was injected through a 7125-Ti Rheodyne valve.

A QSTAR QqTOFMS/MS system (AB Sciex, Framingham, MA, USA) equipped with a TurboIonSpray source operated in negative ion mode was used throughout this work. High-purity nitrogen gas was used as both the curtain and the collision gas, while high-purity air was used as the nebulizer and auxiliary heated gas. The TurboIonSpray interface conditions were: nebulizer voltage,  $-4200\text{ V}$ ; declustering potential,  $-40\text{ V}$ ; focusing potential,  $-120\text{ V}$ ; nebulizer gas flow rate, 1 L/min; curtain gas flow rate, 0.66 L/min; and auxiliary gas (air) delivered by a turbo heated probe, flow rate 5.5 L/min at  $450\text{ }^\circ\text{C}$ . Accurate mass measurements (four decimal places) were carried out at a mass resolution higher than 5000 (full width at half maximum) by obtaining averaged spectra from chromatographic peaks and then recalibrating them using the  $[\text{M}-\text{H}]^-$  ions of a five-acids mix injected post-column:  $\text{C}_2\text{H}_3\text{O}_2^-$  at  $m/z$  59.0139,  $\text{C}_2\text{HO}_3^-$  at  $m/z$  72.9931,  $\text{C}_2\text{H}_2\text{ClO}_2^-$  at  $m/z$  92.9749,  $\text{C}_8\text{H}_7\text{O}_3^-$  at  $m/z$  151.0395 and  $\text{C}_{10}\text{H}_{10}\text{O}_3\text{Cl}^-$  at  $m/z$  213.0324 with its characteristic fragment ion at  $m/z$  126.9956. The product ion mass measurements were carried out by fragmenting the target precursor  $[\text{M}-\text{H}]^-$  ions at an optimized collision voltage (CV) and at a collision gas pressure of 4 mTorr. Each averaged spectrum was recalibrated using, as a lock mass, the precursor ion mass obtained in single MS mode. The collision energy (CE) was optimized for each compound in order to obtain, where possible, spectra showing acceptable signal-to-noise (S/N) ratios in the MS/MS spectra, with both the  $[\text{M}-\text{H}]^-$  ion and the greatest number of product ions of high enough abundance for accurate mass determination.

#### Data analysis

All MS data handling was performed using Analyst QS software (AB Sciex). All mass spectral data acquired by QqTOFMS were exported as ASCII data and analyzed by sCLIPS (self Calibrated Line-shape Isotope Profile search) through Mass Works (version 2.0; Cerno Bioscience, Danbury, CT, USA). sCLIPS is a formula determination tool that performs a peak-shape-only calibration and matches calibrated experimental isotope pattern against possible theoretical ones using the spectral accuracy as discussed later. The mass tolerance for the sCLIPS searches was 10 ppm. The elemental number was restricted to include C, H, O, N, and S. The formula constraints were set by the software on the basis of chemical rules, i.e.  $\text{C}, \text{H}, \text{O} \geq 1, \text{S} \geq 0, \text{and } \text{N} \geq 0 \text{ or } 1$ , following the nitrogen rule. The number of double-bond

equivalents (DBEs) was set between  $-0.5$  and  $5.0$ . The profile mass range, which determines the relative mass spectral range used for the isotope profile comparison and the spectral accuracy calculation, was set between  $-0.5$  and  $2.5$ . The calibration range was centered to the approximate  $m/z$  value of the monoisotopic peak and was 1  $m/z$  unit wide. The spectral accuracy was calculated as  $(1 - \text{RMSE}) * 100$  where RMSE is the fit error between the calibrated and theoretical spectra.

## RESULTS AND DISCUSSION

A detailed screening of the degradation products formed during Uniblu-OH ozonation was carried out. The intermediate degradation products were identified employing conventional reversed-phase HPLC/MS.<sup>[12]</sup> At reaction times longer than 15 min such compounds disappeared completely. Several low molecular weight aldehydes and ketones were identified employing derivatization with 2,4-dinitrophenyl hydrazine (DNPH).<sup>[14]</sup> Once again, these compounds disappeared after time but the total organic carbon content of the aqueous solution did not reduce consistently. This suggested that a number of very polar degradation products had been formed as a result of extensive oxidation. Such compounds are likely to be low molecular weight organic acids. This is also consistent with the acidic pH (3.7) of the reaction mixture at longer ozonation times. Ozonated samples were also analyzed for organic acids on the basis of authentic standards (oxalic and formic acids).<sup>[12]</sup> Preliminary evidence on other minor peaks, not identified for lack of authentic standards, suggested the presence of several novel acids. In addition, on the basis of the low extent of both nitrogen and sulfur mineralization during ozonation, it was reasonable to assume the presence of very polar sulfur- and nitrogen-containing by-products, presumably ionic, and therefore not detectable by reverse phase HPLC.

IC interfaced to ESI-QqTOFMS was employed for the identification of such final by-products allowing 18 unknown by-products to be identified on the basis of accurate mass measurements of the  $[\text{M}-\text{H}]^-$  ions (Table 1). It should be noted that the mass-measured  $[\text{M}-\text{H}]^-$  ions reported in Table 1 often do have not a single unequivocally assigned elemental composition due to the employed QqTOFMS instrumentation (accurate mass error 5 ppm). The number of candidates could be reduced by limiting the possible elements as well as by applying other chemical constraints. In the present investigation it was only possible to set  $-0.5 \leq \text{DBE} \leq 5.0$  and to include C, H, N, O and S for elemental composition, consistent with Uniblu-OH ozonation at a long reaction time. In order for the elemental composition of each by-product to be unequivocally assigned, spectral accuracy was also employed. Spectral accuracy is the measure of similarity between the entire ion isotope pattern spectrum and the theoretical one. Several papers about the calculation of theoretical isotope distributions and on convolution of a peak shape function have been published.<sup>[39-41]</sup> The results obtained using spectral accuracy are also listed in Table 1. It should be noted that, despite the limited instrumental mass accuracy, the employment of spectral accuracy allowed a single elemental composition to be obtained for most of the by-products although the mass accuracy threshold was set to 10 ppm. These results are consistent with the theoretical considerations of

**Table 1.** Possible elemental composition for the unknown  $[M-H]^-$  ions calculated by mass accuracy and by spectral accuracy within error of 10 ppm, without atoms constraints ( $C \geq 1$ ,  $H \geq 1$ ,  $O \geq 1$ ,  $N \geq 0$ ,  $S \geq 0$ ) and with  $-0.5 \leq DBE \leq 5.0$ . The correct match is ranked as number 1 by Spectral accuracy. DBE: double-bond equivalent, RMSE: fit error between the calibrated and theoretical spectrum

By-product number	Measured mass, $[M-H]^- (m/z)$	Elemental composition	Calculated mass ( $m/z$ )	Error (ppm)	DBE	Elemental composition	Spectral accuracy	RMSE
1	138.9704	$C_2H_3O_5S^-$	138.9707	-1.9	1.5	$C_2H_3O_5S^-$	95.3373	14
2	140.9860	$C_2H_5O_5S^-$	140.9863	-2.2	0.5	$C_2H_5O_5S^-$	95.4909	8
3	196.9758	$C_4H_5O_7S^-$	196.9761	-1.8	2.5	$C_4H_5O_7S^-$	95.6101	2
4	212.9703	$C_5H_9O_2S_3^-$	196.9770	-6.2	1.5			
		$C_4H_5O_8S^-$	212.9711	-3.6	2.5	$C_4H_5O_8S^-$	96.2591	0
		$CH_5N_6OS_3^-$	212.9692	4.9	2.5	$CH_5N_6OS_3^-$	95.1599	1
5	212.9693	$C_5H_9O_3S_3^-$	212.9719	-7.6	1.5			
		$CH_5N_6OS_3^-$	212.9692	0.3	2.5	$C_4H_5O_8S^-$	98.0143	0
		$C_4H_5O_8S^-$	212.9711	-8.3	2.5		1	
6	224.9733	$C_6H_9O_3S_3^-$	224.9719	6.1	2.5	$C_5H_5O_8S^-$	98.2773	0
		$C_2HN_4O_9^-$	224.9749	-7.1	4.5	$C_2HN_4O_9^-$	95.0093	1
		$C_5H_5O_8S^-$	224.9711	9.9	3.5			
7	224.9732	$C_6H_9O_3S_3^-$	224.9719	5.6	2.5	$C_5H_5O_8S^-$	98.1916	0
		$C_2HN_4O_9^-$	224.9749	7.6	4.5			
		$C_5H_5O_8S^-$	224.9711	9.5	3.5			
8	177.9800	$C_4H_4NO_6S^-$	177.9816	-8.8	3.5	$C_4H_4NO_6S^-$	95.1120	0
9	193.9769	$C_4H_4NO_6S^-$	193.9765	2.1	3.5	$C_4H_4NO_6S^-$	99.0034	0
		$C_5H_8NOS_3^-$	193.9773	-2.3	2.5			
10	193.9749	$C_4H_4NO_6S^-$	193.9765	-8.1	3.5	$C_4H_4NO_6S^-$	99.0130	0
11	115.9978	$C_3H_2NO_4^-$	115.9989	-9.7	3.5	$C_3H_2NO_4^-$	95.4047	1
12	119.9939	$C_2H_2NO_5^-$	119.9938	0.4	2.5	$C_2H_2NO_5^-$	95.0147	1
13	116.9829	$C_3HO_5^-$	116.9829	-0.4	3.5	$C_3HO_5^-$	98.0959	3
14	133.0145	$C_4H_5O_5^-$	133.0142	1.9	2.5	$C_4H_5O_5^-$	98.6007	0
15	149.0100	$C_5H_9OS_2^-$	149.0100	-0.2	1.5	$C_4H_5O_6^-$	98.6302	1
		$C_4H_5O_6^-$	149.0092	5.6	2.5			
16	161.0102	$C_6H_9OS_2^-$	161.0100	1.0	2.5	$C_5H_5O_6^-$	97.9233	0
		$C_5H_5O_6^-$	161.0092	6.4	3.5			
17	179.0196	$C_5H_7O_7^-$	179.0197	-0.7	2.5	$C_5H_7O_7^-$	98.3357	0
		$C_6H_{11}O_2S_2^-$	179.0205	-5.5	1.5			
18	192.9994	$C_5H_5O_8^-$	192.9990	2.1	3.5	$C_5H_5O_8^-$	95.7336	0
		$C_6H_9O_3S_2^-$	192.9998	-2.4	2.5			

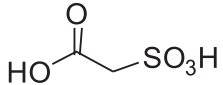
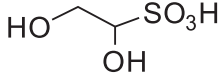
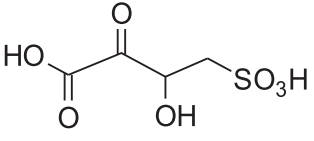
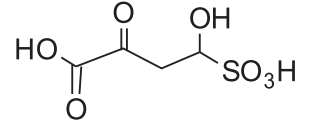
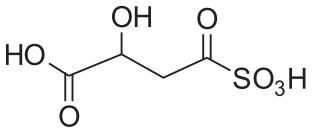
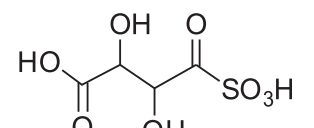
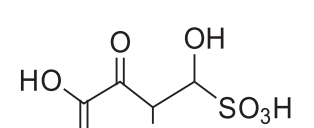
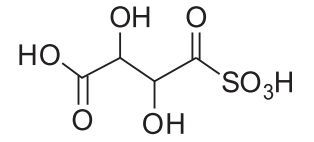
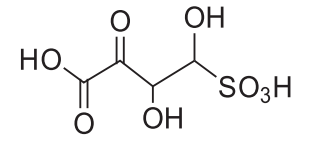
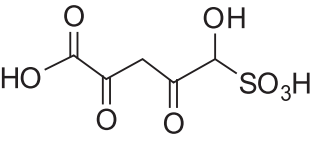
Kind and Fiehn who mentioned that the use of isotopic abundance information (i.e., spectral error) can eliminate 95% of the false candidates.<sup>[42]</sup>

The effectiveness of spectral accuracy is particularly evident for by-products 6 and 7 that being isomers both have the elemental composition for their  $[M-H]^-$  ions of  $C_5H_5O_8S^-$ . Specifically, despite their low mass accuracies (9.9 and 9.3 ppm), the observed isotope patterns achieved a spectral accuracy of better than 98%. The above reported elemental composition was associated to their  $[M-H]^-$  ions using the same s-CLIPS parameters. The comparison between measured and theoretical isotopic pattern profiles for by-product 6 is reported in Supplementary Fig. S1 (Supporting Information). It should also be noted that although a second possible elemental composition ( $C_2HN_4O_9^-$ ) for the  $[M-H]^-$  ion of by-product 6 resulted from the application of spectral accuracy, this was not chemically reasonable due to the low number of hydrogen atoms and high number of oxygen atoms. There was a similar situation for by-product 4 (Table 1) where the second elemental composition obtained employing spectral accuracy was not chemically consistent for an oxidized sulfur-containing compound, as each sulfur atom usually requires at least two oxygen atoms. An excellent result was obtained for by-product 9 at  $m/z$  193.9769 for

which spectral accuracy is able to distinguish between the  $[M-H]^-$  ions of two possible compounds with similar absolute mass accuracy error. A spectral accuracy value of 99.0% was assigned to the ion of elemental composition  $C_4H_4NO_6S^-$ . Once elemental compositions had been obtained the chemical structure of the by-products was assessed by obtaining accurate MS/MS spectra using, as a lock mass, the precursor ion mass obtained in single MS mode. The accurate mass measurements of both the  $[M-H]^-$  ions and their main product ions are listed in Table 2.

By-products 1 and 2 show  $[M-H]^-$  ions at  $m/z$  138.9704 and 140.9860, consistent with the elemental compositions  $C_2H_3O_5S^-$  and  $C_2H_5O_5S^-$  (errors -1.9 and -2.2 ppm, respectively). Their MS/MS spectra (Figs. 1(a) and 1(b)) show product ions at  $m/z$  79.9563 and 79.9582 for by-products 1 and 2, respectively, which were attributed to the radical anion  $SO_3^-$  (errors -13.3 and 10.5 ppm), suggesting that they are sulfur-containing degradation products. Fragmentation of the  $[M-H]^-$  ion of by-product 1 also displayed the presence of a carboxylic group in the parent compound due to the product ion at  $m/z$  94.9815 assigned to  $CH_3O_3S^-$  (error 6.9 ppm). These experimental results suggested that by-product 1 was a carboxymethanesulfonate, probably formed by further oxidation of the carbonyl group of the

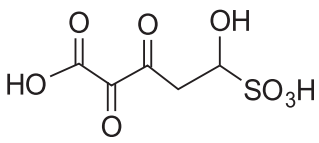
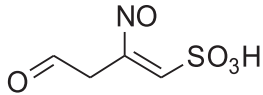
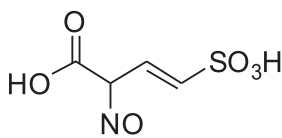
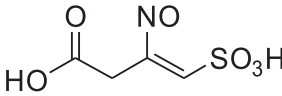
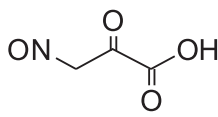
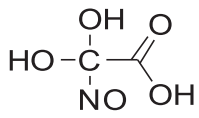
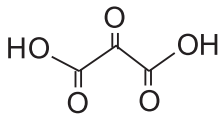
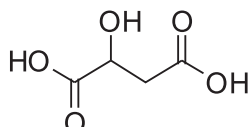
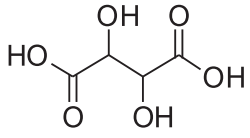
**Table 2.** Chemical structures of identified by-products, accurate mass measurements and elemental compositions of  $[M-H]^-$  ions as well as their product ions detected using IC/QqTOFMS and IC/QqTOFMS/MS analysis. CV: collision voltage

	By-product	Measured $[M-H]^-$ mass ( $m/z$ )	CV (V)	Major ions ( $m/z$ )	Elemental composition	Calculated mass ( $m/z$ )	Error (ppm)	
(1)		138.9704	20	138.9704 94.9815 79.9563	$C_2H_3O_5S^-$ $CH_3O_3S^-$ $SO_3^-$	138.9707 94.9808 79.9574	-1.9 6.9 -13.3	
(2)		140.9860	20	140.9860 122.9793 94.9816 79.9582	$C_2H_5O_5S^-$ $C_2H_3O_4S^-$ $CH_3O_3S^-$ $SO_3^-$	140.9863 122.9758 94.9808 79.9574	-2.2 28.8 8.0 10.5	
(3)	A 	196.9758	20	196.9758 178.9585 152.9847 134.9793 80.9661 71.0167	$C_4H_5O_7S^-$ $C_4H_3O_6S^-$ $C_3H_5O_5S^-$ $C_3H_3O_4S^-$ $HSO_3^-$ $C_3H_3O_2^-$	196.9761 178.9656 152.9863 134.9758 80.9652 71.0139	-1.8 -39.6 10.6 26.3 11.3 40.1	
	B 							
	C 							
								
								
(4)		212.9703	10	212.9703 168.9782 150.9669 96.9471	$C_4H_5O_8S^-$ $C_3H_5O_6S^-$ $C_3H_3O_5S^-$ $HSO_4^-$	212.9711 168.9812 150.9707 96.9601	-3.6 -17.9 -25.2 -134	
(5)		212.9693	10	212.9693 168.9832 120.9626	$C_4H_5O_8S^-$ $C_3H_5O_6S^-$ $C_2HO_4S^-$	212.9711 168.9812 120.9601	-8.3 11.6 20.6	
(6)		224.9733	10	224.9733 180.9802 142.9946 110.9784 96.9623	$C_5H_5O_8S^-$ $C_4H_5O_6S^-$ $C_3H_3O_5^-$ $CH_3O_4S^-$ $HSO_4^-$	224.9711 180.9812 142.9986 110.9758 96.9601	9.9 -5.7 -27.9 23.8 22.7	

(Continues)

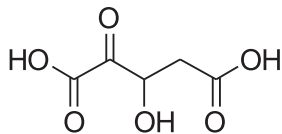
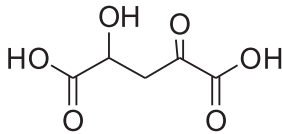
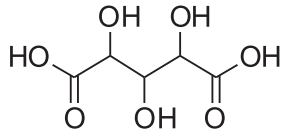
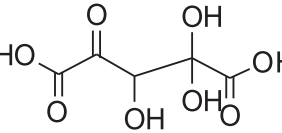


Table 2. (Continued)

By-product	Measured [M-H] <sup>-</sup> mass (m/z)	CV (V)	Major ions (m/z)	Elemental composition	Calculated mass (m/z)	Error (ppm)
	224.9732	10	224.9732	C <sub>5</sub> H <sub>5</sub> O <sub>8</sub> S <sup>-</sup>	224.9711	9.5
			152.9861	C <sub>3</sub> H <sub>5</sub> O <sub>5</sub> S <sup>-</sup>	152.9863	-1.4
			145.0146	C <sub>5</sub> H <sub>5</sub> O <sub>5</sub> <sup>-</sup>	145.0142	2.4
			134.9774	C <sub>3</sub> H <sub>3</sub> O <sub>4</sub> S <sup>-</sup>	134.9758	12.2
			110.9770	CH <sub>3</sub> O <sub>4</sub> S <sup>-</sup>	110.9758	11.2
			106.9830	C <sub>2</sub> H <sub>3</sub> O <sub>3</sub> S <sup>-</sup>	106.9808	20.2
	177.9800	20	96.9579	HSO <sub>4</sub> <sup>-</sup>	96.9601	-22.7
			177.9800	C <sub>4</sub> H <sub>4</sub> NO <sub>5</sub> S <sup>-</sup>	177.9816	-8.8
			159.9744	C <sub>4</sub> H <sub>2</sub> NO <sub>4</sub> S <sup>-</sup>	159.9710	21.2
			96.0104	C <sub>4</sub> H <sub>2</sub> NO <sub>2</sub> <sup>-</sup>	96.0091	13.5
			80.9668	HSO <sub>3</sub> <sup>-</sup>	80.9652	19.9
	193.9769	20	193.9769	C <sub>4</sub> H <sub>4</sub> NO <sub>6</sub> S <sup>-</sup>	193.9765	2.1
			149.9865	C <sub>3</sub> H <sub>4</sub> NO <sub>4</sub> S <sup>-</sup>	149.9867	-1.0
			113.0090	C <sub>4</sub> H <sub>3</sub> NO <sub>3</sub> <sup>-</sup>	113.0118	-25.1
			106.9815	C <sub>2</sub> H <sub>3</sub> O <sub>3</sub> S <sup>-</sup>	106.9808	6.2
			80.9637	HSO <sub>3</sub> <sup>-</sup>	80.9651	-18.4
	193.9749	20	193.9749	C <sub>4</sub> H <sub>4</sub> NO <sub>6</sub> S <sup>-</sup>	193.9765	-8.1
			175.9639	C <sub>4</sub> H <sub>2</sub> NO <sub>5</sub> S <sup>-</sup>	175.9659	-11.5
			119.9876	C <sub>3</sub> H <sub>4</sub> O <sub>3</sub> S <sup>-</sup>	119.9887	-8.9
			112.0060	C <sub>4</sub> H <sub>2</sub> NO <sub>3</sub> <sup>-</sup>	112.004	17.7
			80.9648	HSO <sub>3</sub> <sup>-</sup>	80.9652	-4.8
	115.9978	20	115.9975	C <sub>3</sub> H <sub>2</sub> NO <sub>4</sub> <sup>-</sup>	115.9989	-9.7
			72.0099	C <sub>2</sub> H <sub>2</sub> NO <sub>2</sub> <sup>-</sup>	72.0091	11.1
	119.9939	20	119.9939	C <sub>2</sub> H <sub>2</sub> NO <sub>5</sub> <sup>-</sup>	119.9938	0.4
			89.9968	C <sub>2</sub> H <sub>2</sub> O <sub>4</sub> <sup>-</sup>	89.9959	10.5
	116.9829	10	116.9829	C <sub>3</sub> HO <sub>5</sub> <sup>-</sup>	116.9829	-0.4
			72.9906	C <sub>2</sub> HO <sub>3</sub> <sup>-</sup>	72.9931	-34.5
	133.0145	20	133.0145	C <sub>4</sub> H <sub>5</sub> O <sub>5</sub> <sup>-</sup>	133.0142	-1.9
			115.0026	C <sub>4</sub> H <sub>3</sub> O <sub>4</sub> <sup>-</sup>	115.0037	-9.4
			89.0247	C <sub>3</sub> H <sub>5</sub> O <sub>3</sub> <sup>-</sup>	89.0244	3.2
			72.9931	C <sub>2</sub> HO <sub>3</sub> <sup>-</sup>	72.9931	-0.2
			71.0142	C <sub>3</sub> H <sub>3</sub> O <sub>2</sub> <sup>-</sup>	71.0139	4.9
			59.0144	C <sub>2</sub> H <sub>3</sub> O <sub>2</sub> <sup>-</sup>	59.0139	9.3
	149.0100	20	149.0100	C <sub>4</sub> H <sub>5</sub> O <sub>6</sub> <sup>-</sup>	149.0092	5.6
			130.9991	C <sub>4</sub> H <sub>3</sub> O <sub>5</sub> <sup>-</sup>	130.9986	3.8
			105.0185	C <sub>3</sub> H <sub>5</sub> O <sub>4</sub> <sup>-</sup>	105.0193	-7.9
			87.0078	C <sub>3</sub> H <sub>3</sub> O <sub>3</sub> <sup>-</sup>	87.0088	-11.1

(Continues)

Table 2. (Continued)

By-product	Measured [M-H] <sup>-</sup> mass ( <i>m/z</i> )	CV (V)	Major ions ( <i>m/z</i> )	Elemental composition	Calculated mass ( <i>m/z</i> )	Error (ppm)
(16) A 	161.0102	20	161.0102	C <sub>5</sub> H <sub>5</sub> O <sub>6</sub> <sup>-</sup>	161.0092	-6.4
			142.9980	C <sub>5</sub> H <sub>3</sub> O <sub>5</sub> <sup>-</sup>	142.9986	-4.2
			117.0191	C <sub>4</sub> H <sub>5</sub> O <sub>4</sub> <sup>-</sup>	117.0193	-2.0
			99.0093	C <sub>4</sub> H <sub>3</sub> O <sub>3</sub> <sup>-</sup>	99.0088	5.4
(17) B 	179.0196	20	179.0196	C <sub>5</sub> H <sub>7</sub> O <sub>7</sub> <sup>-</sup>	179.0197	-0.7
			161.0095	C <sub>5</sub> H <sub>5</sub> O <sub>6</sub> <sup>-</sup>	161.0092	2.1
(18) 	179.0196	20	133.0142	C <sub>4</sub> H <sub>5</sub> O <sub>5</sub> <sup>-</sup>	133.0142	-0.3
			103.0028	C <sub>3</sub> H <sub>3</sub> O <sub>4</sub> <sup>-</sup>	103.0037	-8.6
			99.0078	C <sub>4</sub> H <sub>3</sub> O <sub>3</sub> <sup>-</sup>	99.0088	-9.8
			89.0234	C <sub>3</sub> H <sub>5</sub> O <sub>3</sub> <sup>-</sup>	89.0244	-11.4
			71.0128	C <sub>3</sub> H <sub>3</sub> O <sub>2</sub> <sup>-</sup>	71.0139	-15.5
			59.0126	C <sub>2</sub> H <sub>3</sub> O <sub>2</sub> <sup>-</sup>	59.0139	-21.2
(18) 	192.9994	20	192.9994	C <sub>5</sub> H <sub>5</sub> O <sub>8</sub> <sup>-</sup>	192.9990	2.1
			149.0094	C <sub>4</sub> H <sub>5</sub> O <sub>6</sub> <sup>-</sup>	149.0092	1.6
			121.0140	C <sub>3</sub> H <sub>5</sub> O <sub>5</sub> <sup>-</sup>	121.0142	-2.0
			105.0190	C <sub>3</sub> H <sub>5</sub> O <sub>4</sub> <sup>-</sup>	105.0193	-3.2
			77.0236	C <sub>2</sub> H <sub>5</sub> O <sub>3</sub> <sup>-</sup>	77.0244	-10.6

previously detected 2-oxoethanesulfonic acid.<sup>[14]</sup> The product ion mass spectrum of deprotonated by-product 2 (Fig. 1(b)) revealed an ion at *m/z* 122.9793 with elemental composition of C<sub>2</sub>H<sub>3</sub>O<sub>4</sub>S<sup>-</sup>. It was formed through loss of water from the [M-H]<sup>-</sup> ion, indicating the probable presence of a hydroxyl group in by-product 2. This compound was a 1,2-dihydroxyethanesulfonate, formed by cleavage of the Uniblu-OH 2-hydroxyethylsulfonyl group and hydroxylation at the 1-position. All the information obtained from the product ion spectra of by-products 1 and 2 is rationalized in the fragmentation pathways depicted in Supplementary Fig. S2 (Supporting Information) and Fig. 2, respectively.

By-product 3 showed a [M-H]<sup>-</sup> ion at *m/z* 196.9758 consistent with elemental composition C<sub>4</sub>H<sub>5</sub>O<sub>7</sub>S<sup>-</sup> (error -1.8 ppm) for which three possible chemical structures can be proposed (Table 2). Its product ion mass spectrum (Supplementary Fig. S3, Supporting Information) revealed an ion at *m/z* 80.9661 attributed to HSO<sub>3</sub><sup>-</sup> (error 11.3 ppm) suggesting this compound to be another sulfur-containing by-product. Examination of the product ion spectrum reveals other minor ions at *m/z* 178.9585, 152.9847 and 134.9793 with elemental compositions C<sub>4</sub>H<sub>3</sub>O<sub>6</sub>S<sup>-</sup>, C<sub>3</sub>H<sub>5</sub>O<sub>5</sub>S<sup>-</sup> and C<sub>3</sub>H<sub>3</sub>O<sub>4</sub>S<sup>-</sup>, respectively. The first two ions can be rationalized through loss of water and carbon dioxide from the precursor ion, respectively. Both these product ions led to the formation of the third product ion (*m/z* 134.9793) through

further loss of CO<sub>2</sub> and water, respectively. Finally, a product ion at *m/z* 71.0167, assigned to C<sub>3</sub>H<sub>3</sub>O<sub>2</sub><sup>-</sup> (error 40.1 ppm), can be rationalized by loss of sulfurous acid from the above discussed product ion at *m/z* 153. The high errors associated with some of the product ions of by-product 3 are reasonable, due to their low signal intensity. The product ion spectrum of deprotonated by-product 3 did not allow us to unequivocally assign its structure, there being three possible structures: 3-carboxy-3-oxopropane-1-sulfonate, substituted with a hydroxyl group at position 1 (A) or 2 (B) and 3-carboxy-3-hydroxy-1-oxopropane-1-sulfonate (C). All three structures are consistent with the fragmentation pattern outlined in Supplementary Fig. S4 (Supporting Information).

By-products 4 and 5 are two closely eluting isomers having [M-H]<sup>-</sup> ions at *m/z* 212.9703 and 212.9693. On the basis of both spectral accuracy (Table 1) and mass accuracy (Table 2), their elemental composition was assigned as C<sub>4</sub>H<sub>5</sub>O<sub>8</sub>S<sup>-</sup> (errors -3.6 and -8.3 ppm, respectively) suggesting that these by-products were the result of a hydroxylation on by-product 3. Interestingly, the product ion spectrum of deprotonated by-product 5 (Table 2) showed a diagnostic ion at *m/z* 120.9626, not observed for by-product 4, with elemental composition of C<sub>2</sub>HO<sub>4</sub>S<sup>-</sup> (error 20.6 ppm). Its formation was rationalized by consecutive loss of water and formaldehyde from the ion at *m/z* 168.9832 assigned to C<sub>3</sub>H<sub>5</sub>O<sub>6</sub>S<sup>-</sup> (error 11.6 ppm). This

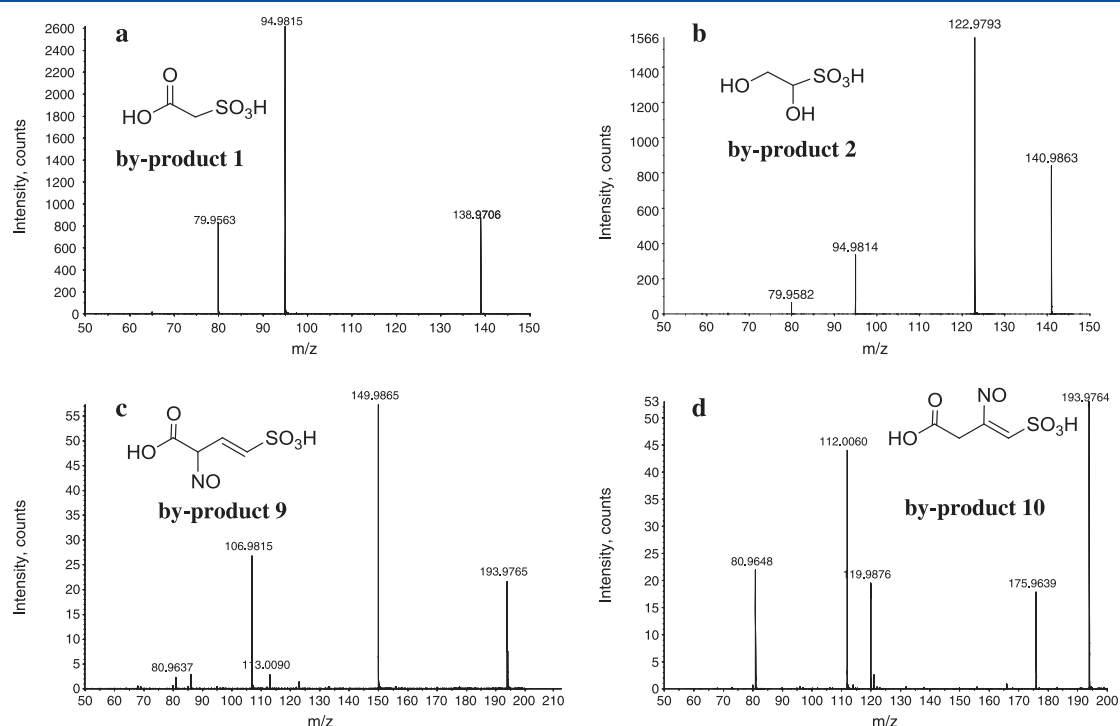


**Figure 1.** Calibrated product ion spectra of  $[M-H]^-$  ions of (a) by-product 1, (b) by-product 2, (c) by-product 9, and (d) by-product 10.  $[M-H]^-$  ions at  $m/z$  138.9707, 140.9863 and 193.9765 were used as lock masses. CV = 20 V.

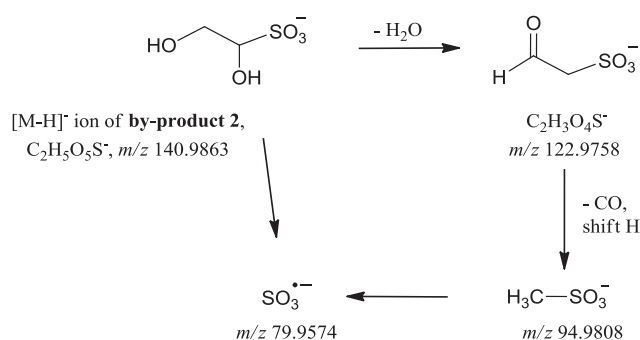


**Figure 2.** Proposed fragmentation pathway of  $[M-H]^-$  ion of by-product 2 from IC/QqTOFMS/MS data at CV = 20 V. Accurate mass measurements of product ions are reported in Table 2.

finding led to by-product 5 being unequivocally assigned as 3-carboxy-1,2-dihydroxy-3-oxopropane-1-sulfonate. The structure of by-product 4 was proposed to be 3-carboxy-2,3-dihydroxy-1-oxopropane-1-sulfonate. The identified product ions of these structures were consistent with the fragmentation patterns outlined in Supplementary Figs. S5 and S6 (Supporting Information).

By-products 6 and 7 were two closely eluting isomers, which showed  $[M-H]^-$  ions at  $m/z$  224.9733 and 224.9732. The elemental composition of both ions was determined to be  $C_5H_5O_8S^-$  based on mass accuracy (errors -9.9 and -9.5 ppm, respectively) and spectral accuracy (Table 2). Their fragmentation patterns showed significant differences, allowing the different chemical structures to be determined. Both

compounds were sulfur-containing by-products as demonstrated by the presence of product ions at  $m/z$  96.9623 and 96.9579 assigned to  $HSO_4^-$  (errors 22.7 and -22.7 ppm, respectively). The ions at  $m/z$  110.9784 and 110.9770 were consistent with the elemental composition  $CH_3O_4S^-$  (errors 23.8 and 11.2 ppm, respectively). The presence of such a product ion made it probable that both compounds had a hydroxyl group at the  $\alpha$ -position of the sulfur group. Two other ions in the product ion spectrum of deprotonated by-product 6 (Supplementary Fig. S7(a), Supporting Information) at  $m/z$  180.9892 and 142.9946 with elemental compositions  $C_4H_5O_6S^-$  and  $C_5H_3O_5^-$  (errors -5.7 and -27.9 ppm, respectively) suggested neutral loss of  $CO_2$  and  $H_2SO_3$ , respectively, from the  $[M-H]^-$  ion. The product ion spectrum of deprotonated by-product 7 (Supplementary Fig. S7(b), Supporting Information) showed a base peak at  $m/z$  152.9861 with elemental composition  $C_3H_5O_5S^-$  (error -1.4 ppm) probably arising from homolytic carbon-carbon cleavage between the carbonyl groups in positions 3 and 4 of the  $[M-H]^-$  ion. This product ion, in turn, gave rise to ions at  $m/z$  134.9774 and then at  $m/z$  106.9830 through consecutive losses of water and CO. On the basis of the identified product ions of deprotonated by-products 6 and 7, the fragmentation patterns outlined in Supplementary Figs. S7(c) and S7(d) (Supporting Information) were proposed.

By-products 8–12 all showed even-mass  $[M-H]^-$  ions suggesting that they were nitrogen-containing compounds. The product ion spectra of deprotonated by-products 8–10 revealed the presence of an ion at  $m/z$  81 whose accurate mass was consistent with the elemental composition  $HSO_3^-$ , as already found for by-product 3. By-products 9 and 10 showed  $[M-H]^-$  ions with the same elemental composition of

$C_4H_4NO_6S^-$  (errors 2.1 and  $-8.1$  ppm, respectively). However, the fragmentation patterns of these ions showed significant differences (Figs. 2(c) and 2(d)). Specifically, the product ion spectrum of deprotonated by-product 9 showed a base peak at  $m/z$  149.9865 with elemental composition  $C_3H_4NO_4S^-$  (error  $-1.0$  ppm). This is consistent with  $CO_2$  loss, indicating the presence of a monocarboxylic acid group. A close examination of this product ion spectrum revealed another minor odd-electron ion at  $m/z$  113.0090, corresponding to the radical ion with an elemental composition of  $C_4H_3NO_3^-$ , which derives from elimination of the  $HSO_3^-$  radical ion from the  $[M-H]^-$  ion. This by-product was assigned as 3-carboxy-3-nitrosoprop-1-ene-1-sulfonate. The product ion mass spectrum of deprotonated by-product 10 revealed an ion at  $m/z$  175.9639 and an odd-electron ion at  $m/z$  119.9876, consistent with elemental compositions  $C_4H_2NO_5S^-$  and  $C_3H_4O_3S^-$  (errors  $-11.5$  and  $-8.9$  ppm), respectively. The former ion was derived through the loss of water, while the latter derived from consecutive elimination of carbon dioxide and an NO radical. Both these product ions suggest the presence of a monocarboxylic acid. In addition, the base peak of the product ion spectrum was at  $m/z$  112.0060 with elemental composition  $C_4H_2NO_3^-$  (error 17.7 ppm) probably arising from loss of  $H_2SO_3$  from the  $[M-H]^-$  ion and further migration of the NO group to the terminal carbon. The structure was thus assigned as 3-carboxy-3-nitrosoprop-1-ene-2-sulfonate, with the nitro group probably located at the  $\beta$ -position of the carboxylic acid group. This compound can

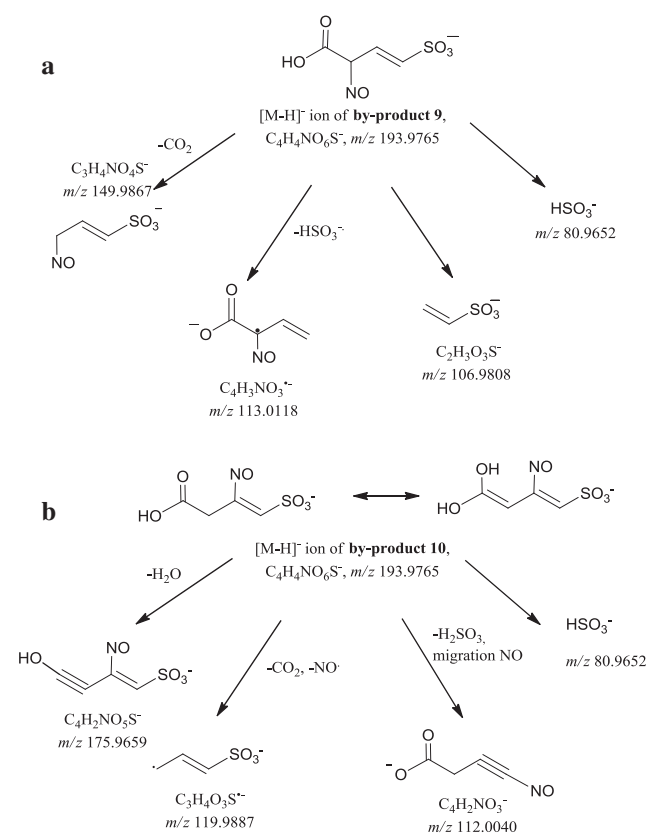


**Figure 3.** Proposed fragmentation pathway of  $[M-H]^-$  ions of by-product 9 (a) and 10 (b) from IC/QqTOFMS/MS data at  $CV = 20$  V. Accurate mass measurements of product ions are reported in Table 2.

be correlated with by-product 8 by a further oxidation of the terminal carbon. Based on the identified product ions of by-products 9 and 10 the fragmentation patterns outlined in Figs. 3(a) and 3(b) were proposed.

Table 1 also shows that by-products 13–18 yielded product ions consistent with consecutive neutral loss of 44 and 18 Da, indicating the presence of a carboxylic acid and a hydroxyl group, respectively. Therefore, the structures of these compounds were consistent with mono- and polyhydroxylated dicarboxylic acids of low molecular weight. By-product 13 with its  $[M-H]^-$  ion at  $m/z$  116.9829, assigned to  $C_3HO_5^-$  (error  $-0.4$  ppm), was previously identified as the corresponding DPNH derivative, derivatized at the oxo position.<sup>[14]</sup> By-product 14 showed a  $[M-H]^-$  ion at  $m/z$  133.0145 with elemental composition  $C_4H_5O_5^-$  (error  $-1.9$  ppm) whose product ion spectrum (Fig. 4) showed an intense ion at  $m/z$  115.0026 and a minor one at  $m/z$  89.0247 with elemental compositions  $C_4H_3O_4^-$  and  $C_3H_5O_3^-$  (errors  $-9.4$  and  $3.2$  ppm, respectively). These ions were formed by competitive loss of water and  $CO_2$ , respectively, and both underwent further fragmentation leading to acrylate and acetate ions through  $CO_2$  and formaldehyde loss. In addition, the ion at  $m/z$  72.9931, assigned to deprotonated glyoxylic acid (error  $-0.2$  ppm), could be rationalized by  $C_2H_4O_2$  loss through cleavage at the 2-3 position on the  $[M-H]^-$  ion. This information allowed us to assign by-product 14 to 2-hydroxysuccinic acid whose fragmentation pathway is depicted in Fig. 5. On the basis of exact mass measurement data, and confirmed by high spectral accuracy (better than 98%), by-products 15–17 were assigned as listed in Table 2. In particular, by-product 15 showed a  $[M-H]^-$  ion at  $m/z$  149.0100 with elemental composition  $C_4H_5O_6^-$  (error 5.6 ppm), consistent with the conjugated form of 2,3-dihydroxysuccinic acid. This suggested that the compound was formed by a further hydroxylation of by-product 14. The product ion spectrum of deprotonated by-product 16 did not allow us to distinguish between two possible dicarboxylic acid structures: 3-hydroxy-2-oxopentanedioic acid and 2-hydroxy-4-oxopentanedioic acid. By-product 17 showed a  $[M-H]^-$  ion at  $m/z$  179.0196 with elemental composition  $C_5H_7O_7^-$  (error  $-0.7$  ppm), assigned as deprotonated 2,3,4-trihydroxypentanedioic acid.

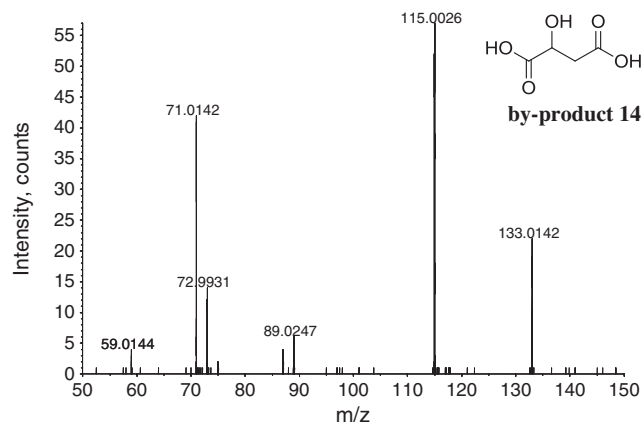


**Figure 4.** Calibrated product ion spectrum of  $[M-H]^-$  ion of by-product 14 at  $CV = 20$  V.  $[M-H]^-$  ion at  $m/z$  133.0142 was used as a lock mass.

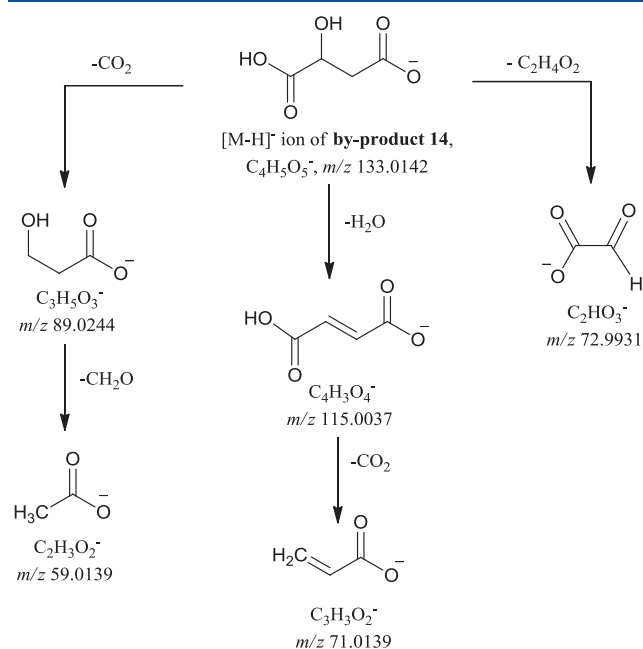


**Figure 5.** Proposed fragmentation pathway of  $[M-H]^-$  ion of by-product 14 from IC/QqTOFMS/MS data at  $CV=20$  V. Accurate mass measurements of product ions are reported in Table 2.

The last identified compound, by-product 18, showed a  $[M-H]^-$  ion at  $m/z$  192.9994, with elemental composition  $C_5H_5O_8^-$  (error 2.1 ppm), whose product ion spectrum (Supplementary Fig. S8, Supporting Information) showed major ions at  $m/z$  149.0094 and 105.0190 with elemental compositions  $C_4H_5O_6^-$  and  $C_3H_5O_4^-$  (errors 1.6 and  $-3.2$  ppm, respectively). These ions were formed by consecutive losses of  $CO_2$  from the  $[M-H]^-$  ion, indicating that this by-product was a dicarboxylic acid. A product ion at  $m/z$  121.0140 of elemental composition  $C_3H_5O_5^-$  (error  $-2.0$  ppm) was derived by CO elimination from  $m/z$  149. This finding allowed the oxo group to be located at the 4-position. The structure of this compound was assigned as 2,2,3-trihydroxy-4-oxopentanedioic acid. Interestingly, the absence of any water loss in the product ion spectrum could be explained by the fact that all positions on the aliphatic chain are locked and thus the dehydration pathway was not possible. The information obtained from the product ion spectrum was rationalized in the fragmentation pathway depicted in Supplementary Fig. S9 (Supporting Information).

#### Formation mechanism of identified low molecular weight organic acids

The formation/degradation of identified organic acids was monitored over a long ozonation time in order to gain insights into their formation mechanism, and selected measured profiles are depicted in Fig. 6. The identified by-products were consistent with further oxidation and decarboxylation of the previously identified carbonyl by-products.<sup>[14]</sup> From Fig. 6 it can be seen that by-product 12 was always formed at ozonation times longer than 90 min, suggesting that it was an end by-product. A careful analysis of the measured profiles shown in Fig. 6, including possible structures of low molecular weight carboxylic acids

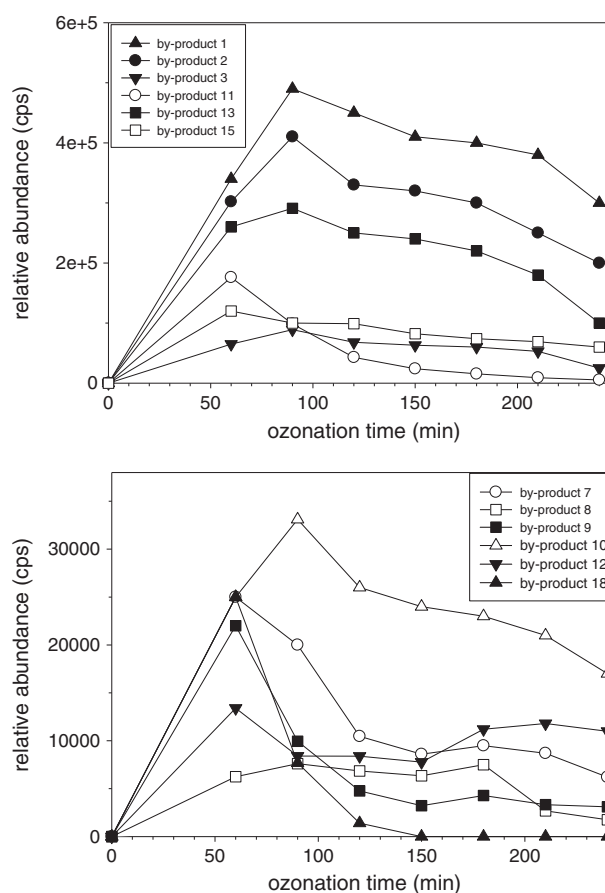


**Figure 6.** Formation/degradation profiles of selected identified carboxylic acids (extracted ion peak area from IC/ESI-QqTOFMS) during ozonation of Uniblu-OH.

identified over a long ozonation time, could help in understanding the reaction pathway depicted in Fig. 7. The identified organic acids (Table 1) arose from further degradation of low molecular weight carbonyl compounds, namely keto-acids and aliphatic aldehydes detected in the early stage of the ozonation process.<sup>[14]</sup> Although complex competitive and consecutive reactions occurred during ozonation, it was possible to describe a degradation pathway on the basis of reasonable chemistry, supported by some observed correlations between the by-products belonging to the same class. After the formation of the sulfur-containing by-products 1–7 and by-products 16 and 17, the degradation proceeded further with the decarboxylation of by-product 16 (A) and 16 (B) followed by oxidation of the terminal carbon of the formed intermediate, leading to by-product 14. This oxidation process was based on hydrogen homolytic abstraction by a hydroxyl radical leading to a peroxy radical which, in turn, was transformed into a hydroperoxide. By-product 13 was formed from by-product 17 by means of the same oxidation route. It followed that three of the detected by-products all led to the formation of a single compound, 2-oxomalonic acid (by-product 13). This was also consistent with the formation/decomposition profiles of the detected by-products. By-product 13 was the lowest molecular weight dicarboxylic acid detected and it persisted in high abundance at long reaction times (Fig. 6). The finding that 2-oxomalonic acid slowly disappeared at longer ozonation time suggested that it was



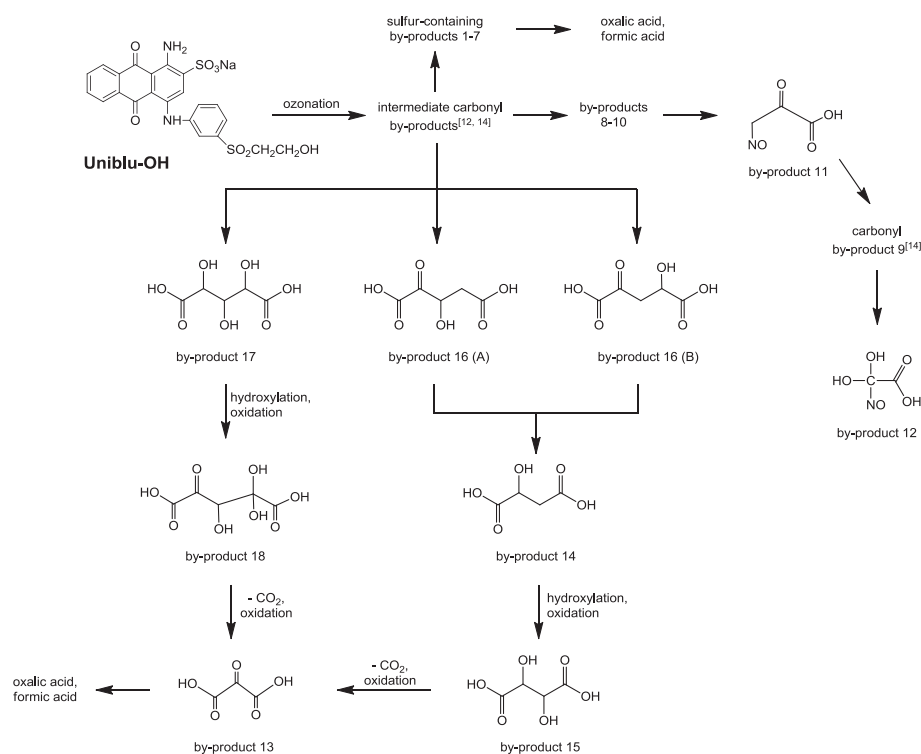


**Figure 7.** Proposed degradation pathway for Uniblu-OH ozonation leading to low molecular weight organic acids.

degraded to oxalic and/or formic acid, according to previous investigation employing authentic standards.<sup>[12]</sup> The same aforementioned mechanisms including decarboxylation and subsequent oxidation can be applied to all the sulfur- and nitrogen-containing by-products 1–12 in order to explain the formation of their lower molecular weight homologues. Sulfur-containing by-products were still persistent at longer ozonation time confirming that the sulfur present in Uniblu-OH did not undergo complete mineralization. Finally, by-product 12 was still formed at longer ozonation time (Fig. 6) and therefore was another end product. This confirmed the finding that the organic nitrogen compound, Uniblu-OH, was not completely mineralized.

## CONCLUSIONS

The coupling of ion chromatography (IC) and electrospray ionization mass spectrometry (ESI-MS), proved to be a powerful technique for the identification of low molecular weight organic acids formed as final by-products of Uniblu-OH degradation by the ozonation process, an oxidation method widely employed to degrade recalcitrant organic pollutants in industrial wastewater. Organic acid identification was possible due to the employment of a NaOH gradient and a membrane ion suppressor that minimized the background spectral interferences and enhanced the signals of the  $[M-H]^-$  ions. The combination of mass accuracy, MS/MS information and high spectral accuracy was demonstrated to be a powerful method for unequivocally assigning a single chemical composition to each identified compound. Specifically, the employment of the spectral accuracy concept using

the sCLIPS algorithm allowed the unequivocal identification of 18 low molecular weight organic acids as a result of extensive oxidation of the parent organic pollutant. Excellent spectral accuracy of better than or close to 95% was found for most of the identified compounds. Most of the by-products gave rise in the MS collision cell to either single or double  $CO_2$  and water loss, consistent with assignment to polyhydroxylated carboxylic acids. Some of identified organic acids were shown to be both sulfur- and nitrogen-containing carbonyl by-products. Due to the complexity of reactions involved during Uniblu-OH ozonation it was possible to assess the presence of correlations between different identified by-products, such as polyhydroxylated carboxylic acids. These compounds in turn decompose to known low molecular weight organic acids through decarboxylation and further oxidation and then undergo complete mineralization. However, sulfur- and nitrogen-containing compounds still remain at longer ozonation times. This result is of environmental interest due to the potential toxicity of such compounds.

## SUPPORTING INFORMATION

Additional supporting information may be found in the online version of this article.

## Acknowledgements

This work was partially supported by Apulia Region by funding from the Relu-Valbior Project within the Scientific Research Framework Program 2007-2013.

## REFERENCES

- [1] A. Lopez, C. Di Iaconi, G. Mascolo, A. Pollice, in *Innovative and Integrated Technologies for the Treatment of Industrial Wastewater (INNOWATECH)*, IWA Publishing, 2011.
- [2] P. R. Gogate, A. B. Pandit. A review of imperative technologies for wastewater treatment II: hybrid methods. *Adv. Environ. Res.* **2004**, *8*, 553.
- [3] M. Pera-Titus, V. Garcia-Molina, M. A. Baños, J. Giménez, S. Esplugas. Degradation of chlorophenols by means of advanced oxidation processes: a general review. *Appl. Catal. B Environ.* **2004**, *47*, 219.
- [4] S. Devipriya, S. Yesodharan. Photocatalytic degradation of pesticide contaminants in water. *Solar Energy Materials and Solar Cells* **2005**, *86*, 309.
- [5] J. J. Pignatello, E. Oliveros, A. MacKay. Advanced oxidation processes for organic contaminant destruction based on the Fenton reaction and related chemistry. *Crit. Rev. Environ. Sci. Technol.* **2006**, *36*, 1.
- [6] C. Comninellis, A. Kapalka, S. Malato, S. A. Parsons, I. Poullos, D. Mantzavinos. Advanced oxidation processes for water treatment: advances and trends for R&D. *J. Chem. Technol. Biotechnol.* **2008**, *83*, 769.
- [7] M. A. Shannon, P. W. Bohn, M. Elimelech, J. G. Georgiadis, B. J. Marinas, A. M. Mayes. Science and technology for water purification in the coming decades. *Nature* **2008**, *452*, 301.
- [8] L. Rizzo. Bioassays as a tool for evaluating advanced oxidation processes in water and wastewater treatment. *Water Res.* **2011**, *45*, 4311.
- [9] S. Malato, P. Fernández-Ibáñez, M. I. Maldonado, J. Blanco, W. Gernjak. Decontamination and disinfection of water by solar photocatalysis: Recent overview and trends. *Catal. Today* **2009**, *147*, 1.
- [10] M. Constapel, M. Schellenträger, J. M. Marzinkowski, S. Gäb. Degradation of reactive dyes in wastewater from the textile industry by ozone: Analysis of the products by accurate masses. *Water Res.* **2009**, *43*, 733.
- [11] A. Detomaso, G. Mascolo, A. Lopez. Characterization of carbofuran photodegradation by-products by liquid chromatography/hybrid quadrupole time-of-flight mass spectrometry. *Rapid Commun. Mass Spectrom.* **2005**, *19*, 2193.
- [12] G. Mascolo, A. Lopez, A. Bozzi, G. Tiravanti. By-products formation during the ozonation of the reactive dye Uniblu-A. *Ozone-Sci. Eng.* **2002**, *24*, 439.
- [13] D. Deng, J. Guo, G. Zeng, G. Sun. Decolorization of anthraquinone, triphenylmethane and azo dyes by a new isolated *Bacillus cereus* strain DC11. *Int. Biodeter. Biodegr.* **2008**, *62*, 263.
- [14] A. Amorisco, V. Locaputo, G. Mascolo. Characterization of carbonyl by-products during Uniblu-A ozonation by liquid chromatography/hybrid quadrupole time-of-flight mass spectrometry. *Rapid Commun. Mass Spectrom.* **2011**, *25*, 1801.
- [15] J. A. Cruwys, R. M. Dinsdale, F. R. Hawkes, D. L. Hawkes. Development of a static headspace gas chromatographic procedure for the routine analysis of volatile fatty acids in wastewaters. *J. Chromatogr. A* **2002**, *945*, 195.
- [16] W.-J. Huang, G.-C. Fang, C.-C. Wang. The determination and fate of disinfection by-products from ozonation of polluted raw water. *Sci. Total Environ.* **2005**, *345*, 261.
- [17] J. Chen, B. P. Preston, M. J. Zimmerman. Analysis of organic acids in industrial samples comparison of capillary electrophoresis and ion chromatography. *J. Chromatogr. A* **1997**, *781*, 205.
- [18] Y. Deng, X. Fan, A. Delgado, C. Nolan, K. Furton, Y. Zuo, R. D. Jones. Separation and determination of aromatic acids in natural water with preconcentration by capillary zone electrophoresis. *J. Chromatogr. A* **1998**, *817*, 145.
- [19] S. Uchiyama, E. Matsushima, S. Aoyagi, M. Ando. Simultaneous determination of C1–C4 carboxylic acids and aldehydes using 2,4-dinitrophenylhydrazine-impregnated silica gel and high-performance liquid chromatography. *Anal. Chem.* **2004**, *76*, 5849.
- [20] S.-F. Chen, R. A. Mowery, V. A. Castleberry, G. P. v. Walsum, C. K. Chambliss. High-performance liquid chromatography method for simultaneous determination of aliphatic acid, aromatic acid and neutral degradation products in biomass pretreatment hydrolysates. *J. Chromatogr. A* **2006**, *1104*, 54.
- [21] K. Fischer. Environmental analysis of aliphatic carboxylic acids by ion-exclusion chromatography. *Anal. Chim. Acta* **2002**, *465*, 157.
- [22] K. Ohta, M. Ohashi, J.-Y. Jin, T. Takeuchi, C. Fujimoto, S.-H. Choi, J. J. Ryoo, K.-P. Lee. Retention behavior of C1–C6 aliphatic monoamines on anion-exchange and polymethacrylate resins with heptylamine as eluent. *J. Chromatogr. A* **2004**, *1039*, 179.
- [23] M. C. Bruzzoniti, E. Mentasti, C. Sarzanini, P. Hajós. Ion chromatographic separation of carboxylic acids prediction of retention data. *J. Chromatogr. A* **1997**, *770*, 13.
- [24] S. A. Cassidy, C. W. Demarest, P. B. Wright, J. B. Zimmerman. Development and application of a universal method for quantitation of anionic constituents in active pharmaceutical ingredients during early development using suppressed conductivity ion chromatography. *J. Pharm. Biomed. Anal.* **2004**, *34*, 255.
- [25] J. Qiu, X. Jin. Development and optimization of organic acid analysis in tobacco with ion chromatography and suppressed conductivity detection. *J. Chromatogr. A* **2002**, *950*, 81.
- [26] K.-H. Bauer, T. P. Knepper, A. Maes, V. Schatz, M. Voihsel. Analysis of polar organic micropollutants in water with ion chromatography–electrospray mass spectrometry. *J. Chromatogr. A* **1999**, *837*, 117.
- [27] L. Charles, D. Pépin, B. Casetta. Electrospray ion chromatography – tandem mass spectrometry of bromate at sub-ppb levels in water. *Anal. Chem.* **1996**, *68*, 2554.
- [28] K. Gamoh, H. Saitoh, H. Wada. Improved liquid chromatography/mass spectrometric analysis of low molecular weight carboxylic acids by ion exclusion separation with electrospray ionization. *Rapid Commun. Mass Spectrom.* **2003**, *17*, 685.
- [29] S. B. Mohsin. Ion chromatography coupled with mass spectrometry for the determination of ionic compounds in agricultural chemicals. *Anal. Chem.* **1999**, *71*, 3603.
- [30] M. I. H. Helaleh, K. Tanaka, H. Taoda, W. Hu, K. Hasebe, P. R. Haddad. Qualitative analysis of some carboxylic acids by ion-exclusion chromatography with atmospheric pressure chemical ionization mass spectrometric detection. *J. Chromatogr. A* **2002**, *956*, 201.
- [31] R. Roehl, R. Slingsby, N. Avdalovic, P. E. Jackson. Applications of ion chromatography with electrospray mass spectrometric detection to the determination of environmental contaminants in water. *J. Chromatogr. A* **2002**, *956*, 245.
- [32] J. M. Käkölä, R. J. Alén, J. P. Isoaho, R. B. Matilainen. Determination of low-molecular-mass aliphatic carboxylic acids and inorganic anions from kraft black liquors by ion chromatography. *J. Chromatogr. A* **2008**, *1190*, 150.
- [33] X. Xiang, C. Y. Ko, H. Y. Guh. Ion-exchange chromatography/electrospray mass spectrometry for the identification of organic and inorganic species in topiramate tablets. *Anal. Chem.* **1996**, *68*, 3726.
- [34] G. Mascolo, A. Lopez, A. Detomaso, G. Lovecchio. Ion chromatography–electrospray mass spectrometry for the identification of low-molecular-weight organic acids during the 2,4-dichlorophenol degradation. *J. Chromatogr. A* **2005**, *1067*, 191.

- [35] W. Buchberger, W. Ahrer. Combination of suppressed and non-suppressed ion chromatography with atmospheric pressure ionization mass spectrometry for the determination of anions. *J. Chromatogr. A* **1999**, *850*, 99.
- [36] W. W. Buchberger. Detection techniques in ion analysis: what are our choices? *J. Chromatogr. A* **2000**, *884*, 3.
- [37] W. Jiang, J. C. L. Erve. Spectral accuracy of a new hybrid quadrupole time-of-flight mass spectrometer: application to ranking small molecule elemental compositions. *Rapid Commun. Mass Spectrom.* **2012**, *26*, 1014.
- [38] Y. Wang, M. Gu. The concept of spectral accuracy for MS. *Anal. Chem.* **2010**, *82*, 7055.
- [39] A. L. Rockwood, S. L. Van Orden. Ultrahigh-speed calculation of isotope distributions. *Anal. Chem.* **1996**, *68*, 2027.
- [40] A. L. Rockwood, S. L. Van Orden, R. D. Smith. Ultrahigh resolution isotope distribution calculations. *Rapid Commun. Mass Spectrom.* **1996**, *10*, 54.
- [41] J. A. Yergey. A general approach to calculating isotopic distributions for mass spectrometry. *Int. J. Mass Spectrom. Ion Phys.* **1983**, *52*, 337.
- [42] T. Kind, O. Fiehn. Seven Golden Rules for heuristic filtering of molecular formulas obtained by accurate mass spectrometry. *BMC Bioinformatics* **2007**, *8*, 105.

Rapid Commun. Mass Spectrom. 2012, 26, 1014–1022  
(wileyonlinelibrary.com) DOI: 10.1002/rcm.6197

# Spectral accuracy of a new hybrid quadrupole time-of-flight mass spectrometer: application to ranking small molecule elemental compositions

Wei Jiang and John C. L. Erve\*

Analytical Sciences, Novartis Institutes for Biomedical Research, Cambridge, MA, USA

**RATIONALE:** Determining the elemental compositions of unknown molecules is an important goal of analytical chemistry. The isotope pattern revealed by a mass spectrometer provides valuable information regarding the elemental composition of a molecule. In order to employ spectral accuracy considerations for elemental composition determination, it is important to know how faithfully a mass spectrometer can record the isotope pattern and to understand the magnitude of the errors of the relative isotopic abundances.

**METHODS:** Twenty-four small molecule drugs and two natural products representing a diverse range of elemental compositions and ranging in molecular weight from 236 to 1663 Da were measured on a new hybrid orthogonal acceleration quadrupole time-of-flight (Q-TOF) mass spectrometer by flow infusion analysis. The similarity between the observed profile isotope pattern and the theoretical isotope pattern, denoted spectral accuracy, was calculated using a computational algorithm in the program MassWorks.

**RESULTS:** The spectral accuracy for all compounds averaged better than 98%. When using spectral accuracy to rank elemental compositions with the elemental constraints ( $C_{1-100}H_{0-200}N_{0-50}O_{0-50}F_{0-5}S_{0-5}Cl_{0-5}Br_{0-5}$ ) further restricted by empirical rules and a mass tolerance  $\leq 5$  parts-per-million, the correct formula was ranked first over 80% of the time. In contrast, when using mass accuracy for ranking, only two compounds (8%) were ranked first. For quinidine and troglitazone, the initial spectral accuracy measurements were lower than expected and further analysis indicated that minor, structurally related components were present.

**CONCLUSIONS:** Our work has determined the magnitude of spectral accuracy that can be expected on a new Q-TOF mass spectrometer. In addition, we demonstrate the utility of spectral accuracy measurements both for ranking elemental compositions and also for obtaining insight into the chemical nature of the analyte that might otherwise be overlooked. Copyright © 2012 John Wiley & Sons, Ltd.

Using mass spectrometry for elemental composition (EC) determination is an important application of analytical chemistry in diverse scientific fields including forensics,<sup>[1]</sup> toxicology,<sup>[2]</sup> environmental chemistry,<sup>[3]</sup> petrochemicals,<sup>[4]</sup> metabolomics,<sup>[5]</sup> and pharmaceuticals.<sup>[6]</sup> For molecules up to ~500 Da containing the elements  $(CH)_{no\ limit}N_{0-5}O_{0-10}S_{0-3}$ , a theoretical study reported that a mass accuracy of 0.1 mDa would give a unique EC.<sup>[7]</sup> Such mass accuracies are typically only obtained on Fourier transform ion cyclotron resonance (FTICR) mass spectrometers capable of resolving powers of  $m/\Delta m$  (full width at half maximum (FWHM))  $>400\,000$ . For peptides with masses up to 700–800 Da, a theoretical study argued that a mass accuracy of  $\pm 1$  ppm would give rise to a unique EC<sup>[8]</sup> in part because not all monoisotopic masses are possible for peptides. Small molecules have a greater variety of elements to consider and for this reason are more challenging than peptides. For low molecular weight analytes (<200 Da) high accuracy mass measurements (<1 ppm) may give a single EC. However, as the mass of the analyte increases, the number of feasible ECs increases exponentially and another

theoretical study demonstrated that for metabolites from 0–500 Da with C, H, N, S, O, P, and potentially F, Cl, Br and Si as elements, even a mass accuracy  $< \pm 1$  ppm is not sufficient to arrive at a unique EC when searching metabolite databases.<sup>[9]</sup> In such situations, adding constraints to the type and number of elements considered can reduce the number of ECs although with true unknowns this poses the risk of missing the correct EC.

Due to the limitations of mass accuracy alone, approaches have been developed to use other readily obtainable mass spectrometric information for EC determination. Making high mass accuracy measurements of both the protonated molecule and product ions following collision-induced dissociation allows the elimination of ECs inconsistent with observed product ions and neutral losses. When applied to 113 environmental chemicals with masses <410 Da using MS data collected on a quadrupole time-of-flight (Q-TOF) mass spectrometer, a unique EC was obtained for 65% of the compounds measured.<sup>[10]</sup> Recently, a software program called Multi-stage Elemental Formula has been developed which uses as input  $MS^n$  spectra from the mass spectral tree for a compound of interest.<sup>[11]</sup> Applying this program to 12 spectra for metabolites with masses from 150 to 450 Da acquired on an Orbitrap mass spectrometer at 30 000 resolving power (RP) provided a unique EC when considering

\* Correspondence to: J. C. L. Erve, 250 Massachusetts Ave, Cambridge, MA 02139, USA.  
E-mail: john\_erve@hotmail.com



the data acquired in MS<sup>n</sup> experiments ( $n = 2-5$ ) and it was also shown that when acquiring higher order spectra (MS<sup>n</sup>), greater mass error was tolerated.

Isotopic peak ratios (i.e. isotope abundances) are a valuable source of information for EC determination as the natural abundances of isotopes of elements such as S, Br and Cl can give rise to informative isotopic clusters.<sup>[12]</sup> Including isotopic peak ratios can further limit the number of possible ECs for a given mass and should thus be considered, especially as the mass of the analyte increases.<sup>[9]</sup> Various workers have demonstrated the utility of including isotope abundances in addition to accurate mass of (1) precursor ion<sup>[1,13,14]</sup> and (2) precursor, product ions and neutral losses<sup>[15-17]</sup> for EC determination for a variety of analytes and matrices. Several reports have examined the accuracy of isotopic abundance measurements. In one study, 137 commercially available compounds with masses in the range of 75–810 Da were analyzed on an LTQ/Orbitrap mass spectrometer and the experimentally measured relative isotopic abundance (RIA) of  $[A+1]/A$  was compared with the theoretical one.<sup>[18]</sup> Approximately 40% of compounds had RIA errors between 0 and 3% with the remaining compounds equally distributed from 3–5%, 5–10%, 10–20% and >20%, respectively. Although another study that compared the quality of isotopic abundance measurements on an Orbitrap-Velos mass spectrometer at 100 000 RP and an LTQ/FT Ultra between 100 000 and 750 000 RP reported that these measurements were strongly dependent on the signal-to-noise ratio of the protonated molecule under investigation, these measurements did increase the number of single EC assignments by >3-fold compared with measuring accurate mass alone.<sup>[19]</sup>

Spectral accuracy (SA%), or spectral error ( $SE\% = 100 - SA\%$ ), describes the goodness-of-fit between an observed and a theoretical isotope profile.<sup>[20]</sup> The commercially available software program MassWorks uses the algorithm self-Calibrated Line-shape Isotope Profile Search (sCLIPS) to calculate spectral accuracy. Briefly, this approach involves self calibrating the experimentally observed mass spectral peak shape to give a mathematically defined mass spectral profile spectrum which is then compared with an MS profile spectrum for a given EC calculated with the same mass spectral peak shape. The self-calibration algorithm uses the isotopically pure monoisotopic peak (e.g. the calibration range indicated in the Experimental section) of any ion as the model line-shape for calibration, which is then applied to the entire ion isotope pattern (e.g. the profile mass range indicated in the Experimental section). Unlike mass accuracy, a higher SA% implies a better match for a given EC. Spectral accuracy was evaluated on an Orbitrap-XL mass spectrometer for ten natural products with masses between 639 and 1663 Da at five RP settings. At a RP setting of 30 000, SA% ranged from 96.2 to 98.4% and for thioestrepton (1663 Da) the correct EC was within the top seven hits out of 1900 ECs, consistent with the elemental and 2 ppm mass accuracy constraints.<sup>[21]</sup> Instrument manufacturers have also developed algorithms to quantitatively score the match of a measured isotope pattern such as Bruker's Sigma-Fit<sup>®</sup> and Water's i-FIT<sup>®</sup>. The algorithm SIRIUS, which stands for Sum formula Identification by Ranking Isotope patterns Using mass Spectrometry, similarly determines ECs based solely on the exact mass and isotope distribution of the analyte under investigation which, when applied to spectra of organic compounds (100–900 Da) obtained on a Q-TOF mass spectrometer, correctly identified >90% of the metabolites as a top hit.<sup>[22]</sup>

With the growing recognition of the importance of using isotope abundance considerations for EC determination, it is important to know the fidelity of a mass spectrometer with regards to not only mass accuracy of the monoisotopic peak, but also the relative abundances of the isotopic peaks ( $A+1$ ,  $A+2$ , etc.), i.e. the spectral accuracy. Thus, the aim of the present work was to evaluate spectral accuracy on a new oaQ-TOF mass spectrometer. To this end, a diverse range of elemental compositions was obtained consisting of 24 commercially available small molecule drugs ranging in mass from 236 to 704 Da, and two natural products with masses of 639 and 1663 Da (Table 1). Flow infusion analysis (FIA) was performed, the mass accuracy and SA% were determined, and the resulting ECs were ranked based on their SA%.

## EXPERIMENTAL

### Chemicals

Tenidap and citalopram were purchased from Tocris Bioscience (Bristol, UK), prochlorperazine and trifluoperazine were purchased from MP Biomedicals (Solon, OH, USA) and moxidectin was purchased from Fluka (Stenheim, Switzerland). Troglitazone was purchased from Calbiochem (Gibbstown, NJ, USA). All other compounds analyzed in

**Table 1.** Molecular formulae and exact masses of the molecules investigated in the study

Group I	Formula	Exact Mass
Carbamazepine	C <sub>15</sub> H <sub>12</sub> N <sub>2</sub> O	236.0944
Trimeterene	C <sub>12</sub> H <sub>11</sub> N <sub>7</sub>	253.1070
Ketoprofen	C <sub>16</sub> H <sub>14</sub> O <sub>3</sub>	254.0937
Propranolol	C <sub>16</sub> H <sub>21</sub> NO <sub>2</sub>	259.1567
Metoprolol	C <sub>15</sub> H <sub>25</sub> NO <sub>3</sub>	267.1829
Amitriptyline	C <sub>20</sub> H <sub>23</sub> N	277.1825
Imipramine	C <sub>19</sub> H <sub>24</sub> N <sub>2</sub>	280.1934
Diclofenac	C <sub>14</sub> H <sub>11</sub> Cl <sub>2</sub> NO <sub>2</sub>	295.0161
<b>Group II</b>		
Tenidap	C <sub>14</sub> H <sub>9</sub> ClN <sub>2</sub> O <sub>3</sub> S	320.0017
Quinidine	C <sub>20</sub> H <sub>24</sub> N <sub>2</sub> O <sub>2</sub>	324.1832
Citalopram	C <sub>20</sub> H <sub>21</sub> FN <sub>2</sub> O	324.1632
Omeprazole	C <sub>17</sub> H <sub>19</sub> N <sub>3</sub> O <sub>3</sub> S	345.1142
Meloxicam	C <sub>14</sub> H <sub>13</sub> N <sub>3</sub> O <sub>4</sub> S <sub>2</sub>	351.0342
Oxybutynin	C <sub>22</sub> H <sub>31</sub> NO <sub>3</sub>	357.2298
Prochlorperazine	C <sub>20</sub> H <sub>24</sub> ClN <sub>3</sub> S	373.1374
Prazosin	C <sub>19</sub> H <sub>21</sub> N <sub>5</sub> O <sub>4</sub>	383.1588
<b>Group III</b>		
Trifluoperazine	C <sub>21</sub> H <sub>24</sub> F <sub>3</sub> N <sub>3</sub> S	407.1638
Ziprasidone	C <sub>21</sub> H <sub>21</sub> ClN <sub>4</sub> OS	412.1119
Troglitazone	C <sub>24</sub> H <sub>27</sub> NO <sub>5</sub> S	441.1604
Verapamil	C <sub>27</sub> H <sub>38</sub> N <sub>2</sub> O <sub>4</sub>	454.2826
Nicardipine	C <sub>26</sub> H <sub>29</sub> N <sub>3</sub> O <sub>6</sub>	479.2051
OH-taurosporine	C <sub>28</sub> H <sub>26</sub> N <sub>4</sub> O <sub>4</sub>	482.1949
Ketoconazole	C <sub>26</sub> H <sub>28</sub> Cl <sub>2</sub> N <sub>4</sub> O <sub>4</sub>	530.1482
Moxidectin	C <sub>37</sub> H <sub>53</sub> NO <sub>8</sub>	639.3766
Itraconazole	C <sub>35</sub> H <sub>38</sub> Cl <sub>2</sub> N <sub>8</sub> O <sub>4</sub>	704.2388
Thioestrepton	C <sub>72</sub> H <sub>85</sub> N <sub>19</sub> O <sub>18</sub> S <sub>5</sub>	1663.4918



the study were purchased from Sigma-Aldrich (St. Louis, MO, USA) as were di-butylamine acetate (DBAA), dimethyl isopropanolamine (DMIPA) and dimethyl sulfoxide (DMSO). Formic acid (>99%) was purchased from Acros Organics (Geel, Belgium) and HPLC grade acetonitrile was purchased from Thermo Fisher Scientific (Fair Lawn, NJ, USA). Water used was prepared from a MilliQ water system (Billerica, MA, USA).

### FIA by electrospray ionization (ESI) on a Q-TOF mass spectrometer

Stock solutions (1 mM) for all standard compounds prepared in DMSO were diluted in water to 1–20  $\mu\text{M}$  for positive or negative mode mass spectrometric analysis. This typically produced maximum ion abundances of the order of one to five million ions/scan although, for data processing, spectra with ion abundances of one hundred thousand ions/scan were averaged. A tripleTOF 5600 hybrid Q-TOF mass spectrometer (AB Sciex, Foster City, CA, USA) equipped with a Shimadzu UFLC system (Kyoto, Japan), consisting of a CBM-20A control module, an SIL-30 AC autosampler, a DGU-20A5 degasser, and two LC-30 AD pumps, was used for FIA. The mass spectrometer was operated in the positive ion mode with a spray voltage of 5 kV or in the negative ion mode with a spray voltage of  $-4.5$  kV. Ion source gas 1, ion source gas 2 and curtain gas ( $\text{N}_2$ ) were set at pressures of 45, 50, 30 psi, respectively, and the source temperature was maintained at 600  $^\circ\text{C}$ . Samples (10  $\mu\text{L}$ ) were introduced into the mass spectrometer via the UFLC system by flow injection (no column) under isocratic conditions (50% A) at a flow rate of 0.3 mL/min. In positive ion mode, the mobile phase consisted of 0.1% formic acid in water (A) and 0.1% formic acid in acetonitrile (B). In negative ion mode, the mobile phase consisted of 5 mM DBAA in water (A) and acetonitrile with 0.2% DMIPA (B).

Full scan mass spectra were acquired over the range of  $m/z$  100–800 (except for thioestrepton, where the scan range was from  $m/z$  900–1700) with an accumulation time of 0.1 s. A data-dependent experiment collecting three product ion spectra (70 ms each) was also included. The total acquisition time was 1.5 min per sample and all four time-to-digital converter channels were used for detection. Samples were injected on three separate days in randomized order. The tripleTOF instrument was calibrated by an integrated calibration delivery system (AB Sciex) using the manufacturer's positive and negative calibration solutions, with an injection flow rate of 200–300  $\mu\text{L}/\text{min}$ . These calibrant ions were introduced via an orthogonal atmospheric pressure chemical ionization source together with mobile phase flow from the UFLC system. For sample analysis, calibration was performed every six samples. Mass spectral data acquisition and processing were performed using Analyst TF 1.5 (AB Sciex) and Peak View 1.1.1.2 software (AB Sciex).

SA% was calculated by MassWorks software (version 3.0.0, Cerno Bioscience, Danbury, CT, USA) using sCLIPS, which is a formula determination tool that first performs peak shape calibration and then matches the calibrated experimental isotope pattern against possible theoretical ones. The mass spectra were first converted into text files (.txt) and loaded sequentially into MassWorks for processing. The calculated ECs were ranked by decreasing SA% with the chemical elemental constraints ( $\text{C}_{1-100}\text{H}_{0-200}\text{N}_{0-50}\text{O}_{0-50}\text{F}_{0-5}\text{S}_{0-5}\text{Cl}_{0-5}\text{Br}_{0-5}$ )

further restricted by enabling empirical rules<sup>[23]</sup> and a mass tolerance of 5 ppm, except for thioestrepton in which the elements Cl and Br were excluded. The profile mass range was chosen to include the monoisotopic peak and all other isotope peaks, e.g.  $-0.5$  to  $3.5$   $m/z$  units (relative to monoisotopic mass) depending on the compound, and the calibration range was  $\pm 0.2$   $m/z$  units from the monoisotopic peak. Searching was limited to even-electron ions. The standard deviations (SDs) reported in Table 2 were calculated over the three replicate analyses.

## RESULTS

The results for the compounds analyzed will be described in three groups depending on the mass of the compound: group I <300 Da; group II >300 Da and <400 Da; group III >400 Da. When appropriate, specific compounds will be discussed in greater detail. SA%, SE%, mass error and resolving power ( $m/\Delta m$ , FWHM) for the compounds in each group are presented in Table 2.

### Group I: compounds <300 Da

There were eight compounds in group I. All except ketoprofen were analyzed using (+) ESI. SA% values ranged from  $96.77 \pm 0.41$  for diclofenac to  $99.15 \pm 0.03$  for trimeterene, based on triplicate measurements corresponding to SE% between 3.23 and 0.85, respectively. The mass errors were less than 3 ppm for all compounds and averaged  $1.59 \pm 0.24$  ppm. The distribution of SE and mass errors in mDa are illustrated in Fig. 1. The average resolving power ( $m/\Delta m$ ) for these eight compounds was 29082. All compounds in group I were ranked first based on having the highest SA% of the possible ECs consistent with the search parameters (Table 3). In contrast, if mass accuracy was used for ranking, only metoprolol and imipramine were ranked first with other compounds in this group ranging from 2 to 15. The difference in SA% between rank one and two averaged 2.66% for the compounds in group I.

### Group II: compounds >300 Da and <400 Da

There were eight compounds in group II. All except tenidap were analyzed using (+) ESI. SA% values ranged from  $98.25 \pm 0.25$  for tenidap to  $99.13 \pm 0.04$  for citalopram based on triplicate measurements, corresponding to SE% between 1.75 and 0.87, respectively. The mass errors were less than 2.5 ppm for all compounds and averaged  $1.48 \pm 0.28$  ppm. The average resolving power ( $m/\Delta m$ ) for these eight compounds was 31285. All compounds in group II were ranked first, based on having the highest SA% of the possible ECs consistent with the search parameters (Table 3). In contrast, if mass accuracy was used for ranking, no correct ECs were ranked first in this group. The difference in SA% between the top two ranks averaged 1.5% for the compounds in group II.

### Quinidine

The initial results for quinidine gave a SA% of  $86.57 \pm 0.26$ , which was significantly different from that for the other compounds in this group. Upon closer evaluation of the

**Table 2.** Spectral accuracy, spectral error, mass error and resolving power for compounds analyzed

Group	Compound	SA% ± SD	SE (%)	ppm	m/Δm
I	Carbamazepine	98.66 ± 0.03	1.33 ± 0.03	0.82	29 104
	Trimeterene	99.15 ± 0.03	0.85 ± 0.03	1.94	27 666
	Ketoprofen	97.49 ± 0.04	2.51 ± 0.04	2.89	30 097
	Propranolol	98.55 ± 0.22	1.45 ± 0.22	1.61	27 745
	Metoprolol	98.88 ± 0.20	1.12 ± 0.20	1.11	28 176
	Amitriptyline	97.81 ± 0.20	2.19 ± 0.20	2.07	29 736
	Imipramine	98.35 ± 0.30	1.65 ± 0.30	0.98	30 289
	Diclofenac	96.77 ± 0.41	3.23 ± 0.41	1.27	29 842
	Average	98.21 ± 0.59	1.79 ± 0.59	1.59	29 082
II	Tenidap	98.25 ± 0.25	1.75 ± 0.25	1.63	31 742
	Quinidine <sup>a</sup>	86.57 ± 0.26	13.43 ± 0.26	1.74	31 555
	Quinidine <sup>b</sup>	98.85 ± 0.05	1.15 ± 0.05	1.74	31 555
	Citalopram	99.13 ± 0.04	0.87 ± 0.04	2.44	29 700
	Omeprazole	99.09 ± 0.11	0.91 ± 0.11	0.23	30 454
	Meloxicam	99.10 ± 0.13	0.90 ± 0.13	2.20	31 281
	Oxybutynin	98.98 ± 0.08	1.02 ± 0.08	1.90	32 011
	Prochlorperazine	98.82 ± 0.01	1.18 ± 0.01	0.60	31 332
	Prazosin	99.07 ± 0.06	0.93 ± 0.06	1.06	31 936
	Average	98.91 ± 0.29	1.09 ± 0.29	1.50	31 285
III	Trifluoperazine	99.27 ± 0.09	0.73 ± 0.09	0.83	32 329
	Ziprasidone	96.61 ± 0.92	3.39 ± 0.92	0.34	32 129
	Troglitazone <sup>a</sup>	86.97 ± 3.66	13.03 ± 3.66	1.48	30 925
	Troglitazone <sup>b</sup>	97.13 ± 0.10	2.87 ± 0.10	1.48	30 925
	Verapamil	98.99 ± 0.09	1.01 ± 0.09	2.06	31 651
	Nicardipine	99.15 ± 0.03	0.85 ± 0.03	0.15	32 661
	7-Hydroxytaurosp	99.04 ± 0.19	0.96 ± 0.19	2.16	31 590
	Ketoconazole	98.53 ± 0.17	1.47 ± 0.17	1.35	33 089
	Moxidectin	98.09 ± 0.37	1.91 ± 0.37	0.88	37 974
	Itraconazole	98.19 ± 0.32	1.81 ± 0.32	0.73	34 390
	Average	98.33 ± 0.94	1.67 ± 0.94	1.15	32 766
	Thiostrepton <sup>c</sup>	97.86 ± 0.83	2.14 ± 0.83	0.68	39 416
	Thiostrepton <sup>d</sup>	95.77 ± 1.30	4.23 ± 1.30	1.08	39 416

<sup>a</sup>Excluded from average; <sup>b</sup>mixture search; <sup>c</sup>best case n = 3; <sup>d</sup>n = 9. SD = standard deviation.

spectrum, it appeared that the A+2 isotope peak was slightly higher than expected (Fig. 2). A subsequent sCLIPS search was performed which allowed for the possibility that quinidine and dihydroquinidine (+2 hydrogens) were present as a mixture. A mixture search fitted the observed isotope pattern with more than one elemental composition. SA% for quinidine in this mixture search improved by over 10% to 98.85 ± 0.05.

### Group III: compounds >400 Da

There were ten compounds in group III, which comprised eight small molecules and two natural products. All except moxidectin were analyzed using (+) ESI. SA% values ranged from 96.61 ± 0.92 for ziprasidone to 99.27 ± 0.09 for trifluoperazine, based on triplicate measurements, corresponding to SE% between 3.39 and 0.73, respectively. The mass errors were less than 2.2 ppm for all the compounds and averaged 1.01 ± 0.24 ppm. The average resolving power (m/Δm) for these ten compounds was 33 875. In group III, all replicates of trifluoperazine, ziprasidone, verapamil, and nicardipine were ranked first, based on having the

highest SA% of the possible ECs consistent with the search parameters. Except for thiostrepton, which is discussed below, all the other compounds in group III were not ranked first for all replicates although no compound ranked lower than 5<sup>th</sup> place. For example, itraconazole was ranked in place one, two or five for the three replicates. In contrast, if mass accuracy was used for ranking, only nicardipine and ziprasidone were ranked in the top ten, with the other compounds ranked between 15 and 266. Except for thiostrepton, the difference in SA% between the top two ranks was less than 1% and averaged 0.47% for the compounds in this group.

#### Troglitazone

Initial results for troglitazone revealed a SA% of 86.97 ± 3.66, which was significantly different from that for the other compounds in the group. Upon closer evaluation of the spectrum, it appeared that there were two peaks lower in mass by one and two hydrogens (Fig. 3). A subsequent sCLIPS search was performed which allowed for the possibility that troglitazone and oxidized troglitazones with

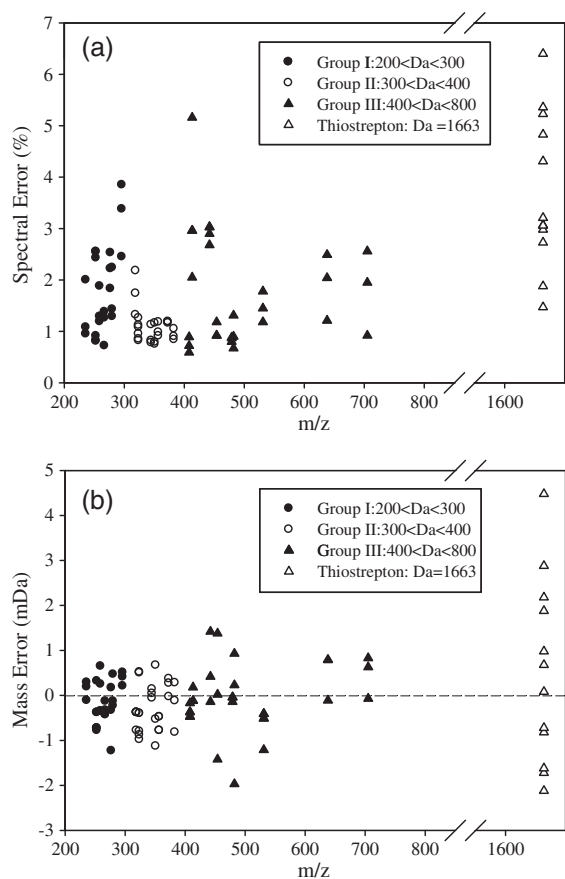


**Figure 1.** Mass errors in mDa (a) and spectral errors (SE%) (b) for compounds in groups I, II and III.

either 1 or 2 fewer hydrogens were present as a mixture. SA% for troglitazone in this mixture search improved by over 10% to  $97.13 \pm 0.10$ .

#### Thiostrepton

The highest mass compound analyzed, the natural product thiostrepton, posed some challenges when performing the sCLIPS calculations. When using our standard elemental and mass accuracy constraints, the number of possible ECs was found to be more than 146 000. Processing took several hours but was never completed before the program aborted. To overcome this problem, the elements Cl and Br were excluded and subsequent calculations generated about 7500 possible ECs. Although the first thiostrepton sample analyzed showed a very good SA% (98.53) and the correct EC tied for first place out of 7484 possible ECs, subsequent replicates had SA% values which were as much as 3% lower. Due to this variability, we carried out an additional six replicate analyses to get a better estimate of SA%. Again, of these six replicates only one sample was found to have a SA% of 98.12 and the variability remained larger than was observed for the other compounds (average SA% =  $95.88 \pm 1.28$ ). The best ranking of thiostrepton was place one, five or ten for the three best SA% values obtained. However, for the other thiostrepton samples with lower SA%, rankings were in the hundreds (68–985) or even in the thousands (1035).

## DISCUSSION

An early study by Ibanez and coworkers on a Q-TOF mass spectrometer noted that the accuracy of relative isotope abundance measurements was approximately 20% although the errors could be as high as 50% or less than 10%, depending on the ion intensity.<sup>[24]</sup> A more recent study by Abate and coworkers reported that the overall accuracies for the  $[A+1]/A$  and  $[A+2]/A$  isotope ratios for 344 species were  $2.6 \pm 2.5\%$  and  $2.1 \pm 2.6\%$ , respectively.<sup>[13]</sup> In our investigation, the overall fidelity for the measurement of protonated (or deprotonated) molecules was determined on a new oaQ-TOF mass spectrometer. To accomplish this objective, we obtained a set of small molecules and two natural products with a diverse set of ECs and used the sCLIPS algorithm to determine SA% of each protonated (or deprotonated) molecule. SA% (or SE% =  $100\% - SA\%$ ) is a measure of the overall goodness-of-fit between an observed and a theoretical protonated (or deprotonated) molecule for a given EC and thus considers not only the measured accurate mass of the monoisotopic peak, but also the relative abundances of the isotopic peaks (A+1, A+2, A+3, etc.). Based on the compounds that we measured, the results demonstrate that SA% averages better than 98% for an average SE% of 1.6%. The mass errors of the protonated (or deprotonated) molecules were also determined and it was found that on average the mass errors were better than 2.5 ppm. These findings indicate that the AB Sciex 5600 Q-TOF instrument meets the conditions suggested by Kind and Fiehn who predict that a mass spectrometer with both mass errors better than 3 ppm and isotope abundance accuracies of about 2% should outperform a mass spectrometer which has higher mass accuracy but which does not consider isotopic abundances for EC determination.<sup>[9]</sup> In contrast to the observations of Bristow and coworkers who found on a Bruker microQ-TOF mass spectrometer that simple isotope patterns (C, H, N, F, O) had higher ranking (i.e. better quality isotope pattern match),<sup>[25]</sup> our data indicates that SA% was not influenced by the presence of heteroatom(s) in the molecule. Specifically, the fifteen compounds in this study without heteroatoms had an average SA% of  $98.68 \pm 0.52\%$  compared with the twelve compounds with heteroatoms (Cl, Br, or S) which had an average SA% of  $98.16 \pm 0.95\%$  – not statistically different.

Limited elemental constraints and a 5 ppm mass tolerance were used for the EC determination. For compounds with masses between 236 and 412 Da, which included all compounds in groups I and II, the correct EC was ranked first out of as few as 20 (e.g. oxybutynin) to as many as 168 (e.g. ziprasidone) formulae. In contrast to SA%, when mass accuracy was used for ranking, only for two compounds in group I was the correct EC ranked first, as shown in Table 3. The significance of a large difference in SA% between the first and second hit compared with the standard deviation of the measurement is that it increases confidence in the top hit. For compounds in group I, the differences between the first and second rank were, as shown in Table 3, typically greater than 1% and as high as 4% (e.g. imipramine), which is about 5–10 times the standard deviation. For group II compounds, the difference between the first and second rank was still more than 1% but for compounds in group III this averaged much less than 1% and although the correct EC was ranked first at least in one analysis, at times the rank was two, three,

**Table 3.** Ranking of compounds elemental composition based on spectral or mass error

Group	Compound	Rank (spectral error)	N <sup>a</sup>	SA% (1st - 2nd)	Formulae with SA ≥ 98%	Formulae with SA ≥ 95%	Rank (mass error)
I	Carbamazepine	1	8	3.71	1	1	2
	Trimeterene	1	10	1.02	2	4	7
	Ketoprofen	1	13	1.56	0	3	3
	Propranolol	1	9	3.53	1	1	3
	Metoprolol	1	5	2.43	1	3	1
	Amitriptyline	1	8	2.30	0	2	5
	Imipramine	1	7	4.14	1	2	1
	Diclofenac	1	38	2.57	0	1	15
	Average	1	12	2.66	1	2	5
II	Tenidap	1	83	1.64	1	6	22
	Quinidine	1	24	0.84	0	0	9
	Quinidine <sup>b</sup>	1	24	3.07	1	2	9
	Citalopram	1	29	2.53	1	3	8
	Omeprazole	1	48	2.49	1	5	2
	Meloxicam	1	89	1.67	2	7	33
	Oxybutynin	1	20	1.05	2	4	7
	Prochlorperazine	1	66	1.85	1	2	2
	Prazosin	1	66	0.66	3	7	5
Average	1	46	1.77	1	4	11	
III	Trifluoperazine	1	91	0.58	2	7	16
	Ziprasidone	1	168	0.55	0	2	7
	Troglitazone	1,2 or 4	162	0.12	0	0	15
	Troglitazone <sup>b</sup>	1 or 2	684	0.32	0	9	15
	Verapamil	1	89	0.70	2	7	51
	Nicardipine	1	194	0.59	4	13	5
	OH-taurosporine	1	253	0.93	2	9	24
	Ketoconazole	1, 2 or 3	590	0.30	3	12	266
	Moxidectin	1 or 4	527	0.50	2	24	16
	Itraconazole	1, 3 or 5	2121	0.14	4	32	44
	Average	N/A	488	0.47	2	12	46
	Thiostrepton <sup>c</sup>	1, 5 or 10	7491	0.04	0–36	273–330	68
Thiostrepton <sup>d</sup>	68–1035	7498	N/A	0–48	198–656	1452	

<sup>a</sup>N = number of ECs obtained following the search; <sup>b</sup>mixture search; <sup>c</sup>best case n = 3; <sup>d</sup>n = 9.

four or even five. This indicates that slight variations in the spectral data quality can have an impact on SA% and be enough to alter the rank, especially when the number of possible ECs is in the hundreds or thousands (e.g. itraconazole, thiostrepton). Böcker and coworkers also divided the 86 compound spectra in their data set, acquired on a MicroQ-TOF from Bruker, into groups and showed a similar trend to ours with respect to correct ranking and mass.<sup>[22]</sup> For compounds with masses 200–300 Da or 300–400 Da, the correct EC was ranked first for every compound except one. However, of the ten compounds with mass 500–600 Da, only seven were ranked first and of three compounds with mass 800–900 Da, only two were ranked first.

Initially, SA% of both quinidine and troglitazone was determined to be approximately 87% and this led to further investigation of these two compounds since this was much lower than for the other compounds. Dihydroquinidine is the reduced form of quinidine that is present in various amounts in commercially available sources.<sup>[26]</sup> Thus, we next calculated SA% based on a mixture of quinidine and dihydroquinidine and this increased SA% to >98%. Moreover,

our analysis indicated that the amount of dihydroquinidine was approximately 11%, consistent with literature reports.<sup>[27]</sup> Figure 2 shows the increased intensity of the A+2 peak of quinidine due to the contribution of the monoisotopic peak of dihydroquinidine. Troglitazone can undergo oxidative metabolism on the chromane system to form a quinone metabolite (loss of two hydrogen atoms). Electrochemical oxidation, which can occur during ESI, also readily generated this quinone.<sup>[28]</sup> Furthermore, generation of a radical with loss of a single hydrogen atom has also been reported.<sup>[29]</sup> Thus, we calculated SA% based on a mixture of troglitazone/oxidized troglitazone with loss of one and two hydrogen atoms and this increased SA% to >97%. Although initially overlooked due to their low abundance, a closer examination of protonated troglitazone revealed two peaks, 1 and 2 Da lower than the monoisotopic peak of troglitazone. Figure 3 shows that the change in the monoisotopic peak of troglitazone due to the presence of these other species significantly reduces SA% although their absolute intensity is low. In a previous investigation on an orbitrap in which both rifampicin and its quinone oxidation product were present



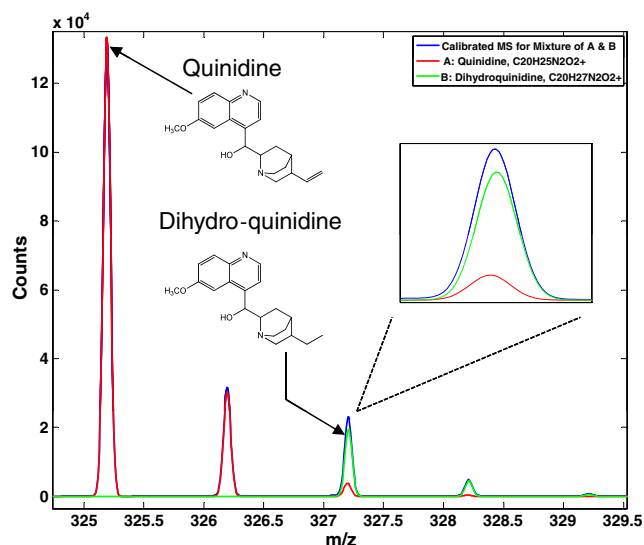


**Figure 2.** Spectrum of quinidine (red) with a small amount of dihydroquinidine (+2  $m/z$  units, green) detected as a minor component. The observed spectrum (blue) is a summation of these two components. Dihydroquinidine increases the abundance of the A+2 isotope peak of quinidine as can be seen clearly in the insert. Note that the resolution of the spectrum was set to 0.7  $m/z$  units (FWHM) for illustrative purposes.

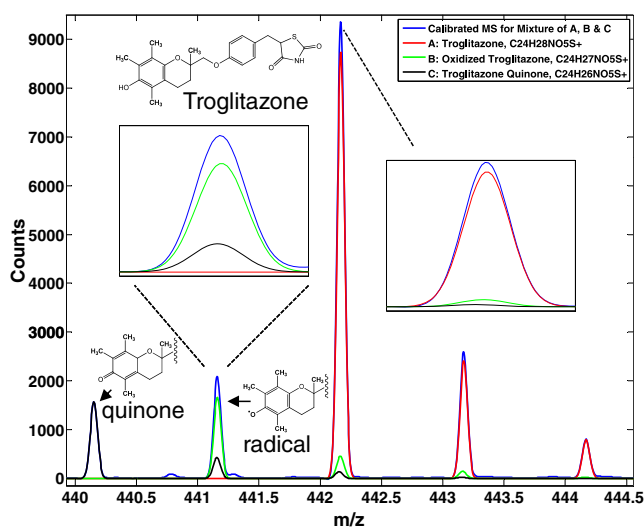


**Figure 3.** Spectrum of troglitazone (red) with smaller amounts of troglitazone quinone ( $-2 m/z$  units, black) and oxidized troglitazone ( $-1 m/z$  unit, green) detected as a minor components. The observed spectrum (blue) is a summation of these three components. The monoisotopic isotope peaks of oxidized troglitazone and troglitazone are increased slightly because of the presence of these components as can be seen clearly in the insert. Note that the resolution of the spectrum was set to 0.7  $m/z$  units (FWHM) for illustrative purposes.

together in a commercially available source, SA% also improved when a mixture search was performed, although the improvement ( $\sim 1\%$ ) was much smaller than the 10% improvements observed here.<sup>[21]</sup> These examples demonstrate that SA% determinations can point the investigator towards additional structural information and chemical insight into the analyte that might otherwise be easily overlooked.

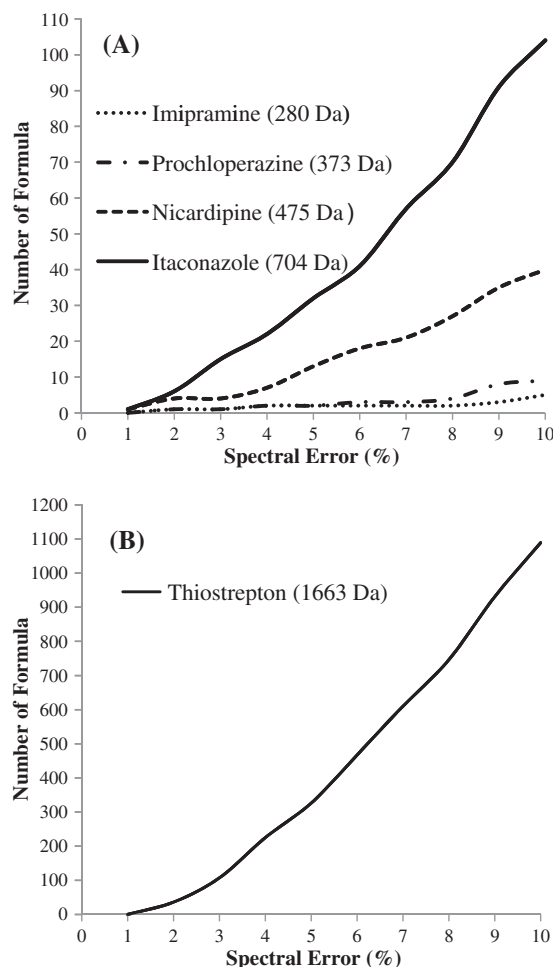


**Figure 4.** (a) Relationship between SE% and number of ECs for imipramine, prochlorperazine and itraconazole as representative compounds of groups I, II and III, respectively. (b) Relationship between SE% and number of ECs for thioestrepton, which shows that when the SE% increases above approximately 3%, the number of ECs is in the hundreds.

In similar experiments to ours on an LTQ/Orbitrap-XL instrument, SA% values of ten natural products were determined at five different RP settings.<sup>[21]</sup> At a RP setting of 30 000, equivalent to the RP obtained on the present Q-TOF instrument, SE% values ranged from 1.62 to 3.8%. Fortunately, a direct comparison of SE% for two compounds is possible: moxidectin 2.11% vs. 1.9% and thioestrepton 3.1% vs. 3.7% on the Orbitrap and Q-TOF, respectively. However, at lower RP settings on the LTQ/Orbitrap-XL, the SE% values were better than on the Q-TOF: 1.58% for moxidectin at 15 000; 2.38% and 1.41% for thioestrepton at 15 000 and 7500, respectively. At higher RP settings (i.e. 60 000 and 100 000), SA% was shown to decrease on the orbitrap, especially with compounds, such as thioestrepton, possessing extensive fine structure. This was manifested as decreasing isotope abundances in the higher isotope peaks (i.e. A+3, A+4, A+5 ...). Erve and coworkers suggested that destructive interference between isotopic fine structure components that can occur in FTICR instruments accounts for these decreased isotopic abundances and hence lower SA%.<sup>[21]</sup> Although the Q-TOF would not be expected to



be subject to these effects, thiostrepton displayed a better SE% (3.59) on the orbitrap at 60 000 RP and was only worse than the Q-TOF at 100 000 RP (SE% = 5.64). It is not clear why the Q-TOF used in this study could not provide SA% values consistently of the order of 98% for thiostrepton.

The findings with thiostrepton best illustrate the importance of having a high SA% when the mass of the compound increases. With the best SE% values obtained, namely 1.47, 1.88 and 3.06, thiostrepton did rank among the top ten ECs (among >7400 ECs). However, for unknown reasons, this SE% was not consistently obtained and the greater SE% resulted in thiostrepton rankings in the hundreds or even thousands. Employing a lower mass tolerance of 2.7 ppm in the sCLIPS search could not improve the rankings enough to make them truly useful (data not shown). The relationship between the number of possible ECs and SE% is further illustrated in Fig. 4(a) using imipramine (group I), prochlorperazine (group II), itraconazole (group III) and Fig. 4(b) with thiostrepton (group III) as examples. With groups I and II, significantly greater SEs (up to 10%) could be tolerated and still only give rise to a small number of ECs. However, as the mass increases, especially above 600 Da, having SE% <2 becomes extremely important both for ranking of and confidence in EC findings.

## CONCLUSIONS

Determination of elemental composition (EC) for unknowns remains an analytical challenge and a strategy involving SA% determination on a mass spectrometer with high fidelity of isotope measurement capability (<3% SE), such as the AB Sciex 5600 Q-TOF, should be a powerful tool. For analytes with mass <400 Da, ranking based on SA% produced the top hit exclusively. Only with masses >400 Da did the rankings become more variable although, except for thiostrepton, the rank was always in the top ten. SA% determinations in our work were based on commercially available compounds and thus ion intensity was not an issue as the full isotope profile was readily observed. Although we did not systematically investigate the influence of ion intensity on SA%, others have reported that ion intensity is a major factor influencing overall quality of isotope ratio measurements.<sup>[13,19,25]</sup> For this reason, the SA% values that we obtained should be considered as a 'best case' scenario and for real-world applications, such as metabolite identification in complex biological matrices, SA% could be lower due to (1) insufficient ion intensity and/or (2) matrix peaks overlapping the isotopic profile of interest. Importantly, we also demonstrated that SA% determinations can alert the investigator when the analyte under investigation may exist as a mixture (1) due to the presence of structurally related components (e.g. dihydroquinidine) or (2) due to chemical or metabolic oxidation (e.g. troglitazone). In addition, this analysis may provide quantitative estimates as to the components of the mixture when the components are similar structurally. The results of our work demonstrate the utility of SA and should encourage manufacturers of mass spectrometers to determine the specifications of not only the mass accuracy, but also the spectral accuracy of their instruments.

## Acknowledgements

We thank AB Sciex and Shimadzu for kindly lending the mass spectrometer and UFLC system used in this study. We thank Dr Yongdong Wang of Cerno Biosciences for creating Figs. 2 and 3 as well as helpful discussions on spectral accuracy.

## REFERENCES

- [1] S. Ojanpera, A. Pelander, M. Pelzing, I. Krebs, E. Vuori, I. Ojanpera. Isotopic pattern and accurate mass determination in urine drug screening by liquid chromatography/time-of-flight mass spectrometry. *Rapid Commun. Mass Spectrom.* **2006**, *20*, 1161.
- [2] S. Hudson, J. Ramsey, L. King, S. Timbers, S. Maynard, P. I. Dargan, D. M. Wood. Use of high-resolution accurate mass spectrometry to detect reported and previously unreported cannabinomimetics in "herbal high" products. *J. Anal. Toxicol.* **2010**, *34*, 252.
- [3] I. Ferrer, E. M. Thurman. Existence and use of accurate mass databases and elemental composition tools for target and non-target analyses. *Chem. Anal.* **2009**, *173*, 57.
- [4] A. G. Marshall, R. P. Rodgers. Petroleomics: chemistry of the underworld. *Proc. Natl. Acad. Sci. USA.* **2008**, *105*, 18090.
- [5] T. Kind, O. Fiehn. Seven Golden Rules for heuristic filtering of molecular formulas obtained by accurate mass spectrometry. *BMC Bioinformatics* **2007**, *8*, 105.
- [6] A. M. Starrett, G. C. DiDonato. High resolution accurate mass measurement of product ions formed in an electrospray source on a sector instrument. *Rapid Commun. Mass Spectrom.* **1993**, *7*, 12.
- [7] S. Kim, R. P. Rodgers, A. G. Marshall. Truly "exact" mass: Elemental composition can be determined uniquely from molecular mass measurement at ~0.1 mDa accuracy for molecules up to ~500 Da. *Int. J. Mass Spectrom.* **2006**, *251*, 260.
- [8] R. A. Zubarev, P. Hakansson, B. Sundqvist. Accuracy requirements for peptide characterization by monoisotopic molecular mass measurements. *Anal. Chem.* **1996**, *68*, 4060.
- [9] T. Kind, O. Fiehn. Metabolomic database annotations via query of elemental compositions: mass accuracy is insufficient even at less than 1 ppm. *BMC Bioinformatics* **2006**, *7*, 234.
- [10] S. Suzuki, T. Ishii, A. Yasuhara, S. Sakai. Method for the elucidation of the elemental composition of low molecular mass chemicals using exact masses of product ions and neutral losses: Application to environmental chemicals measured by liquid chromatography with hybrid quadrupole/time-of-flight mass spectrometry. *Rapid Commun. Mass Spectrom.* **2005**, *19*, 3500.
- [11] M. Rojas-Cherto, P. T. Kasper, E. L. Willighagen, R. J. Vreeken, T. Hankemeier, T. H. Reijmers. Elemental composition determination based on MS<sup>n</sup>. *Bioinformatics* **2011**, *27*, 2376.
- [12] A. H. Grange, G. W. Sovocool. Ion compositions determined with increasing simplicity. *Chem. Anal.* **2009**, *173*, 35.
- [13] S. Abate, Y. G. Ahn, T. Kind, T. R. I. Cataldi, O. Fiehn. Determination of elemental compositions by gas chromatography/time-of-flight mass spectrometry using chemical and electron ionization. *Rapid Commun. Mass Spectrom.* **2010**, *24*, 1172.
- [14] K. F. Blom. Enhanced selectivity in determining elemental composition: concerted precise mass and isotope pattern moment analysis. *Org. Mass Spectrom.* **1988**, *23*, 783.
- [15] A. H. Grange, M. C. Zumwalt, G. W. Sovocool. Determination of ion and neutral loss compositions and deconvolution of product ion mass spectra using an orthogonal acceleration time-of-flight mass spectrometer and an ion correlation program. *Rapid Commun. Mass Spectrom.* **2006**, *20*, 89.
- [16] A. Kaufmann. Determination of the elemental composition of trace analytes in complex matrices using exact masses

- of product ions and corresponding neutral losses. *Rapid Commun. Mass Spectrom.* **2007**, *21*, 2003.
- [17] M. Meringer, S. Reinker, J. Zhang, A. Muller. MS/MS data improves automated determination of molecular formulas by mass spectrometry. *MATCH* **2011**, *65*, 259.
- [18] Y. Xu, J. F. Heilier, G. Madalinski, E. Genin, E. Ezan, J. C. Tabet, C. Junot. Evaluation of accurate mass and relative isotopic abundance measurements in the LTQ-Orbitrap mass spectrometer for further metabolomics database building. *Anal. Chem.* **2010**, *82*, 5490.
- [19] R. J. M. Weber, A. D. Southam, U. Sommer, M. R. Viant. Characterization of isotopic abundance measurements in high resolution FT-ICR and orbitrap mass spectra for improved confidence of metabolite identification. *Anal. Chem.* **2011**, *83*, 3737.
- [20] Y. Wang, M. Gu. The concept of spectral accuracy for MS. *Anal. Chem.* **2010**, *82*, 7055.
- [21] J. C. L. Erve, M. Gu, Y. Wang, W. DeMaio, R. E. Talaat. Spectral accuracy of molecular ions in an LTQ/Orbitrap mass spectrometer and implications for elemental composition determination. *J. Am. Soc. Mass Spectrom.* **2009**, *20*, 2058.
- [22] S. Böcker, M. C. Letzel, Z. Liptak, A. Pervukhin. SIRIUS: decomposing isotope patterns for metabolite identification. *Bioinformatics* **2009**, *25*, 218.
- [23] M. Gu. Enhancing mass spectral formula determination by heuristic rules. *LCGC North Am.* **2010**, *42*.
- [24] M. Ibanez, J. V. Sancho, O. J. Pozo, W. Niessen, F. Hernandez. Use of quadrupole time-of-flight mass spectrometry in the elucidation of unknown compounds present in environmental water. *Rapid Commun. Mass Spectrom.* **2005**, *19*, 169.
- [25] T. Bristow, J. Constantine, M. Harrison, F. Cavoit. Performance optimisation of a new-generation orthogonal-acceleration quadrupole-time-of-flight mass spectrometer. *Rapid Commun. Mass Spectrom.* **2008**, *22*, 1213.
- [26] M. S. Ching, C. L. Blake, H. Ghabrial, S. W. Ellis, M. S. Lennard, G. T. Tucker, R. A. Smallwood. Potent inhibition of yeast-expressed CYP2D6 by dihydroquinidine, quinidine, and its metabolites. *Biochem. Pharmacol.* **1995**, *50*, 833.
- [27] K. A. Thompson, J. J. Murray, I. A. Blair, R. L. Woosley, D. M. Roden. Plasma concentrations of quinidine, its major metabolites, and dihydroquinidine in patients with torsades de pointes. *Clin. Pharmacol. Ther.* **1988**, *43*, 636.
- [28] K. G. Madsen, G. Groenberg, C. Skonberg, U. Jurva, S. H. Hansen, J. Olsen. Electrochemical oxidation of troglitazone: Identification and characterization of the major reactive metabolite in liver microsomes. *Chem. Res. Toxicol.* **2008**, *21*, 2035.
- [29] K. He, R. E. Talaat, W. F. Pool, M. D. Reily, J. E. Reed, A. J. Bridges, T. F. Woolf. Metabolic activation of troglitazone: Identification of a reactive metabolite and mechanisms involved. *Drug Metab. Dispos.* **2004**, *32*, 639.



# Characterization of sulfur compounds in whisky by full evaporation dynamic headspace and selectable one-dimensional/two-dimensional retention time locked gas chromatography–mass spectrometry with simultaneous element-specific detection

Nobuo Ochiai<sup>a,\*</sup>, Kikuo Sasamoto<sup>a</sup>, Kevin MacNamara<sup>b</sup>

<sup>a</sup> GERSTEL K.K., 1-3-1 Nakane, Meguro-ku, Tokyo 152-0031, Japan

<sup>b</sup> Aubrey-16, Seanchill, Dublin 18, Ireland

## ARTICLE INFO

### Article history:

Received 26 August 2012

Received in revised form 30 October 2012

Accepted 1 November 2012

Available online 8 November 2012

### Keywords:

Whisky

Sulfur compounds

Full evaporation dynamic headspace (FEDHS)

Selectable <sup>1</sup>D/<sup>2</sup>D RTL GC–MS

Element-specific detection

Principal component analysis (PCA)

## ABSTRACT

A method is described for characterization of sulfur compounds in unaged and aged whisky. The method is based on full evaporation dynamic headspace (FEDHS) of 100  $\mu$ L of whisky samples followed by selectable one-dimensional (<sup>1</sup>D) or two-dimensional (<sup>2</sup>D) retention-time-locked (RTL) gas chromatography (GC)–mass spectrometry (MS) with simultaneous element-specific detection using a sulfur chemiluminescence detector (SCD) and a nitrogen chemiluminescence detector (NCD). Sequential heart-cuts of the 16 sulfur fractions were used to identify each individual sulfur compound in the unaged whisky. Twenty sulfur compounds were positively identified by a MS library search, linear retention indices (LRI), and formula identification using MS calibration software. Additionally eight formulas were also identified for unknown sulfur compounds. Simultaneous heart-cuts of the 16 sulfur fractions were used to produce the <sup>2</sup>D RTL GC–SCD chromatograms for principal component analysis. PCA of the <sup>2</sup>D RTL GC–SCD data clearly demonstrated the difference between unaged and aged whisky, as well as two different whisky samples. Fourteen sulfur compounds could be characterized as key sulfur compounds responsible for the changes in the aging step and/or the difference between two kinds of whisky samples. The determined values of the key sulfur compounds were in the range of 0.3–210  $\text{ng mL}^{-1}$  (RSD: 0.37–12%,  $n = 3$ ).

© 2012 Elsevier B.V. All rights reserved.

## 1. Introduction

Sulfur compounds in alcoholic beverages such as wine, beer, and spirits are of particular interest because of their low sensory threshold and possible resulting effect on product flavor [1–5]. Moreover, the presence of several medium and high boiling sulfur compounds can improve the flavor. These sulfur compounds have hydrophilic properties and are present at  $\text{ng mL}^{-1}$  levels in complex matrices, which include several high concentration compounds ( $\mu\text{g mL}^{-1}$  levels) such as fusel alcohols, fatty acids, and esters. Therefore, in order to analyze sulfur compounds in those alcoholic beverages, it is essential to have powerful extraction and enrichment steps before gas chromatographic analysis. Although liquid–liquid extraction (LLE) has been the most widely used technique, LLE is tedious, time consuming, labor intensive, and requires large amounts of organic solvents. Headspace techniques, e.g. static headspace (SHS), dynamic headspace (DHS), and headspace solid

phase microextraction (HS–SPME), have been frequently used in analysis of sulfur compounds in wine because they are simple, solvent-less, and (can be) fully automated [1]. However, these techniques are generally more selective for more volatile and/or hydrophobic compounds. In 2012, a full evaporation dynamic headspace (FEDHS) method, based on a classical full evaporation technique (FET) developed by Markelov and Guzowski in 1993 [6], was demonstrated for uniform enrichment of odor compounds including hydrophilic sulfur compounds (e.g. 2-acetylthiazole and 2-formylthiophene) in aqueous samples at  $\text{ng mL}^{-1}$  levels [7]. By using FEDHS of 100  $\mu$ L of aqueous sample at 80 °C, a wide range of odor compounds with different polarities could be uniformly recovered (>85%) in contrast with conventional DHS and HS–SPME, while leaving most of the low volatile matrix behind [8].

Several authors reported that gas chromatography–mass spectrometry (GC–MS) in combination with simultaneous selective detection is a powerful tool for the identification of sulfur compounds [1]. Bouchilloux et al. demonstrated combinations of GC with olfactometry, flame photometry, and MS for identification of three aromatic thiols in red wine [9]. In certain cases, identification of trace sulfur compounds in complex samples by GC–MS with

\* Corresponding author. Tel.: +81 3 5731 5321; fax: +81 3 5731 5322.  
E-mail address: [nobuo.ochiai@gerstel.co.jp](mailto:nobuo.ochiai@gerstel.co.jp) (N. Ochiai).

simultaneous selective detection can be challenging because co-elution interferes with mass spectral identification of individual compounds. A more effective way to improve the identification capability and separation resolution is through two-dimensional ( $^2D$ ) GC with simultaneous mass spectrometric and selective detection. There are two established  $^2D$  GC approaches: heart-cutting  $^2D$  GC (GC–GC) [10,11] and comprehensive  $^2D$  GC (GC  $\times$  GC) [10,12]. The former approach is commonly used in target analysis of specific compounds in a sample. The latter approach is mainly used in exhaustive analysis of a sample for total profiling. Although several injections are often required for the identification of multiple target compounds, heart-cutting  $^2D$  GC–MS with simultaneous selective detection has higher ability to obtain a clean mass spectrum for each target peak because of a much longer second column and proper temperature programming, resulting in higher peak capacity and sample capacity in the second dimensional separation compared to GC  $\times$  GC. Heart-cutting  $^2D$  GC–MS in combination with a sulfur chemiluminescence detector (SCD) and nitrogen chemiluminescence detector (NCD) was successfully applied for analysis of trace sulfur and nitrogen compounds in whisky [13–15]. Recently, a novel selectable one-dimensional ( $^1D$ ) or  $^2D$  GC–MS ( $^1D/^2D$  GC–MS) with simultaneous selective detection was demonstrated for simple and fast operation of both  $^1D$  GC–MS and  $^2D$  GC–MS using GC equipped with LTM-technology in combination with single quadrupole MS [8,16,17]. With this system, simultaneous mass spectrometric and selective detection can be performed for both  $^1D$  GC and  $^2D$  GC separations, without any instrumental set-up change. Therefore, the selection and confirmation of target compounds in  $^2D$  GC analysis can be easily performed with both mass spectral and olfactometric/element-specific information.

In this study, a combined approach consisting of FEDHS,  $^1D/^2D$  GC–MS with SCD and NCD for characterization of sulfur compounds in two kinds of unaged and aged whisky is described.

## 2. Experimental

### 2.1. Reagents and materials

4,5-Dimethyl-1,3-thiazole, ethyl 2-methyl sulfanyl acetate, ethyl 3-methyl sulfanyl propanoate, 1-(1,3-thiazol-2-yl)ethanone (2-acetyl thiazole), 3-methylthiophene-2-carbaldehyde (3-methyl-2-formylthiophene), 5-methylthiophene-2-carbaldehyde (5-methyl-2-formylthiophene), (methyltrisulfanyl)methane (dimethyl trisulfide), thiophene-2-carbaldehyde (2-formyl thiophene), 1-thiophen-2-ylethanone (2-acetyl thiophene), and 1-thiophen-3-ylethanone (3-acetyl thiophene) were kindly obtained from Dr. Katsumi Umamo of Takata Koryo Co., Ltd. (Hyogo, Japan).

Two kinds of malt whisky (“A” from Speyside, Scotland and “G” from Highland, Scotland), unaged and 15 years old, were used for the analysis. Both whiskies were of the “single malt” variety, i.e. produced exclusively in the same distillery and not a mixture of malt whiskies from different distilleries. The unaged whisky was at 65% (v/v) ethanol. The aged whisky was at 40% (v/v) ethanol.

### 2.2. Instrumentation

FEDHS was performed using a GERSTEL DHS module (GERSTEL, Mülheim an der Ruhr, Germany) that enables dynamic purging of the headspace above a sample combined with trapping of purged analytes on an adsorbent trap using a dual-needle design [18]. The trapped compounds were subsequently analyzed by thermal desorption (TD)- $^1D/^2D$  GC–SCD/NCD/MS using a MPS2 robotic arm and a TDU thermal desorption unit placed on top of a CIS4 programmable temperature vaporizing (PTV) inlet (GERSTEL). The Agilent 7890 gas chromatograph (host GC) was equipped with

a CTS2 cryo-trap system from GERSTEL, a dual LTM–GC system (Agilent), a SCD (Agilent) and a NCD (Agilent). A 5975C mass spectrometer from Agilent was used. The dual LTM–GC–SCD/NCD/MS system was configured as  $^1D/^2D$  GC–MS with simultaneous selective detection previously described [16], which enables simple and fast operation of both  $^1D$  GC–MS and  $^2D$  GC–MS with simultaneous selective detection without any instrumental setup change.

The  $^1D/^2D$  GC–SCD/NCD/MS system was equipped with dual wide format LTM–GC column modules (5 in.; 1 in. = 2.54 cm), an Agilent capillary flow technology (CFT) Deans switch, a 2-Way splitter and a 3-way splitter (with make-up gas line), which were controlled with a pressure control module (PCM). PCM has two pressure control capabilities. One is called PCM (main) and the other is called Auxiliary (AUX).

### 2.3. Sample preparation

One hundred micro-liters of whisky sample were transferred into an empty 10 mL screw cap headspace vial. No further sample preparation was necessary.

### 2.4. FEDHS and thermal desorption (TD)

For FEDHS, samples were transferred from the sample tray to the DHS module at 80 °C. Analytes in the headspace vial were immediately purged with 3 L of nitrogen gas at a flow rate of 100 mL min<sup>−1</sup> and trapped at 40 °C on a TDU tube packed with Tenax TA. The TDU tube was transported to, and subsequently desorbed in the TDU. The TDU was programmed from 30 °C (held for 0.5 min) to 240 °C (held for 3 min) at 720 °C min<sup>−1</sup> with 50 mL min<sup>−1</sup> desorption flow. Desorbed compounds were focused at 10 °C on a Tenax TA packed liner in the PTV inlet. After desorption, the PTV inlet was programmed from 10 °C to 240 °C (held for GC run time) at 720 °C min<sup>−1</sup> to inject trapped compounds onto the analytical column. The injection was performed in the split mode with a split ratio of 1–1 using the low split option (Gerstel KK, Tokyo, Japan) controlled by the pneumatic box of the TDU system.

### 2.5. Selectable $^1D/RTL$ $^2D$ RTL GC–SCD/NCD/MS

Separations were performed on a 30 m, 0.25 mm i.d., 1.0  $\mu$ m film thickness DB-1 column (Agilent) as the first dimensional ( $^1D$ ) column and a 30 m, 0.25 mm i.d., 0.25  $\mu$ m film thickness DB-Wax column (Agilent) as the second dimensional ( $^2D$ ) column. The column temperature for the  $^1D$  DB-1 was programmed from 40 °C (held for 2 min) to 240 °C (held for 8 min) at 5 °C min<sup>−1</sup>. After the retention time of 50 min, the sample matrix was back flushed. The column temperature for the  $^2D$  DB-Wax was kept at 40 °C during  $^1D$  GC analysis, and programmed from 40 °C at 10 °C min<sup>−1</sup> to 280 °C (held for 10 min) for  $^2D$  GC analysis. The host GC oven was kept at a constant temperature of 250 °C. The inlet pressure and the pressure of AUX of PCM for the 3-way splitter were 361 and 27 kPa, respectively. For the  $^2D$  RTL GC–SCD/NCD/MS analysis, five individual runs, each at a different constant pressure of the PCM for the Deans switch, were initially performed with injections of the locking compound {3-methylthiophene-2-carbaldehyde (3-methyl-2-formylthiophene)}. This is followed by a 3-methyl-2-formylthiophene retention time versus the Deans switch pressure (for the  $^2D$  column) regression calibration [19] to allow calculation of the exact required pressure to achieve the desired retention time of the locking compound. The pressure of the PCM was initially set at 261 kPa so that the retention time of 3-methyl-2-formylthiophene is exactly 64.80 min. A single run with injection of 3-methyl-2-formylthiophene was performed to check and relock the PCM pressure before every sequence.



For simultaneous mass spectrometric and element-specific detection, a split ratio of 1:1:1 was set to the MS, the SCD, and the NCD. A deactivated fused silica capillary with 1.0 m × 0.20 mm i.d., was used for connecting from the splitter to the SCD, and 1.2 m × 0.20 mm i.d., for connecting from the splitter to the NCD and the MS. The MS was operated in scan mode using electron ionization at 70 eV. Scan range was set from  $m/z$  29 to 300 and a sampling rate equal to three was used, resulting in scan rate of 2.68 scan  $s^{-1}$ . For the formula identification using MassWorks software ver. 2.0.2.0 (Cerno Bioscience, CT, USA), the MS was operated in “raw scan mode” which generates a profile mass spectrum (10–20 measurements per each integer  $m/z$  value in the spectrum). The SCD burner temperature was set to 800 °C and its flow rate was 63 mL  $min^{-1}$  and 45 mL  $min^{-1}$  for air and hydrogen, respectively. The NCD burner temperature was set to 950 °C and its flow rate was 10 mL  $min^{-1}$  and 5 mL  $min^{-1}$  for oxygen and hydrogen, respectively.

## 2.6. Data analysis

ChemStation ver. E.02.01.1177 (Agilent) and Aroma Office 2D database ver. 2.01.00 (Gerstel KK) were used for a combined search using a MS library and a linear retention indices (LRI) database. Aroma Office 2D contains the most comprehensive database of odor compounds available (>73,000 entries). This software is a searchable database which contains LRI information for a wide range of odor compounds from many literature references. MassWorks software ver. 2.0.2.0 (Cerno Bioscience) was used for the formula identification. MassWorks is a novel MS calibration software which calibrates for isotope profile as well as for mass accuracy allowing highly accurate comparisons between calibrated and theoretical spectra. This calibration process has been published and detailed elsewhere [20,21]. Principal component analysis (PCA) was performed using Pirouette software ver. 4.0 (Infometrix, WA, USA).

## 3. Results and discussion

### 3.1. FEDHS recovery of sulfur compounds in ethanol–water samples

Table 1 shows FEDHS recovery at 80 °C for the test sulfur compounds in 40% ethanol–water and 65% ethanol–water at 100 ng  $mL^{-1}$ . The logarithm of the octanol–water distribution coefficient ( $\log K_{ow}$ ) of the test sulfur compounds ranged from 0.67 {1-(1,3-thiazol-2-yl)ethanone (2-acetyl thiazole)} to 2.09 (4,5-dimethyl-1,3-thiazole). The  $\log K_{ow}$  values were calculated with a SRC-KOWWIN v1.68 software package (Syracuse Research, Syracuse, NY, USA). FEDHS was performed in six replicate analyses. The recovery was calculated by comparing peak areas with those of a calibration curve prepared by automated direct liquid injection of a standard solution injected into a micro-vial in a thermal desorption

**Table 1**

FEDHS recovery at 80 °C for the test sulfur compounds in 40% ethanol–water and 65% ethanol–water at 100 ng  $mL^{-1}$ .

Compound (common name) <sup>a</sup>	$\log K_{ow}$ <sup>b</sup>	40% ethanol–water		65% ethanol–water	
		Recovery (%)	RSD (%), $n = 6$	Recovery (%)	RSD (%), $n = 6$
1-(1,3-Thiazol-2-yl)ethanone (2-acetyl thiazole)	0.67	92	2.0	98	1.1
Ethyl 2-methyl sulfanyl acetate	0.95	95	3.0	93	2.1
Ethyl 3-methyl sulfanyl propanoate	1.44	99	3.7	94	2.7
1-Thiophen-2-yl ethanone (2-acetyl thiophene)	1.49	93	2.1	96	1.7
Thiophene-2-carbaldehyde (2-formyl thiophene)	1.53	94	1.8	98	2.0
(Methyltrisulfanyl)methane (dimethyl trisulfide)	1.87	92	2.4	88	3.9
5-Methylthiophene-2-carbaldehyde (5-methyl-2-formyl thiophene)	2.08	93	1.9	96	1.9
4,5-Dimethyl-1,3-thiazole	2.09	92	1.5	91	1.7

<sup>a</sup> Common name was shown in a parenthesis.

<sup>b</sup>  $\log K_{ow}$  values were calculated with SRC-KOWWIN software (Syracuse Research, Syracuse, NY, USA).

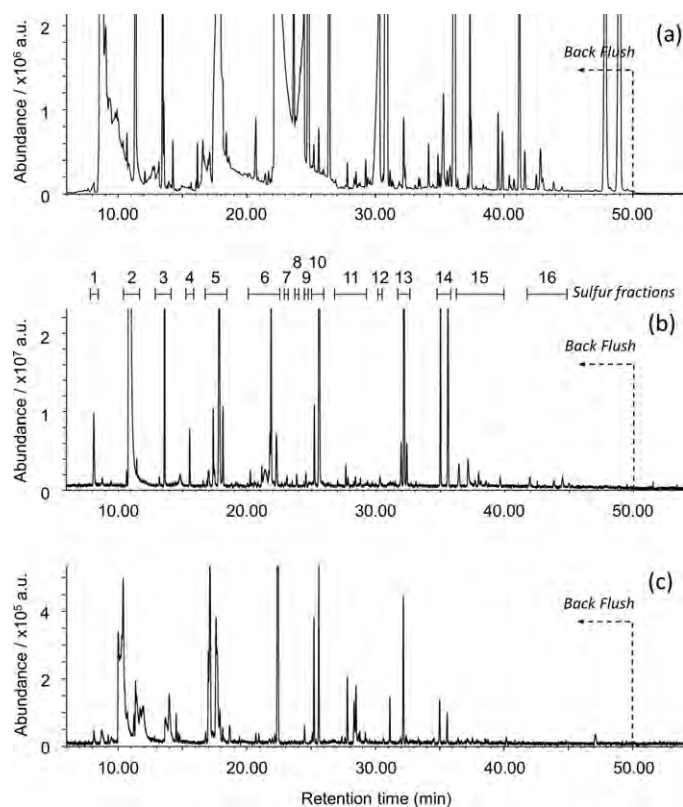


**Fig. 1.**  $^1D$  total ion chromatogram (TIC), SCD and NCD chromatograms of the unaged whisky “A”. (a)  $^1D$  TIC; (b)  $^1D$  SCD chromatogram; (c)  $^1D$  NCD chromatogram.

liner through a septum head of the TDU (TDU liquid option, GERSTEL). Very good recoveries in the range of 92–99% and 88–98% were obtained for both ethanol–water samples. Repeatabilities were also good for both samples resulting in a relative standard deviation (RSD) of less than 3.9%. As already described elsewhere [7], FEDHS allows sample matrix independent analysis. Here, the high concentration level of ethanol is assumed to be the main matrix component during headspace sampling. FEDHS can provide high recovery of hydrophilic sulfur compounds in ethanol–water samples.

### 3.2. Identification of sulfur compounds in single malt whisky

In order to identify sulfur compounds in the whisky samples, the unaged and aged whisky “A” and “G” were first analyzed with FEDHS- $^1D$  GC-SCD/NCD/MS. From the comparison of the  $^1D$  SCD chromatograms, the unaged whisky “A” showed the highest number of sulfur peaks. Fig. 1 shows the  $^1D$  total ion chromatogram (TIC) (Fig. 1a), SCD and NCD chromatograms (Fig. 1b and c) of the unaged



**Table 2**  
Identification of sulfur compounds in the unaged whisky "A" by FEDHS-<sup>1</sup>D/<sup>2</sup>D RTL GC-SCD/NCD/MS.

No.	Compound (common name) <sup>a</sup>	log K <sub>ow</sub> <sup>b</sup>		2 <sub>k</sub> (min) <sup>c</sup>	2 <sup>d</sup> LRI	Database <sup>d</sup>		PBM <sup>e</sup>	Formula	Theoretical m/z	Mass error (mDa)	Spectral accuracy <sup>f</sup>
		Calculated	Deviation									
1	2-Methyl-1,3-thiazole	1.54	57.21	1246	1245 (n=5)	1	83	C <sub>4</sub> H <sub>5</sub> NS	99.0143	-8.6	98.22	
2	1,3-Thiazole	1.81	57.39	1260	1248 (n=5)	12	91	C <sub>3</sub> H <sub>3</sub> NS	84.9986	-6.1	98.51	
3	Diethyl sulfite	0.99	57.98	1301	-	-	96	C <sub>4</sub> H <sub>10</sub> O <sub>3</sub> S	138.0351	-7.9	98.29	
4	Ethyl methanesulfonate	-0.17	58.46	1335	-	-	96	C <sub>3</sub> H <sub>8</sub> O <sub>2</sub> S	108.0245	-6.6	99.71	
5	Ethyl 2-methyl sulfanyl acetate	0.95	60.18	1458	1452 (n=1)	6	64	C <sub>5</sub> H <sub>10</sub> O <sub>2</sub> S	134.0402	-8.8	98.63	
6	Ethyl 3-methyl sulfanyl propanoate	1.44	61.75	1579	1567 (n=3)	12	91	C <sub>6</sub> H <sub>12</sub> O <sub>2</sub> S	148.0558	-5.3	99.13	
7	Methyl sulfanyl methane (dimethyl sulfoxide)	-1.22	61.86	1585	1571 (n=3)	14	94	C <sub>2</sub> H <sub>6</sub> OS	78.0139	-6.5	99.40	
8	(Acetyl thiazole isomer)	0.67	62.42	1633	-	-	95	C <sub>5</sub> H <sub>5</sub> NOS	127.0092	-7.7	99.14	
9	3-Methyl sulfanyl propyl acetate	1.44	62.55	1643	1626 (n=2)	17	83	C <sub>6</sub> H <sub>12</sub> O <sub>2</sub> S	148.0558	-5.1	99.26	
10	1-(1,3-Thiazol-2-yl)ethanone (2-acetyl thiazole)	0.67	62.81	1664	1651 (n=8)	13	96	C <sub>5</sub> H <sub>5</sub> NOS	127.0092	-8.5	99.25	
11	Thiophene-3-carbaldehyde (3-formyl thiophene)	1.53	63.23	1698	1693 (n=2)	5	91	C <sub>5</sub> H <sub>4</sub> OS	111.9983	-7.5	98.65	
12	Thiophene-2-carbaldehyde (2-formyl thiophene)	1.53	63.42	1714	1718 (n=1)	4	95	C <sub>5</sub> H <sub>4</sub> OS	111.9983	-7.2	99.19	
13	3-Methyl sulfanyl propan-1-ol (Methionol)	0.44	63.64	1734	1734 (n=15)	1	97	C <sub>4</sub> H <sub>10</sub> OS	106.0452	-5.9	99.63	
14	Isothiocyanatobenzene (phenyl isothiocyanate)	3.33	63.87	1753	-	-	90	C <sub>7</sub> H <sub>5</sub> NS	135.0143	9.0	99.06	
15	5-Methylthiophene-2-carbaldehyde (5-methyl-2-formyl thiophene)	2.08	64.43	1800	1785 (n=1)	15	83	C <sub>6</sub> H <sub>6</sub> OS	126.0139	-7.5	99.47	
16	3-Methylthiophene-2-carbaldehyde (3-methyl-2-formyl thiophene)	2.08	64.80	1834	-	-	83	C <sub>6</sub> H <sub>6</sub> OS	126.0139	-8.6	99.59	
17	3-Ethylthiophene-2-carbaldehyde (3-ethyl-2-formyl thiophene)	2.01	65.37	1885	-	-	94	C <sub>7</sub> H <sub>8</sub> OS	140.0296	-6.8	99.18	
18	2-Methyl-1,3-benzothiazole	2.72	66.18	1960	-	-	90	C <sub>8</sub> H <sub>7</sub> NS	149.0299	-9.2	99.14	
19	1,3-Benzothiazole	2.17	66.41	1979	1961 (n=10)	18	91	C <sub>7</sub> H <sub>5</sub> NS	135.0143	-7.1	99.86	
20	3-Ethyl-2(3H)-benzothiazolethione	2.87	78.01	3025	-	-	89	C <sub>9</sub> H <sub>9</sub> NS <sub>2</sub>	195.0176	-6.8	98.70	

<sup>a</sup> Common name was shown in a parenthesis.

<sup>b</sup> log K<sub>ow</sub> values were calculated with SRC-KOWWIN software (Syracuse Research, Syracuse, NY, USA).

<sup>c</sup> Second dimensional retention time (min).

<sup>d</sup> Average LRI obtained from Aroma Office 2D database.

<sup>e</sup> Probability based matching of a Wiley library search. The similarity between the theoretical and measured patterns based on 100.

<sup>f</sup> A measure of the similarity between the measured isotope pattern and the theoretical pattern.

**Table 3**Formula identification of unknown sulfur compounds in the unaged whisky “A” by FEDHS-<sup>1</sup>D/<sup>2</sup>D RTL GC-SCD/NCD/MS.

No.	Compound	<sup>2</sup> t <sub>R</sub> (min) <sup>a</sup>	<sup>2</sup> D LRI	Formula <sup>b</sup>	Theoretical m/z	Mass error (mDa)	Spectral accuracy <sup>c</sup>
S1	S1	58.12	1309	C <sub>5</sub> H <sub>10</sub> O <sub>2</sub> S	134.0402	8.5	99.08
S2	S2 <sup>d</sup>	61.39	1549	C <sub>5</sub> H <sub>12</sub> OS <sub>2</sub>	152.0330	8.6	99.16
S3	S3	66.22	1960	C <sub>11</sub> H <sub>23</sub> NOS	217.1500	4.5	99.47
S4	S4	66.24	1963	C <sub>3</sub> H <sub>8</sub> OS <sub>2</sub>	124.0017	7.6	98.23
S5	S5	67.31	2061	C <sub>8</sub> H <sub>15</sub> NOS	173.0874	4.5	99.47
S6	S6	67.72	2099	C <sub>9</sub> H <sub>9</sub> NOS	179.0405	6.5	99.26
S7	S7	69.22	2236	C <sub>11</sub> H <sub>15</sub> NOS	209.0874	4.0	98.96
S8	S8	69.98	2306	C <sub>7</sub> H <sub>11</sub> NOS	157.0561	8.9	98.76

<sup>a</sup> Second dimensional retention time (min).<sup>b</sup> Formula identification was performed with MassWorks software (Cerno Bioscience, CT, USA).<sup>c</sup> A measure of the similarity between the measured isotope pattern and the theoretical pattern.<sup>d</sup> S2 was identified as 1-ethoxy-2-(methyldisulfanyl)ethane (3,4-dithiapentyl ethyl ether) from Refs. [4,22].

whisky “A”. Although numerous sulfur compounds were detected in the <sup>1</sup>D SCD chromatogram (Fig. 1b), these sulfur compounds were completely buried in the <sup>1</sup>D TIC (Fig. 1a). It is hard to extract a clean mass spectrum for each sulfur compound because of significant interference of co-eluting sample matrix. Therefore, we sequentially performed 16 heart-cuts with 16 sulfur fractions selected by the <sup>1</sup>D SCD chromatogram for the identification in the <sup>2</sup>D chromatograms. The transferred fractions were separated and profiled under <sup>2</sup>D RTL GC-SCD/NCD/MS. Fig. 2 demonstrates an example of a single heart-cut in the <sup>1</sup>D retention time (RT) 16.8–18.8 min (the sulfur fraction 5 in Fig. 1b) and both <sup>1</sup>D and <sup>2</sup>D TIC (Fig. 2a), SCD/NCD chromatograms (Fig. 2b and c) (separation obtained in <sup>2</sup>D is zoomed and given in Fig. 3). After heart-cutting, the heart-cut fraction was cryo-focused in the CTS2 at –100 °C during the rest of <sup>1</sup>D GC run. At the RT 50 min, <sup>1</sup>D GC was back-flushed and the

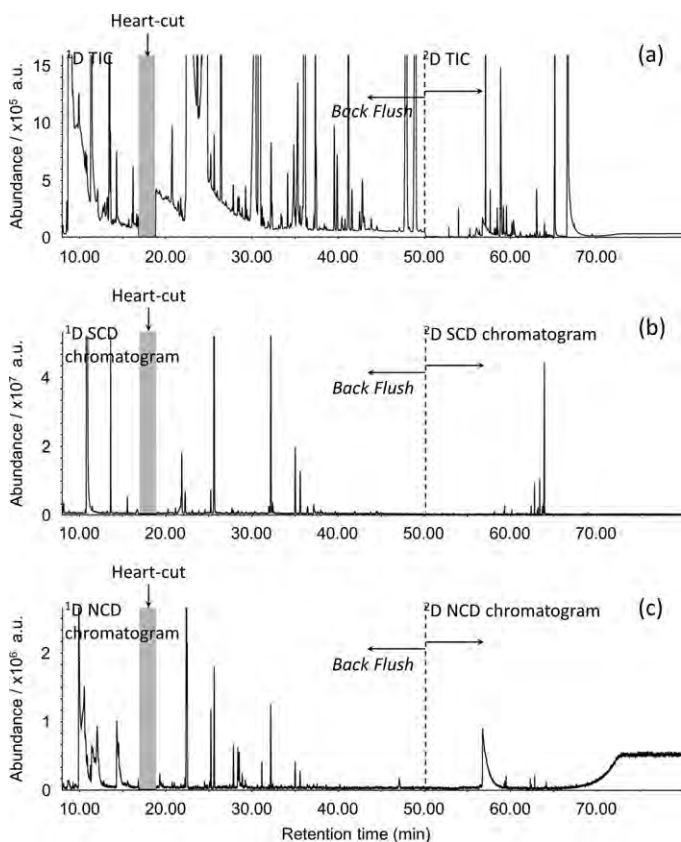


**Fig. 2.** An example of a single heart-cut in the <sup>1</sup>D retention time (RT) 16.8–18.8 min (the sulfur fraction 5 in Fig. 1) and both <sup>1</sup>D and <sup>2</sup>D TIC, and SCD/NCD chromatograms. (a) <sup>1</sup>D/<sup>2</sup>D TIC; (b) <sup>1</sup>D/<sup>2</sup>D SCD chromatogram; (c) <sup>1</sup>D/<sup>2</sup>D NCD chromatogram.

CTS2 was rapidly heated to start <sup>2</sup>D RTL GC. For the identification of sulfur compounds in the <sup>2</sup>D SCD chromatogram, the corresponding peak in the <sup>2</sup>D TIC and the mass spectral data were used and a combined search using the MS library and the LRI database was performed. Besides this, the corresponding nitrogen peak in the <sup>2</sup>D NCD chromatogram was used for confirmation of the presence of nitrogen. Using <sup>2</sup>D LRI, Aroma Office <sup>2</sup>D database, and the MS library search, six sulfur compounds, e.g. ethyl 2-methyl sulfanyl acetate, 1-(1,3-thiazol-2-yl)ethanone (2-acetyl thiazole) and its isomer, thiophene-2-carbaldehyde (2-formyl thiophene), thiophene-3-carbaldehyde (3-formyl thiophene), and 3-methyl sulfanyl propan-1-ol (methionol), were positively identified in this fraction from only 100 μL of sample. Additionally, the same <sup>2</sup>D analysis but with “raw scan mode”, which generates a profile mass spectrum, was done and the formula identification was performed with MassWorks software. After the calibration using MassWorks software, the mass peak shape involving isotope distribution is identical to the theoretical spectrum and the accuracy of mass

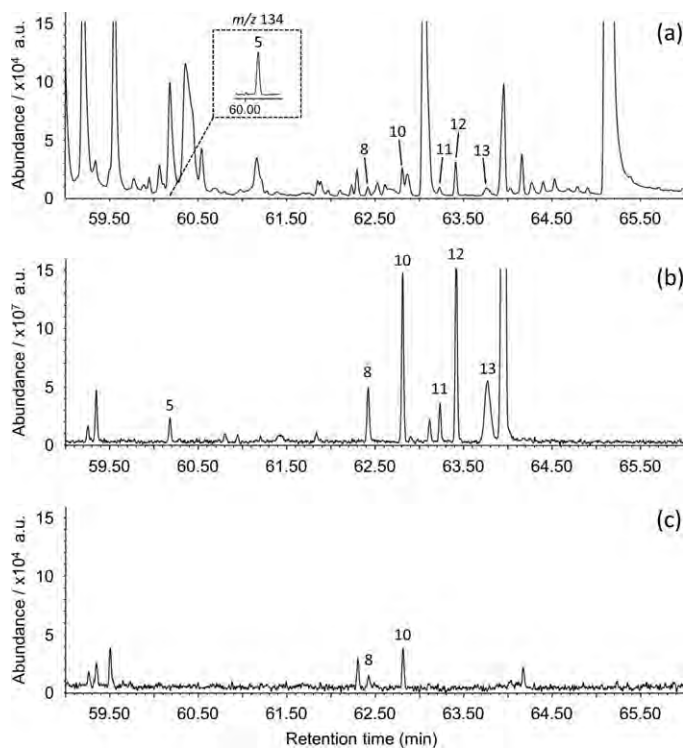


**Fig. 3.** <sup>2</sup>D TIC, SCD and NCD chromatograms of the sulfur fraction 5 of the unaged whisky “A”. (a) <sup>2</sup>D TIC; (b) <sup>2</sup>D SCD chromatogram; (c) <sup>2</sup>D NCD chromatogram. 5, ethyl 2-methyl sulfanyl acetate; 8, acetyl thiazole isomer; 10, 2-acetyl thiazole; 11, 3-formyl thiophene; 12, 2-formyl thiophene; 13, methionol.

position is greatly improved (e.g. down to four decimal places even with the unit resolution quadrupole MS measurement). Consequently, a unique isotope distribution as well as an accurate mass could be used for the formula identification. For these six sulfur compounds, the number one candidate formula obtained by MassWorks software corresponded to the formula of the identified compound by using the MS library and/or the LRI database. The mass errors of molecular ions ranged from  $-5.9$  to  $-8.8$  mDa and the spectral accuracies ranged from 98.63 to 99.63 (the spectral accuracy reflects the correctness of the complete mass spectral response of an ion in the form of continuously sampled spectral error as a function of all relevant  $m/z$  values [21]). From the 16 sulfur fractions selected by the  $^1\text{D}$  SCD chromatograms, 20 sulfur compounds were positively identified in the unaged whisky "A". Table 2 summarizes 20 sulfur compounds with the parameters used for the identification. Since the mass errors of less than  $\pm 10$  mDa and the spectral accuracies of more than 98 were obtained for the identified 20 sulfur compounds, we used these values as criteria for the formula identification of unknown sulfur compounds. Eight additional best candidate formulas were obtained for the unknown sulfur compounds (S1–S8) in the unaged whisky "A" (Table 3). We have succeeded in identifying S2 as 1-ethoxy-2-(methyl-disulfanyl)ethane (3,4-dithiapentyl ethyl ether) [4,22] and the further identification of the others are work in progress. These 28 sulfur compounds were used for multivariate analysis in the next section.

### 3.3. Principal component analysis of sulfur compounds in whisky using $^2\text{D}$ RTL GC-SCD with 16 simultaneous heart-cuts

FEDHS of 100  $\mu\text{L}$  of whisky transfer substantial amounts of non-target compounds such as esters and fatty acids to the  $^1\text{D}$  column, resulting in subtle retention time shift even with the thick film column such as DB-1 with dimensions  $30\text{ m} \times 0.25\text{ mm i.d.} \times 1.0\text{ }\mu\text{m}$  df. In this case, it is essential to have retention time alignment for all the components in all the chromatograms before multivariate analysis. In the meantime,  $^2\text{D}$  GC can reduce the effect of the non-target compounds for the retention time shift. Also, the PCM and the CTS2 cryo-trap system can provide highly reproducible injection of the heart-cut fractions into the  $^2\text{D}$  GC column under RTL condition. Therefore, we applied  $^2\text{D}$  RTL GC-SCD with 16 simultaneous heart-cuts containing 28 sulfur compounds (listed in Tables 2 and 3) to multivariate analysis. Triplicate analyses were performed for each whisky sample. The data set which consists of 12 analyses was used for multivariate analysis to consider repeatability of analysis. Fig. 4 demonstrates an example of the 16 heart-cuts of the unaged whisky "A" and both  $^1\text{D}$  and  $^2\text{D}$  TIC (Fig. 4a), SCD/NCD chromatograms (Fig. 4b and c). Fig. 5 shows a comparison of the  $^2\text{D}$  RTL SCD chromatograms between all whisky samples. Compared to the unaged whisky, many sulfur compounds (3, 5, 6, 8, 9, 13, 18–20, and S1–S8) dramatically decreased or were not detected in the aged whisky. Masuda and Nishimura investigated changes in sulfur compounds during whisky aging in wood casks and found that low boiling sulfur compounds {e.g. methylsulfanyl-methane (dimethyl sulfide) (DMS) and (methyl-disulfanyl)methane (dimethyl disulfide) (DMDS)} and some medium/low boiling sulfur compounds (e.g. 3-methyl sulfanyl propyl acetate and methionol) decrease rapidly during maturation [23]. Similar results have been reported for DMS and DMDS in Irish whiskey [24]. These sulfides have disagreeable aromas (e.g. asparagus, cabbage, and onion), but disappear rapidly during maturation. Natural evaporation is a factor in the decrease, but oak wood is also necessary for their removal. It is reported that the burnt char on the inside of the cask can act as adsorption layer to remove these disagreeable volatile sulfur compounds [25]. On the other hand, several sulfur compounds did not appreciably change (1, 15, and 17) or even increased (4, 11, and 12 for both "A" and "G", 10 for "G", and 16 for "A"). Compounds that

**Table 4**  
Concentration of the key sulfur compounds in unaged and aged single malt whisky samples.

No.	Compound (common name) <sup>a</sup>	Formula	Unaged "A"		Aged "A"		Unaged "G"		Aged "G"	
			Concentration (ng mL <sup>-1</sup> )	RSD (%) n=3	Concentration (ng mL <sup>-1</sup> )	RSD (%) n=3	Concentration (ng mL <sup>-1</sup> )	RSD (%) n=3	Concentration (ng mL <sup>-1</sup> )	RSD (%) n=3
3	Diethyl sulfide	C <sub>4</sub> H <sub>10</sub> O <sub>3</sub> S	100	2.2	0.52	3.4	93	3.7	0.73	7.3
4	Ethyl methanesulfonate	C <sub>3</sub> H <sub>8</sub> O <sub>3</sub> S	28	2.0	62	1.5	50	2.1	75	0.37
9	3-Methyl sulfanyl propyl acetate	C <sub>6</sub> H <sub>12</sub> O <sub>2</sub> S	35	2.5	0.32	12	20	2.6	0.35	6.1
10	1-(1,3-thiazol-2-yl)ethanone (2-acetyl thiazole)	C <sub>5</sub> H <sub>5</sub> NOS	13	7.6	9.1	4.4	15	12	17	3.1
11	Thiophene-3-carbaldehyde (3-formyl thiophene)	C <sub>5</sub> H <sub>4</sub> OS	2.8	5.9	4.5	6.0	3.4	1.7	18	4.5
12	Thiophene-2-carbaldehyde (2-formyl thiophene)	C <sub>5</sub> H <sub>4</sub> OS	28	3.6	21	3.1	22	2.6	28	0.59
13	3-Methyl sulfanyl propan-1-ol (methionol)	C <sub>4</sub> H <sub>10</sub> O <sub>2</sub> S	110	3.5	nd	-	32	5.1	nd	-
16	3-Methylthiophene-2-carbaldehyde	C <sub>6</sub> H <sub>6</sub> OS	9.6	4.6	17	1.1	15	2.2	13	3.2
18+S4	(3-methyl-2-formyl thiophene)	C <sub>8</sub> H <sub>7</sub> NS/C <sub>3</sub> H <sub>8</sub> O <sub>2</sub>	26	4.1	nd	-	31	1.4	nd	-
19	2-Methyl-1,3-benzothiazole+S4	C <sub>7</sub> H <sub>5</sub> NS	210	2.3	1.2	9.5	170	2.5	1.0	4.5
S1	1,3-Benzothiazole	C <sub>5</sub> H <sub>10</sub> O <sub>2</sub> S	11	3.5	nd	-	21	5.1	nd	-
S2	S2 <sup>b</sup>	C <sub>5</sub> H <sub>12</sub> O <sub>2</sub> S	6.4	4.3	0.41	1.3	9.5	2.6	0.30	10
S5	S5	C <sub>8</sub> H <sub>15</sub> NOS	110	6.0	nd	-	100	2.7	nd	-

<sup>a</sup> Common name was shown in a parenthesis.

<sup>b</sup> S2 was identified as 1-ethoxy-2-(methyl-disulfanyl)ethane (3,4-dithiapentyl ethyl ether) from Refs. [4,22].

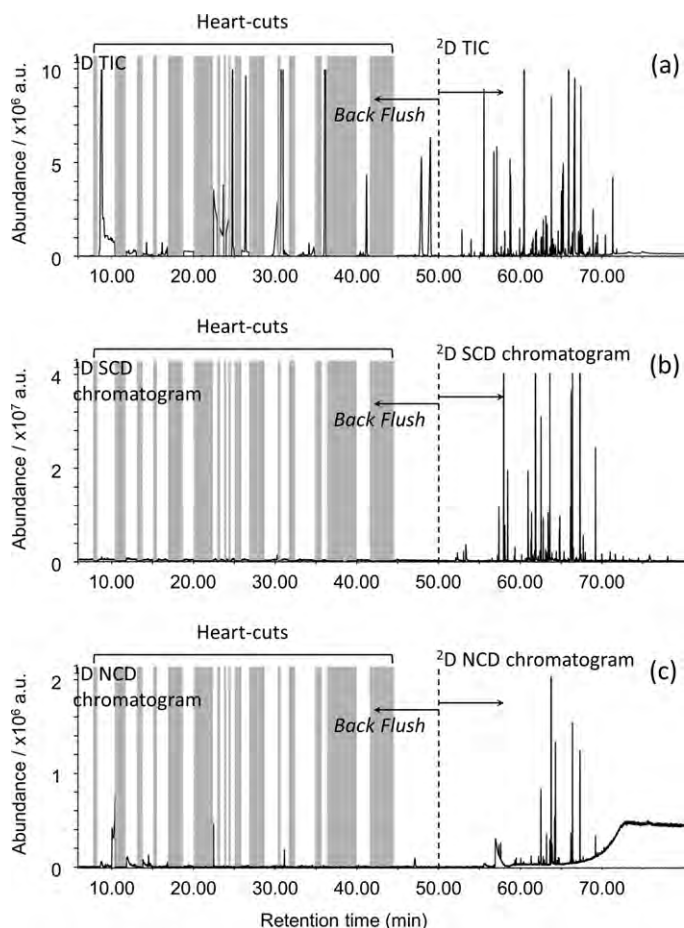


**Fig. 4.** An example of simultaneous 16 heart-cuts in the  $^1\text{D}$  GC and both  $^1\text{D}$  and  $^2\text{D}$  TIC, SCD/NCD chromatograms. (a)  $^1\text{D}/^2\text{D}$  TIC; (b)  $^1\text{D}/^2\text{D}$  SCD chromatogram; (c)  $^1\text{D}/^2\text{D}$  NCD chromatogram.

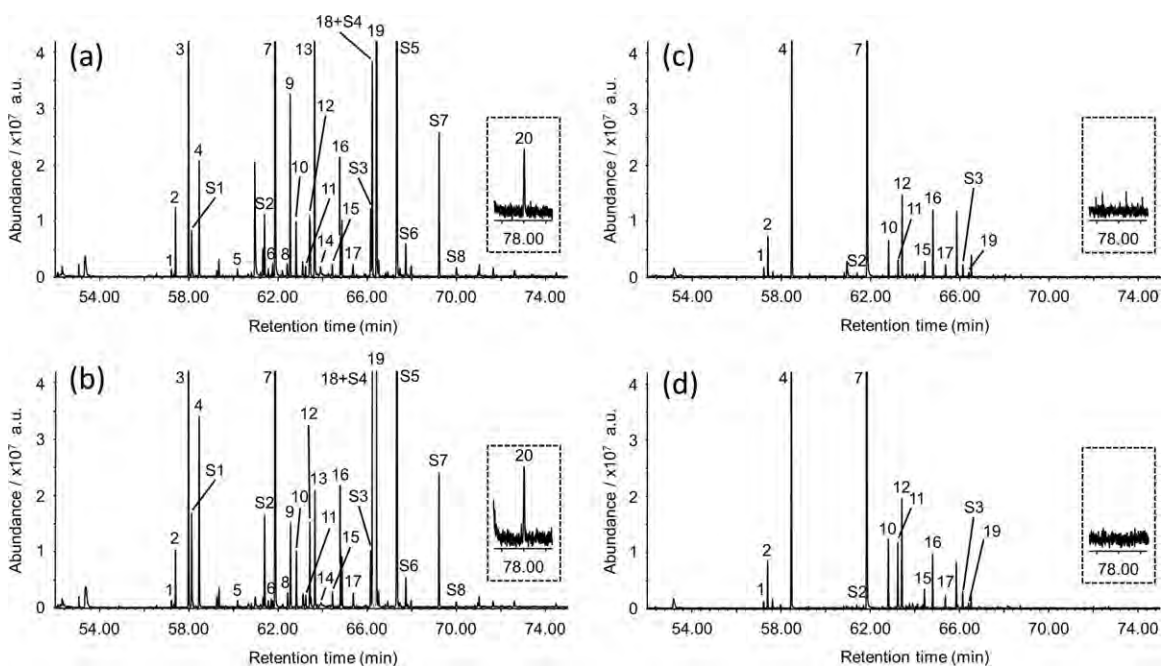


**Fig. 5.** A comparison of the  $^2\text{D}$  RTL SCD chromatograms between all whisky samples. (a) Unaged whisky "A"; (b) unaged whisky "G"; (c) aged whisky "A"; (d) aged whisky "G". The marked peaks represent positively identified sulfur compounds (see Table 2, 1–20) and unknown sulfur compounds which have candidate formulas (see Table 3, S1–S8).

increase during aging, such as thiophenes, originate from the wood as Maillard reaction products. They have a roasted spicy and/or fruity aroma which can contribute positively to the whisky flavor [26].

A principal component analysis (PCA) was applied to all samples to obtain a simplified view of the relationship between unaged and aged whisky, as well as two different whisky samples. The three principal components (PC) account for 99.98% of the total variance of the data (PC1: 97.4%, PC2: 1.6%, and PC3: 0.98%, respectively). Fig. 6a shows a PCA score plot using PC1 and PC2. PC1 clearly differentiates between the unaged and aged whisky samples. From the corresponding loading plot in Fig. 6b, the sulfur compounds can be characterized according to the strength of the contribution to each PC (the compounds which have the PC factor of more than  $\pm 0.1$  are labeled with a bold letter). Diethyl sulfite (3), 1,3-benzothiazole (19), and S5 show higher contribution to the positive PC1, while ethyl methanesulfonate (4) highly contributes to the negative PC1. Also, methionol (13) and 2-methyl-1,3-benzothiazole (18)+S4 (these two compounds were not separated in the  $^2\text{D}$  RTL GC-SCD with the simultaneous 16 heart-cuts) show moderate contribution to the positive PC1, while 2-formyl thiophene (12) and 3-methyl-2-formyl thiophene (16) moderately contribute to the negative PC1. In general, the positive PC1 is correlated with the decrease of sulfur compounds during the aging, while the negative PC1 is correlated with the increase of sulfur compounds. PC 2 clearly differentiates between the unaged whisky "A" and "G", however, the aged whisky samples are not appreciably differentiated. From the loading plot, 2-methyl-1,3-benzothiazole (18)+S4 and S5 show higher contribution to the positive PC2, while methionol (13) highly contributes to the negative PC2. Also, diethyl sulfite (3), ethyl methanesulfonate (4), 3-methyl-2-formyl thiophene (16), S1, and S2 (3,4-dithiapentyl ethyl ether) show moderate contribution to the positive PC2, while 3-methyl sulfanyl propyl acetate (9) moderately contributes to the negative PC2. In general, the positive PC2 is correlated with higher response of sulfur compounds in the unaged whisky "G", while the negative PC2 is correlated with higher response of sulfur compounds in the unaged whisky "A".



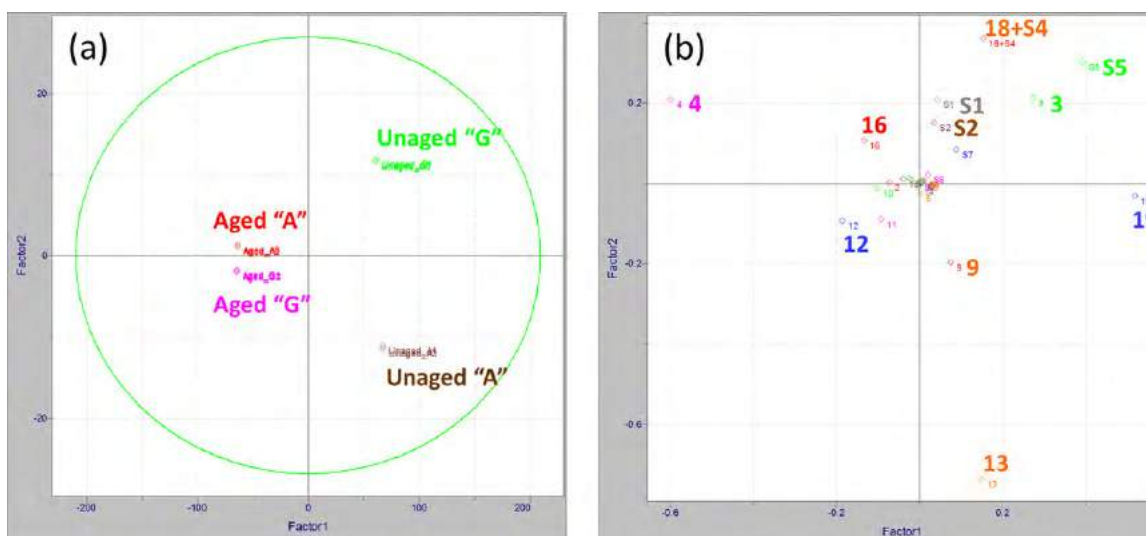


**Fig. 6.** PCA score plot using PC1 and PC2 (a) and the corresponding loading plot (b). The compounds which have the PC factor of more than  $\pm 0.1$  are labeled with a bold letter.

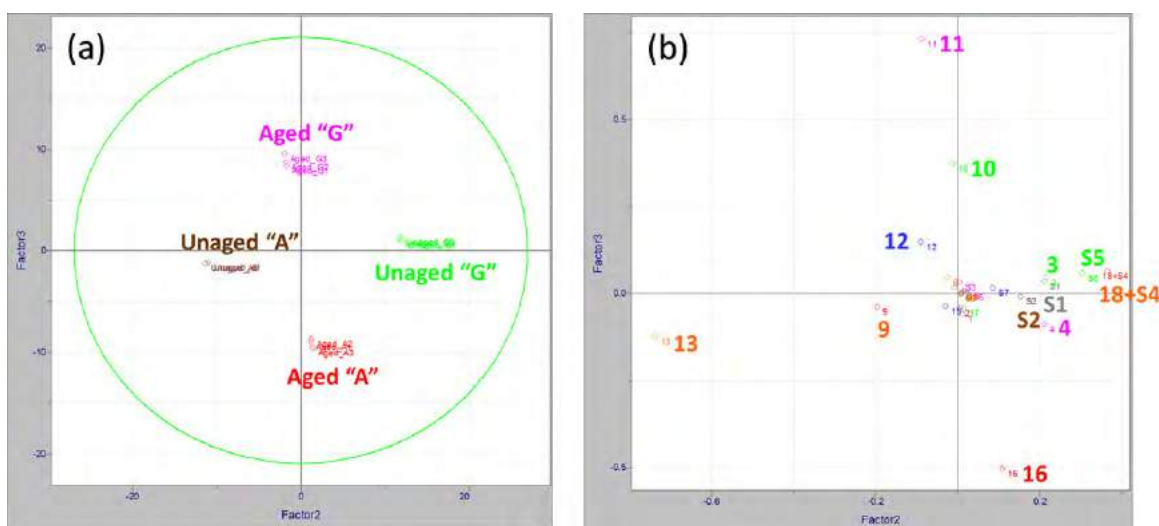


**Fig. 7.** PCA score plot using PC2 and PC3 (a) and the corresponding loading plot (b). The compounds which have the PC factor of more than  $\pm 0.1$  are labeled with a bold letter.

Although PC1 does not differentiate between the aged whisky samples and PC2 shows very small difference, PC3 clearly differentiates those samples. Also, the score plot using PC2 and PC3 can clearly differentiate all whisky samples (Fig. 7a). From the corresponding loading plot in Fig. 7b, 2-acetyl thiazole (10), 3-formyl thiophene (11), and 2-formyl thiophene (12) show higher contribution to the positive PC3, while 3-methyl-2-formyl thiophene (16) highly contribute to the negative PC3. The positive PC3 is correlated with higher response of sulfur compounds in the aged whisky "G", while the negative PC3 is correlated with higher response of sulfur compound in the aged whisky "A", if those sulfur compounds are still detected in the aged samples.

Finally, quantification of fourteen sulfur compounds (3, 4, 9, 10, 11, 12, 13, 16, 18 + S4, 19, S1, S2, and S3), which could be characterized as key sulfur compounds with the PC factor of more than  $\pm 0.1$  in the loading plot, was performed using a linear and equimolar response of the  $^2\text{D}$  RTL GC-SCD to sulfur compounds [27]. 1-Thiophen-3-ylethanone (3-acetyl thiophene) ( $\log K_{ow}$ : 1.49), which was not present in the samples, was chosen as a standard and spiked into the sample between 1 and 200  $\text{ng mL}^{-1}$  (7.9 and 1600  $\text{nmol mL}^{-1}$ ). The recovery of 3-acetyl thiophene in the unaged whiskey "A" spiked at 100  $\text{ng mL}^{-1}$  was 101% (RSD: 2.0%,  $n=5$ ).

Concentrations of the key sulfur compounds in the unaged and aged whisky samples were in the range of 0.3–210  $\text{ng mL}^{-1}$  (RSD: 0.37–12%,  $n=3$ ). Table 4 summarizes the determined values of the key sulfur compounds.

Using the FEDHS- $^1\text{D}/^2\text{D}$  RTL GC-SCD/NCD/MS system, once the key sulfur compounds are identified in  $^2\text{D}$  GC mode (and subsequent PCA), then it may be possible to routinely monitor and quantify them in  $^1\text{D}$  GC mode with the selective detection such as SCD. This would be a very user-friendly option, especially because no instrumental configuration changes need to be made.

#### 4. Conclusion

The combination of FEDHS,  $^1\text{D}/^2\text{D}$  RTL GC-SCD/NCD/MS, the combined search using mass spectra and LRI, formula identification, and PCA, offers a very effective synergy for identifying key sulfur compounds in the unaged and aged whisky. Twenty sulfur compounds were positively identified in the unaged whisky by sequential heart-cuts of the 16 sulfur fractions. Also, 8 formulas could be obtained for unknown sulfur compounds.

$^2\text{D}$  RTL GC-SCD data obtained by simultaneous heart-cuts of the 16 sulfur fractions clearly demonstrated the changes of sulfur



compounds during the aging step. PCA of the <sup>2</sup>D RTL GC-SCD data proved to be a remarkable tool for distinguishing between unaged and aged whisky, as well as two different whisky samples. Fourteen sulfur compounds could be characterized as key sulfur compounds and determined at sub-ngmL<sup>-1</sup> to ngmL<sup>-1</sup> levels.

### Acknowledgements

The authors thank Dr. Katsumi Umano of Takata Koryo Co., Ltd. for the standard sulfur compounds. The authors also thank Mr. Edward Pfannkoch of Gerstel Inc. and Mr. Hirooki Kanda of Gerstel K.K. for their kind support.

### References

- [1] M. Mestres, O. Busto, J. Guasch, J. Chromatogr. A 881 (2000) 569.
- [2] B. Vanderhaegen, H. Neven, H. Verachtert, G. Derdelinckx, Food Chem. 95 (2006) 357.
- [3] L. Nykänen, H. Suomalainen, Aroma of Beer, Wine and Distilled Alcoholic Beverages, D. Daniel Publishing Company, Dordrecht/Boston/Lancaster, 1983.
- [4] Kevin Mac Namara, in: R. Cantagrel (Ed.), Elaboration et Connaissance des Spiritueux, Lavoisier & Doc, Paris, 1993, p. 385.
- [5] J. Ledauphin, B. Basset, S. Cohen, T. Payot, D. Bariller, J. Food Compos. Anal. 19 (2006) 28.
- [6] M. Markelov, J.P. Guzowski Jr., Anal. Chim. Acta 276 (1993) 235.
- [7] N. Ochiai, K. Sasamoto, A. Hoffmann, K. Okanoya, J. Chromatogr. A 1240 (2012) 59.
- [8] C. Devos, N. Ochiai, K. Sasamoto, P. Sandra, F. David, J. Chromatogr. A 1255 (2012) 207.
- [9] P. Bouchilloux, P. Darriet, R. Henry, V. Lavigne-Cruège, D. Dubourdiou, J. Agric. Food Chem. 46 (8) (1998) 3095.
- [10] P.J. Marriott, S.-T. Chin, B. Maikhunthod, H.-G. Schmarr, S. Bieri, TrAC Trends Anal. Chem. 34 (2012) 1.
- [11] P.Q. Tranchida, D. Sciarone, P. Dugo, L. Mondello, Anal. Chim. Acta 716 (2012) 66.
- [12] M. Adahchour, J. Beens, U.A.Th. Brinkman, J. Chromatogr. A 1186 (2008) 67.
- [13] K. MacNamara, A. Hoffmann, Dev. Food. Sci 39 (1998) 303.
- [14] K. MacNamara, A. Hoffmann, in: P. Sandra (Ed.), Proceedings of the 15th International Symposium on Capillary Chromatography, Riva del Garda, Italy, 1993, p. 877.
- [15] K. MacNamara, R. Leardi, A. Hoffmann, LCGC Eur. (December) (2003) 14.
- [16] K. Sasamoto, N. Ochiai, J. Chromatogr. A 1217 (2010) 2903.
- [17] N. Ochiai, K. Sasamoto, J. Chromatogr. A 1218 (2011) 3180.
- [18] F. Poy, L. Cobelli, S. Banfi, F. Fossati, J. Chromatogr. 395 (1987) 281.
- [19] L.M. Blumberg, M.S. Klee, Anal. Chem. 70 (1998) 3828.
- [20] Y. Wang, Methods for Operating MS Instrument Systems, United States Patent No. 6,983,213, 2006.
- [21] Y. Wang, M. Gu, Anal. Chem. 82 (2010) 7055.
- [22] T. Taniguchi, N. Miyajima, H. Komura, Food flavors: generation, analysis and process influence, in: G. Charalambous (Ed.), Proceedings of the 8th International Flavor Conference, Cos, Greece, 1994, p. 1767.
- [23] M. Masuda, K. Nishimura, J. Food Sci. 47 (1989) 101.
- [24] K. MacNamara, C.J. Van Wyk, O.P.H. Augustyn, A. Rapp, S. Afr. J. Enol. Viticult. 22 (2001) 75.
- [25] K. Nishimura, M. Ohnishi, M. Masuda, K. Koga, R. Matsuyama, in: J. Piggott (Ed.), Flavour of Distilled Beverages, Ellis Horwood, Chichester, 1983, p. 241.
- [26] G. Vernin, C. Párkányi, in: G. Vernin (Ed.), Chemistry of Heterocyclic Compounds in Flavors and Aromas, Ellis Horwood, Chichester, 1982, p. 151.
- [27] Agilent Technologies Publication 5989-6785EN, June 2007.

# Application of Spectral Accuracy to Improve the Identification of Organic Compounds in Environmental Analysis

Emmanuel Eysseric,<sup>†</sup> Killian Barry,<sup>†</sup> Francis Beaudry,<sup>‡</sup> Magali Houde,<sup>§</sup> Christian Gagnon,<sup>§</sup> and Pedro A. Segura<sup>\*,†,‡</sup>

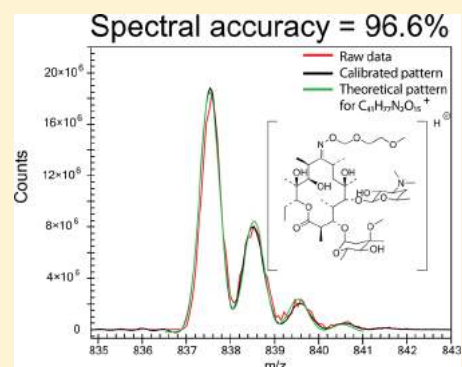
<sup>†</sup>Department of Chemistry, Université de Sherbrooke, Sherbrooke, Quebec J1K 2R1, Canada

<sup>‡</sup>Groupe de Recherche en Pharmacologie Animal du Québec (GREPAQ), Department of Veterinary Biomedicine, Université de Montréal, Saint-Hyacinthe, Quebec J2S 2M2, Canada

<sup>§</sup>Environment and Climate Change Canada, Montreal, Quebec H2Y 2E7, Canada

## S Supporting Information

**ABSTRACT:** Correct identification of a chemical substance in environmental samples based only on accurate mass measurements can be difficult especially for molecules >300 Da. Here is presented the application of spectral accuracy, a tool for the comparison of isotope patterns toward molecular formula generation, as a complementary technique to assist in the identification process of organic micropollutants and their transformation products in surface water. A set of nine common contaminants (five antibiotics, an herbicide, a beta-blocker, an anti-depressant, and an antineoplastic) frequently found in surface water were spiked in methanol and surface water extracts at two different concentrations (80 and 300  $\mu\text{g L}^{-1}$ ). They were then injected into three different mass analyzers (triple quadrupole, quadrupole-time-of-flight, and quadrupole-orbitrap) to study the impact of matrix composition, analyte concentration, and mass resolution on the correct identification of molecular formulas using spectral accuracy. High spectral accuracy and ranking of the correct molecular formula were in many cases compound-specific due principally to conditions affecting signal intensity such as matrix effects and concentration. However, in general, results showed that higher concentrations and higher resolutions favored ranking the correct formula in the top 10. Using spectral accuracy and mass accuracy it was possible to reduce the number of possible molecular formulas for organic compounds of relative high molecular mass (e.g., between 400 and 900 Da) to less than 10 and in some cases, it was possible to unambiguously assign one specific molecular formula to an experimental isotopic pattern. This study confirmed that spectral accuracy can be used as a complementary diagnostic technique to improve confidence levels for the identification of organic contaminants under environmental conditions.



The identification of organic micropollutants, such as pesticides, pharmaceuticals, personal care products, plastic additives, and their metabolites, is a real challenge as a large number and variety of compounds are present in the environment.<sup>1</sup> One of the first steps to identify a compound using mass spectrometry (MS) is to determine the molecular formula from its mass spectrum. Recently, Schymanski et al.<sup>2</sup> proposed to improve the communication of identification confidence using MS based on a five-level approach. According to the authors, accurate mass represents the lowest confidence (level 5), followed by unequivocal molecular formula (level 4), tentative candidate (level 3, based for example on tandem mass spectrometry or other experimental data), probable structure (level 2, which could be reached using library spectrum match or other diagnostic evidence), and finally confirmed structure (level 1, which requires a reference standard). Determination of an unequivocal chemical formula (level 4) with mass accuracy <5 ppm for a unknown peak in the mass spectrum is challenging for compounds with molecular masses >300 Da<sup>3</sup> and can often lead to incorrect conclusions. Using tandem mass spectrometry (MS/MS) databases, such as mzCloud or Mass

Bank, may help to reach confidence level 2 by searching library spectrum matches, however it is difficult to perform such confirmation for less known organic micropollutants or their transformation products that might be absent from those databases. For that reason, complementary techniques have been recently developed to obtain more information on the composition and structure of unknowns such as postcolumn hydrogen–deuterium exchange<sup>4</sup> and comparison of data acquired in the positive and negative ionization mode.<sup>5,6</sup> The former could be used as diagnostic evidence to obtain more information about the presence of specific functional groups (e.g., exchangeable hydrogens present in alcohol and amine groups) on a molecule, while the latter can be employed to confirm the presence of certain compounds. Dual ionization has been used for metabolomic profiling in the past to broaden the range of detection of MS methods. Additionally, for some environmental

Received: May 10, 2017

Accepted: August 2, 2017

Published: August 2, 2017

contaminants, such as pharmaceuticals, herbicides, and fluorinated compounds, electrospray in the negative mode is the preferred ionization polarity.<sup>7</sup> Obtaining additional structural information from the mass spectrum for a precursor ion before carrying on MS/MS experiments is of interest since it could save time and resources. It could also help in the identification process of unknown organic micropollutants and their transformation products, often present in samples at low concentrations, since it is difficult or even impossible to obtain meaningful MS/MS spectra for peaks of low abundance.

Previous studies have explored different approaches to improve the identification of small organic compounds using MS. The “Seven Golden Rules” established by Kind and Fiehn<sup>8</sup> provide a way to limit the sheer number of possible formulas and are now widely used in the identification process of compounds. In these rules, isotope pattern is the major component for the formula determination, along with other rules, such as hydrogen to carbon ratios and probable elements. Recent studies based exclusively on accurate mass to assess molecular formula are rare because MS/MS is normally used to provide additional structural information; however alternatives have been explored. Garcia-Reyes et al.<sup>9</sup> previously developed a workflow for detecting and identifying pesticides and their degradation products using liquid chromatography-time-of-flight MS. The proposed method is efficient for compounds containing S, Cl, or Br, which are a common occurrence in pesticides, because of their very easily distinguishable isotopic patterns. However, if an unknown compound does not contain such elements, the number of possible molecular formulas for a given accurate mass within an acceptable tolerance window cannot be reduced significantly, which impairs the compound identification process. For example, 187 possible molecular formulas, within 5 mDa of mass error and having between 0 to 50 atoms of C, H, N, O, P, and F with up to 20 double bond equivalents, were found for an hypothetical ion of  $m/z$  400.1234. Another approach proposed by Little et al.,<sup>10,11</sup> used accurate mass to perform searches on databases such as the Chemical Abstracts Service or ChemSpider to identify unknown compounds. The authors applied orthogonal filters based on the number of literature references to prioritize the list of potential candidates. Though this approach can be highly successful to identify compounds that are commercially available, it can be less suitable for the identification of transformation products of environmental contaminants that may not be integrated in databases.

An interesting alternative technique to improve the confidence on the identification level of a given unknown is spectral accuracy for MS as introduced by Wang and Gu.<sup>12</sup> Spectral accuracy is a metric that describes the similarity between a calibrated experimental profile data of an ion, obtained through a mathematical transformation of its experimental profile data and the theoretical (calculated) isotopic pattern corresponding to a given molecular formula. Thus, high spectral accuracy (e.g., > 98%) indicates that the experimental isotopic pattern fits well to the isotopic pattern of a specific molecular formula within 2% spectral error<sup>12</sup> (Figure 1). The main advantage of spectral accuracy over mass accuracy is that in the latter error is measured at a single point, while in the former error is measured throughout the whole isotopic distribution. Therefore, spectral accuracy uses all the information embedded in the experimental mass spectrum to rank possible molecular formulas accordingly to their level of likeness to the theoretical mass spectrum. Spectral accuracy was successfully applied to

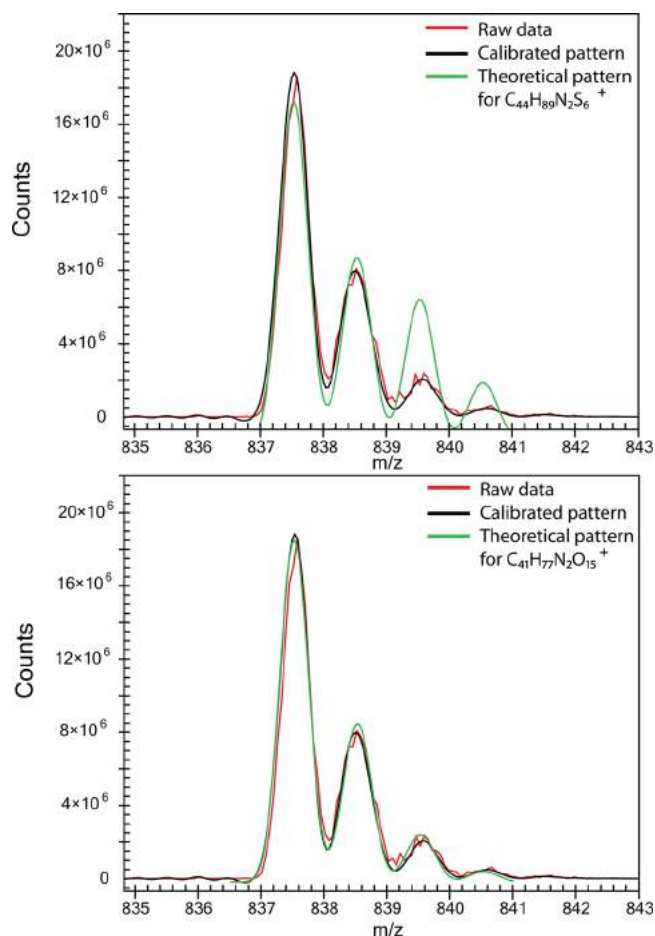


**Figure 1.** Determination of spectral accuracy in the MassWorks software using a known compound spiked in MeOH and analyzed by LC-ESI(+)-QqQMS. The raw data is first calibrated, that is, mathematically transformed, and then compared to the theoretical isotopic pattern of molecular formula candidates. The top figure shows that the isotopic pattern corresponding to an ion of formula  $C_{44}H_{89}N_2S_6^+$  ( $\Delta m = -3.4$  mDa), is not a good match for the calibrated isotopic pattern, therefore the spectral accuracy is 75.00% and was ranked 71st out of 71 possible formulas. The bottom figure shows a better match between the calibrated and the theoretical isotopic pattern of ion  $C_{41}H_{77}N_2O_{15}^+$  ( $\Delta m = -0.7$  mDa) and the spectral accuracy (96.63%), was ranked 6th out of 71 possible for molecular formulas within the software constraints ( $C_{1-66}$ ,  $H_{0-109}$ ,  $N_{0-20}$ ,  $O_{0-25}$ ,  $S_{0-13}$ , mass tolerance = 5 mDa, electron state: even, double bond equivalents range =  $-0.5$  to 50). That ion corresponds to the protonated molecule of roxithromycin, the compound spiked in the sample.

the identification of high mass (639–1664 Da) natural products in a previous study using a linear ion trap-orbitrap mass spectrometer.<sup>13</sup> On the basis of both mass and spectral accuracy, it was possible in some cases to eliminate >99% of formula candidates and the correct formula was usually ranked among the top five candidates. However, data were obtained using millimolar concentrations in pure solvents, experimental conditions that do not correspond to environmental analysis. Moreover, previous works on spectral accuracy showed that ion abundance was a major factor impacting quality of results.<sup>14</sup>

The main objective of the present work was therefore to determine if spectral accuracy could be used as a complementary technique for the identification of organic contaminants in environmental sample analysis. To answer this

question, a set of frequently detected organic contaminants were spiked in methanol and surface water extracts at two different concentrations (80 and 300  $\mu\text{g L}^{-1}$ ). Three different types of mass analyzers (i.e., triple quadrupole, quadrupole-time-of-flight, and quadrupole-orbital ion trap) were used to study the impacts of three important factors in environmental analysis (matrix composition, analyte concentration and mass resolution) on spectral accuracy and formula ranking of the selected organic micropollutants (Figure SI-1).

## ■ EXPERIMENTAL SECTION

**Reagents and Standards.** Water, acetonitrile (ACN), methanol (MeOH), and 0.1% formic acid (FA) in ACN were all LC-MS Optima grade and were obtained from Fisher Scientific (Canada). Analytical standards of atrazine (acronym, ATZ; purity, 98.1%), fluoxetine hydrochloride (FLX, 99.95%), josamycin (JOS,  $\geq 98\%$ ), metoprolol tartrate (MTP,  $\geq 98\%$ ), ofloxacin (OFL, 99.8%) roxithromycin (ROX,  $\geq 90\%$ ), and sulfamethoxazole (SMX, 99.9%) were purchased from Sigma-Aldrich (Canada). Trimethoprim (TRI,  $>98\%$ ) and methotrexate (MTX,  $\geq 98\%$ ) were purchased from Santa Cruz Biotechnology (USA).

**Collection and Preparation of Samples.** Mixture solutions of the aforementioned compounds were prepared in MeOH each at high (300  $\mu\text{g L}^{-1}$ ) and low concentration (80  $\mu\text{g L}^{-1}$ ). River surface water samples (250 mL) were collected from the Magog River (Sherbrooke, Quebec) on September 13, 2016 in amber high density polyethylene bottles and conserved in an ice cooler until arrival to the laboratory, where they were immediately stored at  $-20\text{ }^{\circ}\text{C}$ . Upon extraction, samples were thawed at room temperature and buffered to pH 7 with phosphoric acid monobasic and phosphoric acid dibasic. Water samples were then extracted using a previously reported method.<sup>4</sup> Briefly, samples were loaded in polymeric Strata-X solid-phase extraction cartridges (Phenomenex, USA) and then eluted with  $2 \times 3\text{ mL}$  of an ACN-MeOH (1:1, v/v) solution. Eluates were evaporated under a nitrogen flow and reconstituted to 10 mL with MeOH spiked at the same concentrations as the previous solutions (80 and 300  $\mu\text{g L}^{-1}$ ). Therefore, considering a preconcentration factor of 25 (initial volume = 250 mL, final volume = 10 mL), the high and low concentrations used for each compound are equivalent to 3 and 12  $\mu\text{g L}^{-1}$  respectively, which are in the high range of environmental concentrations of many organic micropollutants detected in surface waters around the globe.<sup>15,16</sup> For all experiments, samples were injected three times in order to evaluate reproducibility of the results.

Another set of analysis at lower concentrations (10, 20, 30, 40, and 50  $\mu\text{g L}^{-1}$ ) was added in order to assess the low concentration limits of spectral accuracy on the quadrupole-time-of-flight mass spectrometer and the quadrupole-orbital ion trap mass spectrometer. Considering the preconcentration factor, those concentrations were equivalent to 0.38, 0.75, 1.1, 1.5, and 1.9  $\mu\text{g L}^{-1}$ . For these experiments, the same sample was injected two times.

**Instruments and Methods.** *Liquid Chromatography-Triple Quadrupole Mass Spectrometry (LC-QqQMS).* The liquid chromatography-triple quadrupole mass spectrometry instrument (LC-QqQMS) used for this work involved an Acquity Ultra Performance LC coupled to a Quattro Premier XE triple quadrupole mass spectrometer both manufactured by Waters (USA). The LC column was a Waters Acquity UPLC HSS T3  $2.1 \times 50\text{ mm}$ ,  $1.8\ \mu\text{m}$ . The mobile phase was

composed of solvent A, water with 0.1% (v/v) formic acid, while solvent B was acetonitrile with 0.1% (v/v) formic acid. Chromatographic separation was obtained using the following elution gradient: at initial time, 5% B; at 5 min, 100% B; at 7 min, 100% B; at 7.01 min, 5% B; at 10 min, 5% B. Run time was 10 min. Mobile phase flow rate was  $500\ \mu\text{L min}^{-1}$  throughout the run. Injection volume was  $10\ \mu\text{L}$ . The QqQMS system was first mass calibrated via MassLynx with a solution of sodium formate before the acquisition. Additional mass calibration was performed through MassWorks by infusing an external calibrant (sodium formate) before the acquisition or by LC-QqQMS analysis of internal calibrants (MTP, FLX, OFL and JOS) mixed with the samples. A detailed description of experiments carried out to evaluate the mass accuracy stability of the QqQMS system is presented in section SI-1 of the Supporting Information.

*Liquid Chromatography-Quadrupole-Time-of-Flight Mass Spectrometry (LC-QqTOF-MS).* The instrument used in these experiments involved a LC system manufactured by Shimadzu (Japan) and composed of a Nexera LC-30AD pump module, a SIL-30AC autosampler and a CTO-30A as column oven module. This LC system was coupled to a high-resolution mass spectrometer, the Maxis quadrupole-time-of-flight mass spectrometer (QqTOFMS) made by Bruker (USA). LC conditions were identical as those used in the LC-QqQMS setup. Injection volume was  $1\ \mu\text{L}$ . The QqTOFMS was calibrated with a sodium formate solution in HPC mode after waiting 30 min for the system to stabilize. The mass drift was monitored and all analyses were done within 4 h of the calibration. No lock mass solution was used. In these conditions, full width at half-maximum mass resolution ( $R_{\text{FWHM}}$ ) at  $m/z\ 455$  was about 25 000.

*Liquid Chromatography-Quadrupole-Orbital Ion Trap Mass Spectrometry (LC-QqOrbitrap MS).* The instrument used in these experiments was composed of a Dionex Ultimate 3000 Rapid Separation System ultrahigh performance liquid chromatograph coupled to a Q-Exactive hybrid quadrupole-orbital ion trap mass spectrometer (QqOrbitrapMS) both manufactured by Thermo (USA). LC conditions were the same as for the LC-QqQMS setup. Injection volume was  $2\ \mu\text{L}$ . As for the QqOrbitrapMS parameters, the ion source was ESI in positive mode, spray voltage was at 4.2 kV, capillary temperature was at  $300\text{ }^{\circ}\text{C}$ , sheath gas was 50 arbitrary units and auxiliary gas was 25 arbitrary units.  $R_{\text{FWHM}}$  was set to 70 000 or 140 000 at  $m/z\ 400$ . Mass range was  $m/z\ 200\text{--}1000$ . The instrument was calibrated using the calibrant solution recommended by the manufacturer, a solution containing *n*-butylamine, caffeine, the tripeptide MRFA and Ultramark 1621, a mixture of fluorinated phosphazines.

**Software Parameters.** Raw profile data of the mass spectrum of the test analytes spiked in MeOH and river water samples were extracted from acquisition files and processed in MassWorks (Cerno Bioscience, USA). This software uses two algorithms for the determination of spectral accuracy and formula ranking: calibrated line shape isotope profile search (CLIPS) and self-calibrated line shape isotope profile search (sCLIPS). The former is used for low resolution data and the latter for high-resolution data. Parameters for both algorithms are shown on Table 1. As the analyses were performed with electrospray ionization in the positive ionization mode, the observed charges were mainly +1 ( $[M + H]^+$ ). Doubly charged species were only observed for ROX, albeit it was not the major ion. Mass tolerance was highly dependent on the type of calibration used for the CLIPS algorithm. For the internal calibration with CLIPS, it was







Table 3. Formula Ranking Results for the Test Compounds in the Three Different Mass Analyzers Employed<sup>a</sup>

compounds	QqQMS ( $R_{\text{FHWM}} = 25\text{K}$ )						QqOrbitrapMS ( $R_{\text{FHWM}} = 70\text{K}$ )						QqOrbitrapMS ( $R_{\text{FHWM}} = 140\text{K}$ )								
	MeOH		matrix		MeOH		matrix		MeOH		matrix		MeOH		matrix		MeOH		matrix		
	300 $\mu\text{g L}^{-1}$	80 $\mu\text{g L}^{-1}$	300 $\mu\text{g L}^{-1}$	80 $\mu\text{g L}^{-1}$	300 $\mu\text{g L}^{-1}$	80 $\mu\text{g L}^{-1}$	300 $\mu\text{g L}^{-1}$	80 $\mu\text{g L}^{-1}$	300 $\mu\text{g L}^{-1}$	80 $\mu\text{g L}^{-1}$	300 $\mu\text{g L}^{-1}$	80 $\mu\text{g L}^{-1}$	300 $\mu\text{g L}^{-1}$	80 $\mu\text{g L}^{-1}$	300 $\mu\text{g L}^{-1}$	80 $\mu\text{g L}^{-1}$	300 $\mu\text{g L}^{-1}$	80 $\mu\text{g L}^{-1}$	300 $\mu\text{g L}^{-1}$	80 $\mu\text{g L}^{-1}$	
ATZ (215)	3 ± 2	1	3.3 ± 0.6	1	1	1	1	1	1	1	1	1	1	1	1	1	1	1	1	1	1
SMX (253)	127 ± 103	1	107 ± 66	1	1	1	1	1	1	1	1	1	1	1	1	1	1	1	1	1	1
MTP (267)	NA	1	NA	1	1	1	1	1	1	1	1	1	1	1	1	1	1	1	1	1	1
TRI (290)	9 ± 8	1	47 ± 69	1	1	1	1	1	1	1	1	1	1	1	1	1	1	1	1	1	1
FLX (309)	NA	1 ± 1	NA	1	1	1	1	1	1	1	1	1	1	1	1	1	1	1	1	1	1
OFL (361)	NA	3 ± 2	NA	2 ± 1	1 ± 1	1	1 ± 1	1	1 ± 1	1	1 ± 1	1	1	1	1	1	1	1	1	1	1
MTX (454)	218 ± 110	5 ± 3	1177 ± 858	1	8 ± 3	2 ± 1	7 ± 1	5 ± 2	9 ± 1	2 ± 1	2 ± 1	6 ± 2	8 ± 1	7 ± 2	8 ± 1	7 ± 2	8 ± 1	7 ± 2	8 ± 1	7 ± 2	8 ± 1
JOS (827)	NA	25 ± 24	NA	3 ± 1	34 ± 33	11 ± 12	1	1 ± 1	2 ± 1	2 ± 1	1	1	1	2 ± 2	1	2 ± 2	1	2 ± 2	1	2 ± 2	2 ± 1
ROX (837)	57 ± 15	2 ± 2	48 ± 17	2 ± 1	4 ± 2	2 ± 1	1	1	1	1	1	1 ± 1	1	1	1 ± 1	1	1	1	1	1	1

<sup>a</sup>NA: Not available. Uncertainty for all values represents standard deviation of three replicate injections. When uncertainty is absent, standard deviation was zero.

Table 4. Spectral Accuracy Results for the Test Compounds in the Three Different Mass Analyzers Employed<sup>a</sup>

compounds	QqTOFMS ( $R_{\text{FHWM}} = 25\text{K}$ )						QqOrbitrapMS ( $R_{\text{FHWM}} = 70\text{K}$ )						QqOrbitrapMS ( $R_{\text{FHWM}} = 140\text{K}$ )								
	MeOH		matrix		MeOH		matrix		MeOH		matrix		MeOH		matrix		MeOH		matrix		
	300 $\mu\text{g L}^{-1}$	80 $\mu\text{g L}^{-1}$	300 $\mu\text{g L}^{-1}$	80 $\mu\text{g L}^{-1}$	300 $\mu\text{g L}^{-1}$	80 $\mu\text{g L}^{-1}$	300 $\mu\text{g L}^{-1}$	80 $\mu\text{g L}^{-1}$	300 $\mu\text{g L}^{-1}$	80 $\mu\text{g L}^{-1}$	300 $\mu\text{g L}^{-1}$	80 $\mu\text{g L}^{-1}$	300 $\mu\text{g L}^{-1}$	80 $\mu\text{g L}^{-1}$	300 $\mu\text{g L}^{-1}$	80 $\mu\text{g L}^{-1}$	300 $\mu\text{g L}^{-1}$	80 $\mu\text{g L}^{-1}$	300 $\mu\text{g L}^{-1}$	80 $\mu\text{g L}^{-1}$	
ATZ (215)	90 ± 2	91 ± 1	98.5 ± 0.5	98.9 ± 0.1	98.96 ± 0.04	98.8 ± 0.7	97.7 ± 0.2	97.27 ± 0.04	97.5 ± 0.4	97.6 ± 0.2	97.08 ± 0.05	95.8 ± 0.2	97.3 ± 0.2	96.5 ± 0.2	97.3 ± 0.2	96.5 ± 0.2	95.8 ± 0.2	97.3 ± 0.2	96.5 ± 0.2	97.3 ± 0.2	96.5 ± 0.2
SMX (253)	86 ± 10	94 ± 4	97.0 ± 0.5	98.5 ± 0.7	97.5 ± 0.5	91 ± 6	85.7 ± 0.5	95.8 ± 0.2	98.2 ± 0.4	98.7 ± 0.1	88 ± 1	95.8 ± 0.3	98 ± 1	98.8 ± 0.1	98 ± 1	98.8 ± 0.1	95.8 ± 0.3	98 ± 1	98.8 ± 0.1	98 ± 1	98.8 ± 0.1
MTP (267)	NA	NA	98.45 ± 0.02	96 ± 1	98.5 ± 0.2	97 ± 5	98.8 ± 0.5	98.2 ± 0.04	99.55 ± 0.08	98.2 ± 0.6	98.3 ± 0.2	96.7 ± 0.8	98.88 ± 0.03	96.0 ± 0.3	98.88 ± 0.03	96.0 ± 0.3	96.7 ± 0.8	98.88 ± 0.03	96.0 ± 0.3	98.88 ± 0.03	96.0 ± 0.3
TRI (290)	97 ± 1	97 ± 1	97.98 ± 0.09	96 ± 1	98.6 ± 0.2	99.3 ± 0.2	97.70 ± 0.08	98.0 ± 0.2	98.5 ± 0.3	97.3 ± 0.8	98.1 ± 0.1	95.0 ± 0.8	98.2 ± 0.4	95 ± 1	98.2 ± 0.4	95 ± 1	95.0 ± 0.8	98.2 ± 0.4	95 ± 1	98.2 ± 0.4	95 ± 1
FLX (309)	NA	NA	97.0 ± 0.4	97.4 ± 0.2	99.1 ± 0.1	97 ± 3	95.2 ± 0.4	98.6 ± 0.1	99.60 ± 0.06	99.3 ± 0.2	98 ± 1	98.90 ± 0.05	99.5 ± 0.1	99.13 ± 0.06	99.5 ± 0.1	99.13 ± 0.06	98.90 ± 0.05	99.5 ± 0.1	99.13 ± 0.06	99.5 ± 0.1	99.13 ± 0.06
OFL (361)	NA	NA	93.17 ± 0.08	99.32 ± 0.07	98.7 ± 0.2	96 ± 6	96.6 ± 0.4	98.07 ± 0.02	98.4 ± 0.5	98.0 ± 0.3	93 ± 1	97.42 ± 0.07	99.03 ± 0.02	95.4 ± 0.4	99.03 ± 0.02	95.4 ± 0.4	97.42 ± 0.07	99.03 ± 0.02	95.4 ± 0.4	99.03 ± 0.02	95.4 ± 0.4
MTX (454)	82 ± 9	86 ± 5	89 ± 6	92.2 ± 0.2	93.3 ± 0.2	97.9 ± 0.5	97.4 ± 0.6	97.82 ± 0.07	96.8 ± 0.1	98.52 ± 0.06	96.7 ± 0.2	96.501 ± 0.009	97.1 ± 0.2	97.2 ± 0.1	97.1 ± 0.2	97.2 ± 0.1	96.501 ± 0.009	97.1 ± 0.2	97.2 ± 0.1	97.1 ± 0.2	97.2 ± 0.1
JOS (827)	NA	NA	92.19 ± 0.06	99.2 ± 0.1	96.8 ± 0.3	97 ± 2	99.5 ± 0.1	99.5 ± 0.1	99.0 ± 0.2	99.2 ± 0.1	99.29 ± 0.07	99.53 ± 0.02	99.5 ± 0.1	99.5 ± 0.1	99.5 ± 0.1	99.5 ± 0.1	99.53 ± 0.02	99.5 ± 0.1	99.5 ± 0.1	99.5 ± 0.1	99.5 ± 0.1
ROX (837)	93 ± 3	95 ± 2	93.3 ± 0.1	99.2 ± 0.1	98.1 ± 0.1	98 ± 1	99.46 ± 0.06	99.46 ± 0.02	99.3 ± 0.1	99.22 ± 0.08	99.4 ± 0.2	99.3 ± 0.1	99.4 ± 0.1	99.65 ± 0.04	99.4 ± 0.1	99.65 ± 0.04	99.3 ± 0.1	99.4 ± 0.1	99.65 ± 0.04	99.4 ± 0.1	99.65 ± 0.04

<sup>a</sup>NA: Not available. Uncertainty for all values represents standard deviation of three replicate injections. When uncertainty is absent, standard deviation was zero.

and spectral accuracy for OFL could be explained by signal enhancement caused by coeluting sample components, which has been reported previously<sup>17,18</sup> and resulted in an improved signal-to-noise ratio. The peak area for OFL was indeed about 3 to 20 times higher in the matrix compared to the MeOH solution (Table SI-2). Matrix effects were quantified by calculating the ratio of peak areas for a test compound in the matrix and MeOH. Thus, for the results presented in Table SI-2, area ratios >1 indicate signal enhancement and area ratios <1 signal suppression. Signal enhancement occurs because matrix components that coelute with target compounds can improve access to the droplet surface during the electrospray ionization process and thus increase ionization efficiency.<sup>17</sup> The opposite effect, known as signal suppression, was also observed during the experiments. Signal suppression can be significant (up to 90%) in some cases in other environmental waters such as hospital and wastewater influents.<sup>19</sup> While these matrix effects can be hardly predicted, they could be reduced by modification in the sample preparation and the chromatographic separation.

**Impact of Analyte Concentration on Spectral Accuracy and Formula Ranking on QqTOFMS Data.** Results in Table 3 show that concentration (80 vs 300  $\mu\text{g L}^{-1}$  spiked in the river water matrix) was an important factor in deciding the correct formula rank for the larger compounds (>350 Da). For smaller compounds (<350 Da), the lower number of possible outcomes for a given accurate mass requires less spectral accuracy for correct formula identification. This was especially true for ATZ and SMX which have very recognizable features due to their Cl and S atoms, respectively. Spectral accuracy of MTX (454 Da) (Table 4) was the most affected by concentration, from 90.7%  $\pm$  0.9% in the 80  $\mu\text{g L}^{-1}$  matrix solution to 97.9%  $\pm$  0.5% in the 300  $\mu\text{g L}^{-1}$  matrix solution. For the other compounds, differences were <4 percentage points. This can be explained by a higher signal for the M+2 and M+3 peaks which allows for a more thorough comparison of the calibrated experimental and theoretical peaks in MassWorks. When peak intensities were <800 counts, major discrepancies are observed between the calibrated experimental and theoretical peaks. These differences result in much lower overall spectral accuracy and less confidence in formula determination. Since the signals for the other compounds were relatively higher than those of MTX in the 80  $\mu\text{g L}^{-1}$  matrix solution, the increase in concentration had a less noticeable effect. Finally, for SMX and OFL, standard deviations >5 percentage points in spectral accuracies were observed. SMX standard deviation was indeed almost 4 times larger in the 300  $\mu\text{g L}^{-1}$  solution compared to the 80  $\mu\text{g L}^{-1}$  solution. Such high variation is due to an outlier value. When the outlier replicate was removed, the variation in spectral accuracy was within 2 percentage points.

**Impact of Mass Analyzer Resolution on Spectral Accuracy and Identification.** *Triple Quadrupole Mass Spectrometer (QqQMS).* Measurements with QqQMS were done using both internal and external mass calibrations. Better results were obtained using internal mass calibration and are discussed here. Results obtained using external calibration are discussed in the Supporting Information (section SI-1).

Mass accuracy results obtained after post-acquisition internal calibration and determination of molecular formulas based on the CLIPS algorithm can be seen in Table 2. For all compounds, average mass accuracy was  $\leq 5$  ppm. As expected, better mass accuracy was obtained in both QqTOFS and

QqOrbitrapMS, but it is remarkable that a QqQMS can attain such low errors in measuring accurate masses. However, concentration had a major impact on both ranking and spectral accuracy on the QqQMS data. In fact, it was possible to obtain meaningful data only for the samples spiked at 300  $\mu\text{g L}^{-1}$  (Tables 3 and 4). In general, the matrix slightly increased spectral accuracy but rank was not significantly affected. As explained previously, the higher spectral accuracy in the river matrix could be explained by signal enhancement during the ESI process, in which the coeluting compounds improve ionization efficiency. As it can be seen in the Supporting Information Table SI-2 for QqQMS data, matrix/MeOH area ratios were between 1.2 and 2.8, indicating that signal enhancement due to the matrix, were observed for all compounds except for ROX (0.9). However, for TRI and MTX, lower rankings despite the matrix induced signal enhancement were observed. These results illustrate the two opposite effects of the matrix on spectral accuracy and formula ranking: (1) ions of coeluting matrix compounds with overlapping  $m/z$  values with the compound of interest may affect intensities of the isotopic pattern and thus lower spectral accuracy and ranking and (2) ions of coeluting matrix compounds of different  $m/z$  from the compound of interest may increase spectral accuracy and formula ranking by increasing the signal-to-noise ratio of the all the peaks of the isotopic pattern.

As shown in Table 3, obtained rankings were not good enough to allow acceptable certainty in formula determination in most cases. Therefore, these results suggest that the use of a QqQMS for the measurement of accurate masses and spectral accuracy of small organic molecules at low concentrations in complex matrices seems to be very challenging. Nevertheless, it could be very helpful for other routine applications that use simpler matrices and compounds at higher concentrations, e.g. monitoring and confirmation of organic synthesis products or impurity and degradation identification in pharmaceutical products.

*Quadrupole-Orbital Ion Trap Mass Spectrometer (QqOrbitrapMS).* Mass accuracy and ranking results at 80 and 300  $\mu\text{g L}^{-1}$  in MeOH and the matrix solution obtained with QqOrbitrapMS at  $R_{\text{FWHM}} = 70$  K and 140 K are shown in Table 2 and 3, respectively. As expected, mass accuracy for the QqOrbitrapMS were generally lower or equal than 2 ppm. Concerning ranking, both low mass compounds (<350 Da) and high mass compounds (between 350 and 837 Da) were not affected by resolution considering that rankings were consistently in the top ten for both resolutions. Generally, lower spectral accuracy was observed for the low mass compounds compared to the high mass compounds, but it did not appear to be affected by resolution at lower concentration. For MTP, TRI and OFL in the matrix samples spiked at the higher concentration (300  $\mu\text{g L}^{-1}$ ), the largest drops in spectral accuracy, caused by an increase in resolution were between 2.2 to 2.7 percentage points. Those differences were statistically significant at the 95% confidence level according to the  $t$  test. Such a reduction in spectral accuracy is only about half of that reported by a previous study using a linear ion trap-orbital ion trap mass spectrometer,<sup>12</sup> where the spectral accuracy of polar organic compounds (masses between 639 to 1664 Da) was higher ( $\geq 97\%$ ) at  $R_{\text{FWHM}} = 7.5$  K than that obtained at  $R_{\text{FWHM}} = 100$  K (<90%). According to the authors of that study, high resolution hinders high spectral accuracy in the orbitrap mass spectrometer. The authors explained those results as the consequence of a phenomenon called "isotope beating". That phenomenon results from destructive interference of signals having close  $m/z$  values, for example, isotopic peaks of

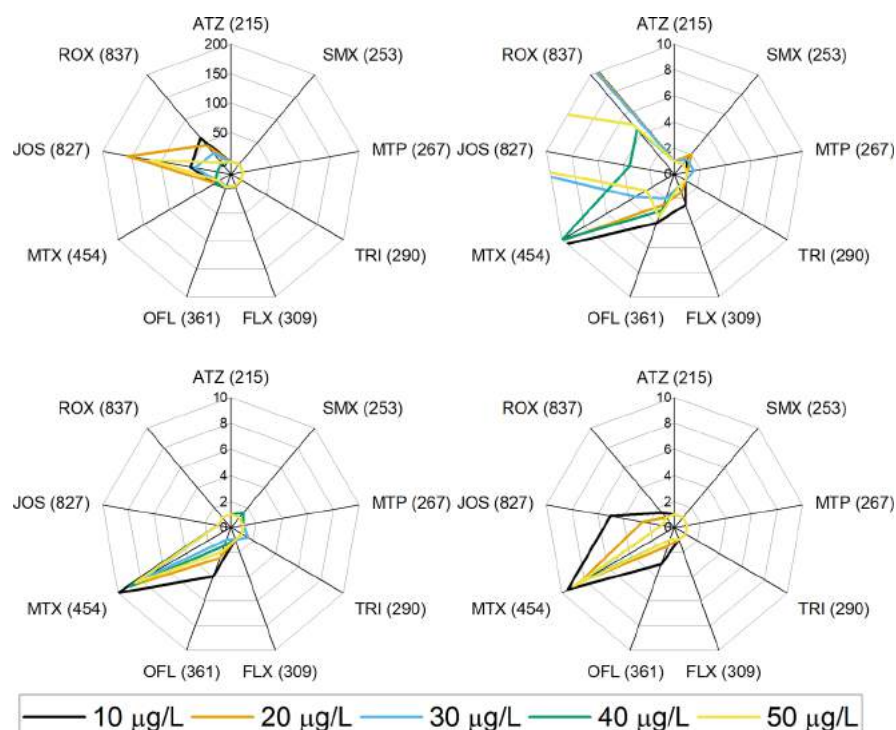


**Figure 2.** Radar plots representing mean formula ranking for the target micropollutants in spiked matrix samples. Top left: QqTOFMS ( $R_{\text{FWHM}} = 25$  K). Top right: QqTOFMS results zoomed in. Bottom left: QqOrbitrapMS ( $R_{\text{FWHM}} = 70$  K). Bottom right: QqOrbitrapMS ( $R_{\text{FWHM}} = 140$  K).

multiply charged ions or closely located isotopes under a given isotope cluster, such as  $M + 3$ , and produce errors in the measurement of isotopic abundances.<sup>20</sup> Such effects have been observed with polymers in ion cyclotron resonance mass spectrometers (ICRMS)<sup>20</sup> and may also be present in the QqOrbitrapMS, which is also an ion trap mass analyzer using Fourier transform signal conversion. Interestingly, such negative correlation between resolution and spectral accuracy was not observed in the present study for compounds with the highest molecular masses (ROX, JOS). It is likely that such issues have been either reduced or corrected in the newer orbital ion trap models, especially at the high masses ( $m/z > 800$ ). It is possible that enhanced Fourier transform for orbitrap mass spectrometry, introduced in 2014, brought some amelioration in peak shape with the addition of apodization and triple zero-filling. These notably helped reducing spectral leakage and side lobes around peaks.<sup>20</sup> Another possibility, proposed by Xu et al.,<sup>14</sup> is the effect of the reduced-profile mode for the recording of mass spectra in orbitraps. In that mode, the noise is subtracted from the acquired mass spectra to reduce raw file size. This signal processing can lead to underestimation of the abundance of  $M + n$  peaks, thus reducing spectral accuracy. It has yet to be confirmed how all these factors played a major role in reducing spectral accuracy with higher resolutions, and it is out of the scope of this article.

Although QqTOFMS are known to measure isotopic patterns very precisely<sup>8</sup> and accurately<sup>13</sup> compared to other mass analyzers, results showed that better spectral accuracies for the tested compounds were obtained with the QqOrbitrapMS at  $R_{\text{FWHM}} = 70$  K and 140 K than with the QqTOFMS at  $R_{\text{FWHM}} = 25$  K. As it can be seen in Table 4, in the data acquired with the QqTOFMS employing the matrix spiked at  $300 \mu\text{g L}^{-1}$ , only 3 out of 9 test compounds had average spectral accuracy  $\geq 98\%$ , while in the QqOrbitrapMS data ( $R_{\text{FWHM}} = 70$  K), 7 out of 9 compounds had average spectral

accuracy  $\geq 98\%$ . Formula rankings were also better with the QqOrbitrapMS at both resolutions compared to the QqTOFMS.

It would be interesting to perform experiments at ultrahigh resolution with an ICRMS to see the effect of full separation of the isotope fine structure on spectral accuracy and formula ranking. Nevertheless, the sCLIPS algorithm does already factors in unresolved isotope fine structures in the calculation of mass accuracy since it takes into account instrument resolution to calibrate the mass spectrum signal.

An important observation from the QqOrbitrapMS results shown in Tables 2 and 3 is that low spectral accuracy (e.g.,  $< 98\%$ ) does not necessarily mean a low ranking as some compounds consistently get low spectral accuracies, in our case SMX data clearly illustrates that. It seldom or never had  $> 98\%$  spectral accuracy but it was always ranked first nevertheless. Since there are less possible formulas for compounds with low molecular masses for a given accurate mass compared to compounds with high molecular masses, the former requires less spectral accuracy for correct formula identification than the latter.

#### Lower Concentration Limits for the Measurement of Spectral Accuracy in Environmental Samples.

Solutions of lower concentrations, ranging from 50 to  $10 \mu\text{g/L}$ , equivalent to environmental concentrations of  $0.38$  to  $1.9 \mu\text{g L}^{-1}$  considering solid-phase extraction preconcentration factor, were analyzed with the intent to assess a minimum working concentration for spectral accuracy. Rankings and spectral accuracies can be seen in Figures 2 and 3, respectively. In the QqTOFMS, the larger compounds such as ROX and in particular JOS were heavily affected by the drop of signal intensity. JOS notably had very low signal intensity; thus  $M+2$  peaks and onward were undistinguishable. Very high variability in the rankings was also observed in the cases of JOS (4–157) and, to a lesser degree, ROX (5–61). ROX did however improve significantly in ranking at 40 and  $50 \mu\text{g L}^{-1}$ . ROX signal intensity was also much superior to that of JOS (16 500 counts at apex at  $50 \mu\text{g L}^{-1}$



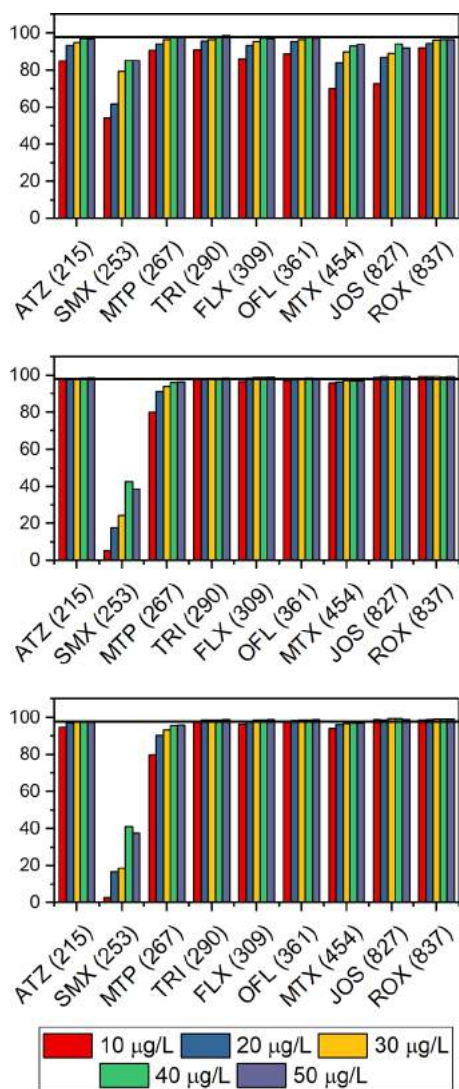


**Figure 3.** Bar plots representing mean spectral accuracy for the target micropollutants in spiked matrix samples. Top: QqTOFMS ( $R_{\text{FHWM}} = 25$  K). Middle: QqOrbitrapMS ( $R_{\text{FHWM}} = 70$  K). Bottom: QqOrbitrapMS ( $R_{\text{FHWM}} = 140$  K). Straight line indicates the threshold of high spectral accuracy (98%). The same sample was injected twice.

compared to 2300 in the same conditions respectively);  $M + 2$  and  $M + 3$  were well-defined. Rankings were never lower than 4 for ATZ, SMX, MTP, TRI, FLX, and OFL in all instances. MTX ranking varied from 3 to 12.

Those lower concentrations mixtures were also analyzed with the QqOrbitrapMS at both 70 K and 140 K resolutions. Ranking and spectral accuracy results can be seen in Figures 2 and 3, respectively. Data showed excellent rankings (within top 5) for all compounds at all concentrations in both resolutions. Except for MTX, which ranked consistently over 5. OFL had higher ranking at the lower concentrations for both resolutions. JOS was also affected at 140K resolution for the 10 and 20  $\mu\text{g L}^{-1}$ . Spectral accuracies were low for SMX, between 5.6% and 38.7% for 70 K. and between 3.0% and 37.7% for 140 K. This was caused by an impurity of high intensity at  $m/z$  256, which although well separated from the  $M + 2$  peak, lowered the match between calibrated and theoretical isotopic patterns of SMX. This impurity was not observed in the QqTOFMS data, thus spectral accuracy for SMX on that instrument was superior (54.2–85.1%) than in the QqOrbitrapMS.

As discussed in the previous sections, adequate measurement of spectral accuracy depends on many factors such as nature of the compound, matrix composition and even the chromatographic and sample preparation methods employed. Therefore, the lower concentration limits for the measurement of spectral accuracy can be improved by using more selective solid-phase extraction or by improving the chromatographic separation of analytes from coeluting matrix compounds having overlapping  $m/z$  values with the compound of interest. In summary, as long as the isotopic pattern is free of interferences and significantly higher than the noise, measurement of spectral accuracy will yield a dependable value that could be used to improve the level of confidence in the assignment of a molecular formula to an accurate mass.

**Rules and Limitations.** Comparison of spectral accuracy to other techniques used for formula determination showed that the algorithms used by MassWorks obtained better ranking of the correct formula of larger compounds (>350 Da), and it was more robust when using lower intensity signals (Supporting Information, section SI-4). However, this spectral accuracy determination has also a few drawbacks. Computing time necessary for determination of ranking and spectral accuracy of the high mass compounds such as JOS (827 Da) and ROX (837 Da) was the biggest downside found in this technique. Depending on the computer performance, the time to generate thousands of formula candidates could go up to 40 min if limitations were not made. Atoms like F and P being monoisotopic means they can be fitted in most formulas while a compound with high  $M+1$  relative abundance like Si compensated for the lack of  $M+1$  distribution from the inclusion of F and P. This results in a high number of generated formulas with low C and H and high Si and P, which are not realistic. In cases where a broad range of atoms are allowed in the formulas, pre- and post-research rules need to be defined to optimize formula generation using MassWorks. First, one must observe the mass spectra and visually assess the presence or absence of Cl and Br in the compounds. These two atoms are very distinct with unmistakable isotope patterns and they could be withdrawn from the allowed atom list if abundant  $M + 2$ ,  $M + 4$ , or higher isotopes are not observed. Such procedure will divide by two the total number of generated formulas and thus save computing time. Additionally, the maximum number of C for a formula using the empirical parameters (Seven Golden Rules) needs to be used with utmost caution since it may exclude the correct formula from consideration. It was observed in one case that the empirical parameters on MassWorks underestimated the maximum number of C on a formula and the correct formula did not appear in the list. Such event was observed with a background contaminant, the plasticizer diisooctyl phthalate ( $\text{C}_{24}\text{H}_{38}\text{O}_4$ ), where the maximum number of C was 23 based on the empirical rules implemented while the compound has 24 C. Setting a more reasonable minimum number of C also helps to reduce the number of generated formulas and saves computing time. A corresponding number of H can be added for the minimum and maximum values. A maximum H/C ratio of 2 was found to help reduce the number of formulas. P tends to be inserted in all formulas and can be monitored by a O/P ratio of minimum 3 as it mainly occurs in the form of organophosphates with high O per P; double bond equivalents (DBE) then also should be monitored as a P–O double bond implies a higher DBE. Na or K adducts were not observed for the selected compounds in this work, but adding them to the allowed atoms might help to uncover the accurate formula in

case positive alkaline adducts are formed. Adjusting pre-search parameters is not necessary with smaller molecules as there are only few possibilities for a compound with a narrow mass error window. Finally, lack of automation is also an issue as each compound mass spectrum needs to be evaluated individually.

## CONCLUSION

This study showed that spectral accuracy is a powerful tool for the determination of chemical formulas from accurate mass data. Spectral accuracy allowed to reduce the number of likely molecular formulas for organic micropollutants of relative high molecular mass (e.g., between 400 and 900 Da) to less than 10, and in some cases, it assigned unambiguously one specific molecular formula to an experimental isotopic pattern. Experiments showed that the major parameter affecting spectral accuracy and correct formula ranking for a set of common organic micropollutants is signal intensity. Thus, conditions increasing signal intensity, such as signal enhancement by the matrix and higher compound concentration, favored higher spectral accuracy and ranking of the correct molecular formula. A significant improvement of both ranking and spectral accuracy was also obtained with higher mass resolution of the mass analyzer. Contrary to a previous study,<sup>13</sup> a moderate (~7 percentage points) decrease in spectral accuracy with higher resolution in the orbitrap mass spectrometer was not observed.

Results also showed that high spectral accuracy (e.g., >98%) and identification of the correct molecular formula were not necessarily correlated for low molecular mass compounds (<350 Da). It was however more prevalent for high molecular mass compounds (>350 Da). Using MassWorks software it was possible to acquire accurate mass data with less than 5 ppm mass accuracy in a QqQMS. While the low resolution of the QqQMS impairs accurate mass and spectral accuracy determination in complex matrices such as river water, application of spectral accuracy to routine analyses is of interest for laboratories without access to high resolution MS technology. Experiments demonstrated that for some compounds, high spectral accuracies and rankings can be obtained at concentrations as low as 10  $\mu\text{g L}^{-1}$  and in general, if the isotopic pattern of the compound is free of major interferences and the signal is above the noise of the instrument, it is possible to measure spectral accuracy correctly.

Finally, this study confirmed that spectral accuracy could be used as a complementary technique to eliminate formula candidates corresponding to an observed accurate mass during identification workflows of organic micropollutants based on liquid chromatography-high resolution MS. Thus, spectral accuracy is a powerful tool to elevate level 5 data (accurate mass) to level 4 (unequivocal molecular formula) according to the identification confidence levels proposed by Schymanski et al.<sup>2</sup> In this way, identification of unknowns present in environmental samples can be a more efficient process.

## ASSOCIATED CONTENT

### Supporting Information

The Supporting Information is available free of charge on the ACS Publications website at DOI: 10.1021/acs.analchem.7b01761.

Molecular structures of the test compounds used in this study, external calibration and stability of the QqQMS system, error in spectral accuracy determination, interference rejection, determination of matrix effects in data acquired the three mass spectrometers, and software comparison (PDF)

## AUTHOR INFORMATION

### Corresponding Author

\*Tel: 1-(819) 821-7922. Fax: 1-(819) 821-8019. E-mail: pa.segura@usherbrooke.ca.

### ORCID

Pedro A. Segura: 0000-0002-4552-4903

### Notes

The authors declare no competing financial interest.

## ACKNOWLEDGMENTS

This study was supported by the Natural Sciences and Engineering Research Council of Canada (NSERC) through a Discovery grant awarded to P.A.S. We would like to thank Yongdong Wang and Don Kuehl of Cerno Biosciences for his help with MassWorks software. Funding sources did not have any involvement in the design, experiments, data interpretation, writing, revision, or submission of this study. We would like to thank Thermo Fisher Scientific for providing a generous access to a QqOrbitrapMS.

## REFERENCES

- (1) Boxall, A.; Rudd, M.; Brooks, B.; Caldwell, D.; Choi, K.; Hickmann, S.; Innes, E.; Ostapyk, K.; Staveley, J.; Verslycke, T.; Ankley, G.; Beazley, K.; Belanger, S.; Berninger, J.; Carriquiriborde, P.; Coors, A.; Deleo, P.; Dyer, S.; Ericson, J.; Gagné, F.; et al. *Environ. Health Perspect.* **2012**, *120*, 1221–1229.
- (2) Schymanski, E. L.; Jeon, J.; Gulde, R.; Fenner, K.; Ruff, M.; Singer, H. P.; Hollender, J. *Environ. Sci. Technol.* **2014**, *48*, 2097–2098.
- (3) Gross, J. H. *Mass Spectrometry: A Textbook*, 2nd ed.; Springer: Berlin, Germany, 2011; p 716.
- (4) Eysseric, E.; Bellerose, X.; Lavoie, J.-M.; Segura, P. A. *Can. J. Chem.* **2016**, *94*, 781–787.
- (5) Yuan, M.; Breitkopf, S. B.; Yang, X.; Asara, J. M. *Nat. Protoc.* **2012**, *7*, 872.
- (6) Zhang, Y.; Ren, Y.; Jiao, J.; Li, D.; Zhang, Y. *Anal. Chem.* **2011**, *83*, 3297–3304.
- (7) Cortés-Francisco, N.; Flores, C.; Moyano, E.; Caixach, J. *Anal. Bioanal. Chem.* **2011**, *400*, 3595–3606.
- (8) Kind, T.; Fiehn, O. *BMC Bioinf.* **2007**, *8*, 105.
- (9) García-Reyes, J. F.; Hernando, M. D.; Molina-Díaz, A.; Fernández-Alba, A. R. *TrAC, Trends Anal. Chem.* **2007**, *26*, 828–841.
- (10) Little, J. L.; Cleven, C. D.; Brown, S. D. *J. Am. Soc. Mass Spectrom.* **2011**, *22*, 348–359.
- (11) Little, J. L.; Williams, A. J.; Pshenichnov, A.; Tkachenko, V. J. *Am. Soc. Mass Spectrom.* **2012**, *23*, 179–185.
- (12) Wang, Y.; Gu, M. *Anal. Chem.* **2010**, *82*, 7055–7062.
- (13) Erve, J. C.; Gu, M.; Wang, Y.; DeMaio, W.; Talaat, R. E. *J. Am. Soc. Mass Spectrom.* **2009**, *20*, 2058–2069.
- (14) Xu, Y.; Heilier, J.-F.; Madalinski, G.; Genin, E.; Ezan, E.; Tabet, J.-C.; Junot, C. *Anal. Chem.* **2010**, *82*, 5490–5501.
- (15) Hughes, S. R.; Kay, P.; Brown, L. E. *Environ. Sci. Technol.* **2013**, *47*, 661–677.
- (16) Segura, P. A.; Takada, H.; Correa, J. A.; El Saadi, K.; Koike, T.; Onwona-Agyeman, S.; Ofosu-Anim, J.; Sabi, E. B.; Wasonga, O. V.; Mghalu, J. M.; dos Santos, A. M., Jr.; Newman, B.; Weerts, S.; Yargeau, V. *Environ. Int.* **2015**, *80*, 89–97.
- (17) Taylor, P. J. *Clin. Biochem.* **2005**, *38*, 328–334.
- (18) Segura, P. A.; Gagnon, C.; Sauvé, S. *Anal. Chim. Acta* **2007**, *604*, 147–157.
- (19) Gros, M.; Rodríguez-Mozaz, S.; Barceló, D. *J. Chromatogr. A* **2013**, *1292*, 173–188.
- (20) Lange, O.; Damoc, E.; Wiegand, A.; Makarov, A. *Int. J. Mass Spectrom.* **2014**, *369*, 16–22.



# 利用 LC-MS 和二维色谱相关光谱技术识别 HPLC 色谱图中杂质峰

陈珍珍<sup>1,2,3</sup>, 张斗胜<sup>1</sup>, 王楠<sup>1</sup>, 冯芳<sup>2</sup>, 胡昌勤<sup>1\*</sup>

(1. 中国食品药品检定研究院, 北京 100050; 2. 中国药科大学, 江苏 南京 210009;  
3. 江西省食品药品检验所, 江西 南昌 330046)

**摘要:** 采用二维色谱相关光谱技术, 实现质控 HPLC 方法与 LC-MS 色谱系统色谱峰的相互识别。本文采用 HPLC-DAD (中国药典 2010 版方法) 得到头孢唑肟和头孢地尼混合降解杂质的色谱图, 建立降解杂质标准色谱光谱数据; 采用 LC-MS 的方法结合 MassWorks 软件的应用鉴别出头孢唑肟和头孢地尼的主要降解产物; 通过计算光谱相关性对杂质色谱峰进行归属。色谱二维光谱相关法在不同色谱系统下能够准确定性, 在没有杂质对照品的情况下, 可为质控 HPLC 方法中的杂质峰的归属提供新的途径和新的思路。

**关键词:** 二维色谱相关光谱技术; 头孢唑肟; 头孢地尼

中图分类号: R917

文献标识码: A

文章编号: 0513-4870 (2012) 04-0492-06

## Identification of impurity peaks in the HPLC chromatogram by LC-MS and two-dimensional chromatographic correlation spectroscopy

CHEN Zhen-zhen<sup>1,2,3</sup>, ZHANG Dou-sheng<sup>1</sup>, WANG Nan<sup>1</sup>, FENG Fang<sup>2</sup>, HU Chang-qin<sup>1\*</sup>

(1. National Institutes for Food and Drug Control, Beijing 100050, China; 2. China Pharmaceutical University, Nanjing 210009, China; 3. Jiangxi Provincial Institute For Food and Drug Control, Nanchang 330046, China)

**Abstract:** A novel qualitative analytical method by using two-dimensional chromatographic correlation spectroscopy techniques for recognizing impurity peaks of HPLC methods of quality control and LC-MS chromatographic system was established. The structures of major degradation products of ceftizoxime and cefdinir were identified by LC-MS and MassWorks application; the standard chromatographic and spectral data of the degradation impurities were obtained by high-performance liquid chromatography with diode array detection. The impurity peaks of two-dimensional chromatography were matched by comparison of spectra and calculating correlation coefficients. Peaks in chromatography can be identified accurately and rapidly in different chromatographic systems such as column and mobile phase changed. The method provides a new way and thought to identify the peaks in quality control of impurities without reference impurity substances.

**Key words:** two-dimensional chromatographic correlation spectroscopy; ceftizoxime; cefdinir

对化学药品中的杂质谱分析是当前药品质量控制的热点<sup>[1,2]</sup>。按 ICH 的要求, 对药物中含量大于或等于 0.1% 的杂质的结构均要进行结构确证, 因此在杂质分析中对 HPLC 色谱图中的每个杂质峰进行定性是目前药品杂质谱分析的关键制约因素。LC-MS 分

析是快速鉴别药品中杂质的有效方法, 已广泛用于对药品中杂质<sup>[3-6]</sup>、降解产物<sup>[7-9]</sup>等的分析。但 LC-MS 分析与常规的质控 HPLC 分析所采用的色谱系统不同, 因此在没有杂质对照品的情况下, 很难直接利用 LC-MS 的鉴别结果确定常规质控 HPLC 方法色谱图中的杂质峰。作者采用二维色谱相关光谱技术已经解决了当色谱柱等色谱条件改变时不同色谱图中色谱峰相互识别的技术问题, 在没有对照品的情况下利用色谱峰的 UV 光谱结合相对保留时间可以实现

收稿日期: 2011-10-24; 修回日期: 2011-12-01.

基金项目: 十一五重大新药创制资助项目 (2010ZX09401-403).

\*通讯作者 Tel: 86-10-67095308, E-mail: hucq@nicpbp.org.cn

对色谱峰的定性识别<sup>[10, 11]</sup>。头孢地尼和头孢唑肟均为 2010 版中国药典收载的品种, 采用了 HPLC 法控制其有关物质, 但尚未对分离出的杂质进行归属<sup>[12]</sup>。本文采用 LC-MS 方法鉴别头孢地尼和头孢唑肟中的主要降解杂质; 再利用二维色谱相关光谱技术, 通过对不同分析方法色谱图中色谱峰的 UV 光谱相似性的比较, 确定 LC-MS 方法鉴别出的降解杂质在中国药典方法色谱图中的位置; 在此基础上归纳出质检 HPLC 色谱图中的杂质峰和 LC-MS 结构鉴别结果相关联的一般方法。

## 材料与方 法

**仪器与试剂** 高效液相色谱仪: Dionex P680A HPLC, PDA-100 二极管阵列监测器。LC-MS 系统: Shiseido 液相色谱仪, ABI3200Q TRAP LC/MS/MS 系统。MassWorks™ Version3.0 为美国 Cerno BioScience 公司产品。头孢唑肟和头孢地尼对照品均来自中国食品药品检定研究院。

**HPLC 方法** 按中国药典 (2010 版)<sup>[12]</sup>方法。均采用 Capcell PAK C<sub>18</sub> (250 mm × 4.6 mm ID, 5 μm) 色谱柱; DAD 波长设定为 190~400 nm; UV 检测波长为 254 nm。

**LC-MS 方法** 头孢唑肟: 以 0.01 mol·L<sup>-1</sup> 醋酸铵溶液 (pH 3.6)-(甲醇-乙腈 1:1) (90:10) 为流动相; DP (去簇电压): 37 V, CE (碰撞气能量): 20 V。头孢地尼: 以 0.01 mol·L<sup>-1</sup> 醋酸铵溶液 (pH 5.2) 为流动相 A, (甲醇-乙腈 1:1) 为流动相 B; 梯度洗脱, 95:5 (0 min), 85:15 (20 min), 75:25 (35 min), 95:5 (36 min), 95:5 (45 min); DP: 45 V, CE: 20 V。均采用 BDS HYPERSIL C<sub>18</sub> (250 mm × 4.6 mm ID, 5 μm) 色谱柱; 柱温 30 °C; 流速为 0.8 mL·min<sup>-1</sup>; DAD 波长设定为 190~400 nm; UV 检测波长为 254 nm; 进样量为 20 μL。ESI 正离子检测, 柱后分流比为 1:1; curtain gas (气帘气): 30 psi (1 psi ≈ 6.9 kPa); IS (喷雾针电压): 4 500 V; TEM (温度): 400 °C; GS1 (辅助气): 65 psi; GS2 (辅助气): 60 psi。

### 降解杂质溶液的制备

头孢唑肟降解溶解制备 分别制备以下降解溶液: 质量浓度为 0.5 mg·mL<sup>-1</sup> 头孢唑肟水溶液 (90 °C 水浴加热 30 min), 加 30% 双氧水 2 mL (静置 5 min); 用 0.1 mol·L<sup>-1</sup> 盐酸溶液配制成 0.5 mg·mL<sup>-1</sup> 头孢唑肟溶液 (室温放置 6 h) 和用 0.1 mol·L<sup>-1</sup> 氢氧化钠溶液配制成 0.5 mg·mL<sup>-1</sup> 头孢唑肟溶液 (室温放置 30 min)。取以上降解溶液充分混匀, 即为混合降解溶液。

头孢地尼降解溶液制备 分别制备以下降解溶液: 质量浓度为 1.0 mg·mL<sup>-1</sup> 头孢地尼水溶液 (90 °C 水浴加热 30 min), 加 30% 双氧水 2 mL (静置 20 min); 用 0.1 mol·L<sup>-1</sup> 盐酸溶液配制成 1.0 mg·mL<sup>-1</sup> 头孢地尼溶液 (室温放置 1 h) 和用 0.1 mol·L<sup>-1</sup> 的氢氧化钠溶液配制成 1.0 mg·mL<sup>-1</sup> 头孢地尼溶液 (室温放置 2 h)。取以上降解溶液充分混匀, 即为混合降解溶液。

**数据处理** 将 HPLC-DAD 采集的三维色谱图数据以 ASC II 码的格式导出 (紫外光谱波长范围为 220~400 nm, 步长为 1.0 nm), 扣除空白后进行归一化处理, 作为标准色谱光谱数据。用 DrugChroCorr 软件进行二维相关计算及作图, 在 PC 上运行。

## 结果与讨论

### 1 对头孢唑肟质控 HPLC 方法色谱图中杂质峰的识别

**1.1 中国药典 2010 版方法分析** 采用中国药典头孢唑肟有关物质方法分析混合降解溶液, 可分离出 8 个杂质峰 (图 1), 7 号峰为头孢唑肟峰。其三维色谱图数据扣除空白并归一化处理, 以 ASC II 码的格式保存, 即构成了头孢唑肟降解杂质的标准色谱-UV 光谱库。各种加速降解条件下产生的杂质峰的相对保留时间见表 1, 据此可以初略判断杂质的来源与产生机制。

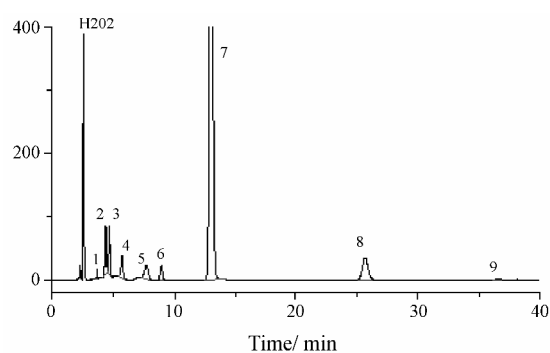


**Figure 1** The chromatogram of mix degradation sample of ceftizoxime under Chinese pharmacopoeia condition. Peaks 1-9 are listed in Table 1. Peak 7: Ceftizoxime

干燥条件下的头孢菌素类药物较稳定, 其水溶液随 pH 和温度不同而易降解。 $\beta$ -内酰胺环是头孢菌素分子中最不稳定的结构, 在一般酸碱催化、中性环境的水分子直接攻击, 其内酰胺环很容易断裂开环。pH 依赖型的立体异构主要有中性或酸性条件下的 C-6 位结构的立体异构、碱性条件下的 C-7 位结构的立体异构和 C-7 位侧链甲氧亚胺键构型的顺反异构。

**Table 1** Relative retention time of impurity peaks in chromatograms under Chinese pharmacopoeia condition

Peak	Degradation sample				
	Mix	H <sub>2</sub> O <sub>2</sub>	Acid	Hydrolysis	Alkaline
1	0.282	0.283			
2	0.336				
3 (F)	0.359	0.359			
4 (A)	0.438				0.435
5 (B)	0.591		0.592		0.593
6 (C)	0.685			0.681	0.685
7 (D)	1.000	1.000	1.000	1.000	1.000
8 (E)	1.972			1.963	1.962
9	2.810				2.790

**1.2 LC-MS 方法分析** 根据一级质谱正负离子扫描得杂质 A 和 B:  $M_r = 401$ ; E 和 C:  $M_r = 383$ ; F:  $M_r = 399$ 。MS 能提供分子离子和分子碎片的质量, 但对分子式的推断有很多不确定性。利用基于同位素峰形校正检索技术 (CLIPS) 的 MassWorks™ 软件可以实现对目标物分子式的准确识别<sup>[13, 14]</sup>。在低分辨率单四级杆液质联用仪上实现了对头孢唑啉水溶液降解杂质元素组成的分析, 进而准确推断出降解杂质的结构<sup>[15]</sup>。

表 2 为目标物经处理所得的分子式。杂质 B、C 和 F 的同位素峰形与目标物的校正同位素峰形的相似度最大, 排在待选分子式的第 1 位, 且其不饱和度 (DBE) 等信息与目标物相符合, 实现了对目标物分子式的准确识别。杂质 A 虽排在第 2 位, 但 MS 得到的是  $[M+H]^+$  的准分子离子峰, 所给出的分子式加 1 个氢, 因此由此分子式算出的不饱和度应不是整数;

排在第 1 位的分子式的 DBE 为 9.0, 而排在第 2 位的分子式的信息与目标物相符合, 故结合不饱和度的信息, 可以确定其为目标物的准确分子式。杂质 E 排在了待选分子式的第 3 位, 但由于杂质 E 为碱降解产物, 其 N 和 O 元素组成与母体化合物相比不会发生太大的变化, 故第 1 位待选分子式可以排除; 根据 DBE 值, 第 2 位待选分子式也可以排除; 而排在第 3 位的分子式的信息与目标物相符合, 即为目标物的准确分子式。从以上结果可知, 杂质 A 和 B 分子式为  $C_{13}H_{15}N_5O_6S_2$ , 杂质 C 和 E 分子式为  $C_{13}H_{13}N_5O_5S_2$ , 杂质 F 的分子式为  $C_{13}H_{13}N_5O_6S_2$ 。

分别进行二级质谱正离子扫描, 杂质 A、B、C、E 和 F 的二级质谱图见图 2。根据碎片离子推断杂质的质谱裂解规律 (图 3), 结合降解机制和已得到的分子式来推断杂质的可能结构式。

杂质 A 和 B 由碱降解得到。其二级质谱图中  $m/z$  358 的碎片峰推测为准分子离子峰 (402) 脱去一分子  $CO_2$ , 碎片峰进一步脱去小分子并环合形成一个六元环, 得到  $m/z$  296 的碎片峰。准分子离子峰发生 A 裂解产生 A1  $m/z$  259 碎片峰。杂质 A 和 B 的二级裂解碎片峰基本一致, 推断可能为同分异构体。

杂质 F 由双氧水降解产生, 分子离子峰比头孢唑啉多 16, 推测头孢唑啉上的硫被氧化成亚砷结构。其二级质谱图中  $m/z$  382 的碎片峰推测为准分子离子峰 (400) 脱去一分子  $H_2O$ 。准分子离子峰的 7 位侧链上的 C-C 键断裂产生了  $m/z$  243 和 156 的碎片峰, 而  $m/z$  243 碎片峰进一步脱去一分子  $H_2O$ , 产生  $m/z$  225 的碎片峰。文献<sup>[4]</sup>报道头孢唑啉有  $M_r$  399 的杂质

**Table 2** Accurate element composition measurement for impurities

Impurity	Rank	M+H	Mono isotope	Mass error		Spectral accuracy	DBE	Formula of target
				mDa	ppm			
A	1	$C_{11}H_{14}N_8O_5S_2$	402.052 9	-0.043 0	-0.107 0	96.920 9	9.0	
	2	$C_{13}H_{16}N_6O_6S_2$	402.054 2	1.299 7	3.232 5	96.786 3	8.5	√
	3	$C_{14}H_{16}N_3O_7S_2$	402.043 0	-9.933 7	-24.707 5	96.695 4	8.5	
B	1	$C_{13}H_{16}N_5O_6S_2$	402.054 2	-6.200 3	-5.421 4	95.523 1	8.5	√
	2	$C_{12}H_{16}N_7O_5S_2$	402.065 4	5.033 0	12.518 1	95.491 3	8.5	
	3	$C_{11}H_{14}N_8O_5S_2$	402.052 9	-7.543 0	-18.760 9	95.472 9	9.0	
C	1	$C_{13}H_{14}N_5O_5S_2$	384.043 6	0.835 0	2.174 1	96.922 3	9.5	√
	2	$C_{11}H_{12}N_8O_4S_2$	384.042 3	-0.507 7	-1.322 0	96.912 3	10.0	
	3	$C_{15}H_{16}N_2O_6S_2$	384.045 0	2.177 6	5.670 3	96.695 0	9.0	
E	1	$C_{12}H_{18}NO_9S_2$	384.042 3	-0.002 4	-0.006 3	96.726 7	4.5	
	2	$C_{11}H_{12}N_8O_4S_2$	384.042 3	-0.007 7	-0.020 1	96.708 1	10.0	
	3	$C_{13}H_{14}N_5O_5S_2$	384.043 6	1.335 0	3.476 1	96.483 7	9.5	√
F	1	$C_{13}H_{14}N_5O_6S_2$	400.038 5	1.549 6	3.873 6	97.742 6	9.5	√
	2	$C_{14}H_{14}N_3O_7S_2$	400.027 3	-9.683 8	-24.207 3	97.732 6	9.5	
	3	$C_{11}H_{12}N_8O_5S_2$	400.037 2	0.206 9	0.517 2	97.596 5	10.0	

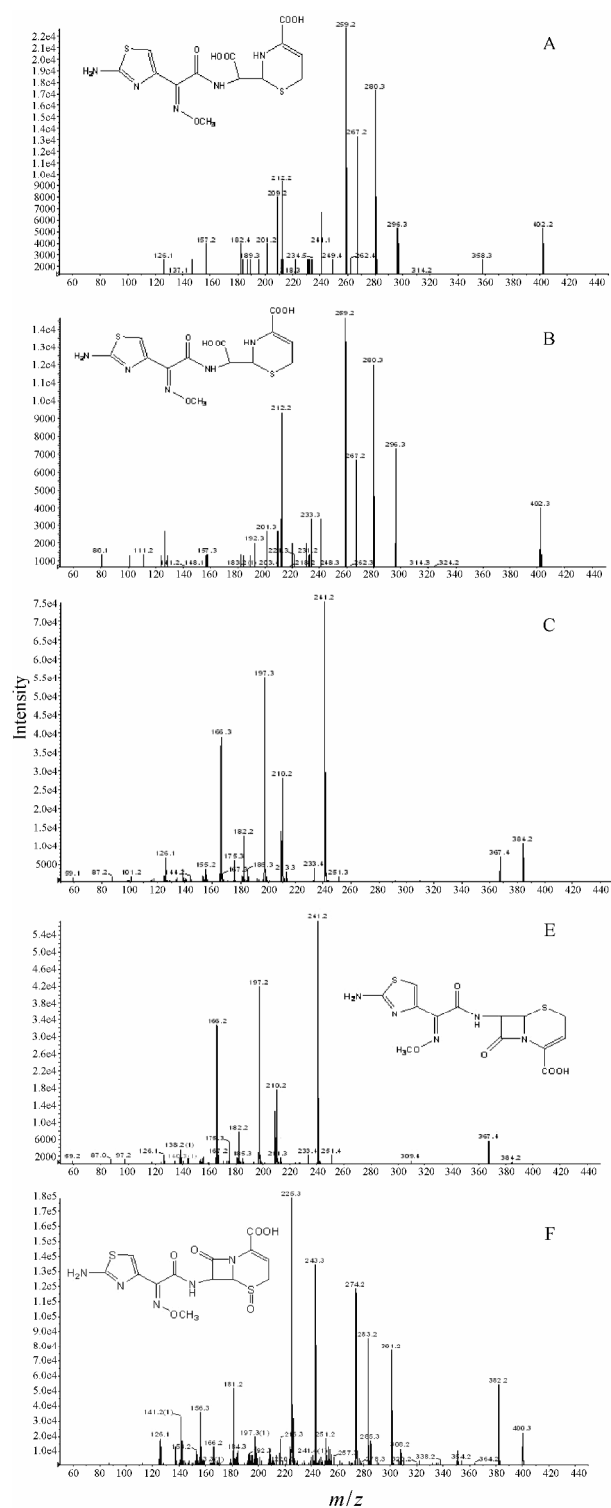


**Figure 2** MS<sup>2</sup> spectra of degradation impurities (A, B, C, E, F represent different degradation impurities under LC-MS condition)

峰且与杂质F有相同的二级碎片离子, 根据以上推断应为杂质F。

杂质E和C由水和碱降解得到, 与头孢唑肟相对分子质量相同, 推测可能为异构体。其二级质谱图中

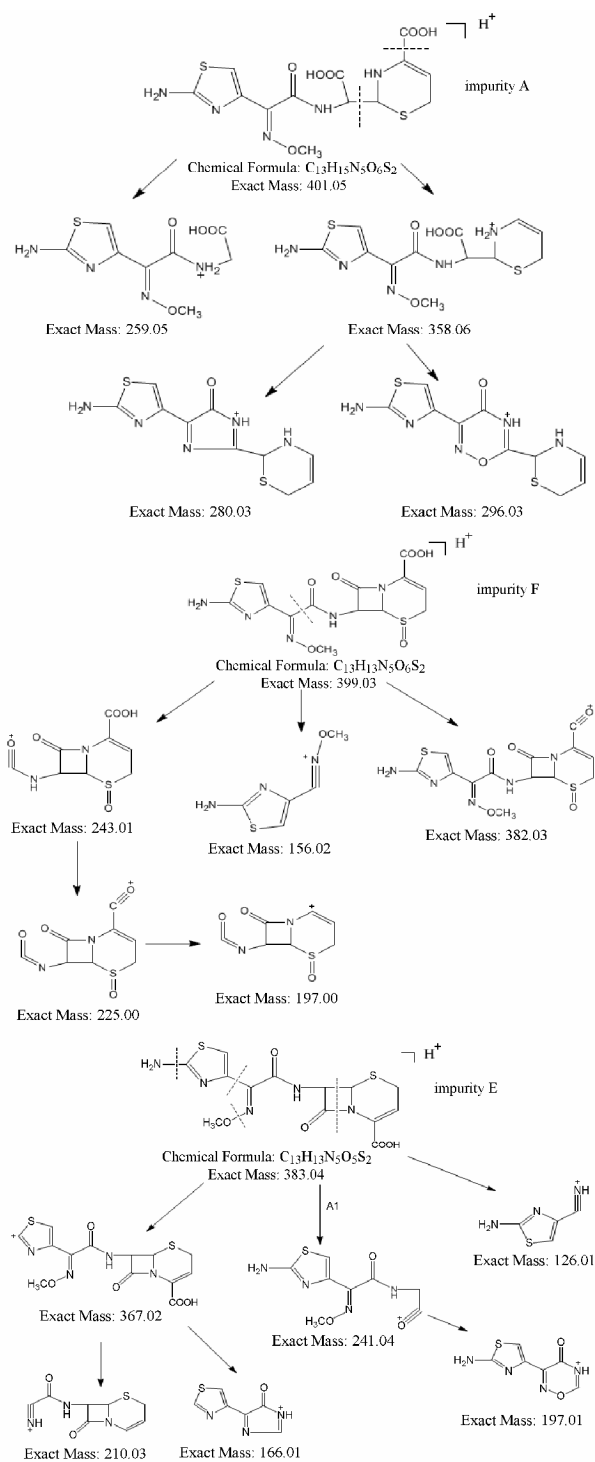


**Figure 3** Proposed fragmentation pathway of impurities (A, E, F represent different degradation impurities under LC-MS condition)

有峰强度很大的  $m/z$  241 碎片峰, 推测为准分子离子峰发生 A 裂解产生的 A1 碎片, 进一步脱去 CO 和 CH<sub>4</sub> 并形成一个六元环  $m/z$  197 的碎片峰。准分子离子峰 (384) 脱去一分子 NH<sub>3</sub> 得到的  $m/z$  367 的碎片峰。文献<sup>[4]</sup>报道头孢唑肟有  $M_r$  383 的杂质, 根据相对保留时间推测杂质 E 为头孢唑肟的反式异构体。



把各降解溶液的三维色谱图数据与头孢唑肟混合降解杂质标准色谱-UV 光谱库进行二维相关分析(图 4), 其中 LC-MS 方法的色谱峰 A~F 分别与混合降解杂质标准色谱图 (Chp2010) 中的色谱峰 4~8 和 3 实现相互识别 (阈值为 0.999)。

## 2 对头孢地尼质控 HPLC 方法色谱图中杂质峰结构的识别

### 2.1 中国药典 2010 版方法分析

采用中国药典头孢地尼有关物质方法分析混合降解溶液, 可分离出 13 个杂质峰, 10 号峰为头孢地尼峰, 得到头孢地尼降解杂质的标准色谱-UV 光谱库。

### 2.2 LC-MS 方法分析

采用 LC-MS 方法, 逐一进样各降解溶液, 进行质谱分析。根据一级质谱正负离子扫描, 得知杂质 C 和 D:  $M_r = 411$ ; A:  $M_r = 395$ 。对目标物经 MassWorks™ 处理所得分子式的结果进行分析。杂质 C 和 D 的同位素峰形与目标物的校正同位素峰形的相似度最大, 排在待选分子式的第 1 位, 且其不饱和度 (DBE) 等信息与目标物相符合, 实现了对目标物分子式的准确识别。杂质 A 排在了待选分子式的第 2 位, 但由于杂质 A 为水降解产物, 其 N 元素组成与母体化合物相比不会发生太大的变化, 故第 1 位

待选分子式 ( $C_{13}H_{14}N_7O_4S_2$ ) 可以排除; 而排在第 2 位的分子式的信息与目标物相符合, 其即为目标物的准确分子式。从以上结果可知杂质 A 分子式为  $C_{14}H_{13}N_5O_5S_2$ , 杂质 C 和 D 分子式为  $C_{14}H_{13}N_5O_6S_2$ 。

分别进行二级质谱正离子扫描, 得到杂质 A、C 和 D 的二级质谱图。

杂质 C 和 D 由过氧化氢降解产生, 推测头孢地尼上的硫被氧化成亚砷结构。其二级质谱图中,  $m/z$  394 的碎片峰推测为准分子离子峰 (412) 脱去一分子  $H_2O$  得到的,  $m/z$  168 的碎片峰, 推测为准分子离子峰的 A 裂解得到的 A2 碎片脱去一分子  $H_2O$  得到的, 而进一步脱去一分子 CO 产生  $m/z$  140 的碎片峰。文献<sup>[5]</sup>报道头孢地尼原料药中存在  $M_r$  411 的杂质峰, 相对保留时间约 0.4 min 与杂质 C 基本相符, 推测杂质 C 与文献报道为同一物质。杂质 D 分子式与二级碎片均与杂质 C 一致, 推断二者为同分异构体。

杂质 A 由水解得到, 与头孢地尼相对分子质量一样, 推测可能为异构体。其二级质谱图中,  $m/z$  227 的碎片峰推测为准分子离子峰 (396) 发生 A 裂解产生的 A1 碎片,  $m/z$  170 碎片峰为 A2 碎片, 进一步脱去一分子的  $H_2O$  为  $m/z$  152 碎片峰。 $m/z$  209 碎片峰

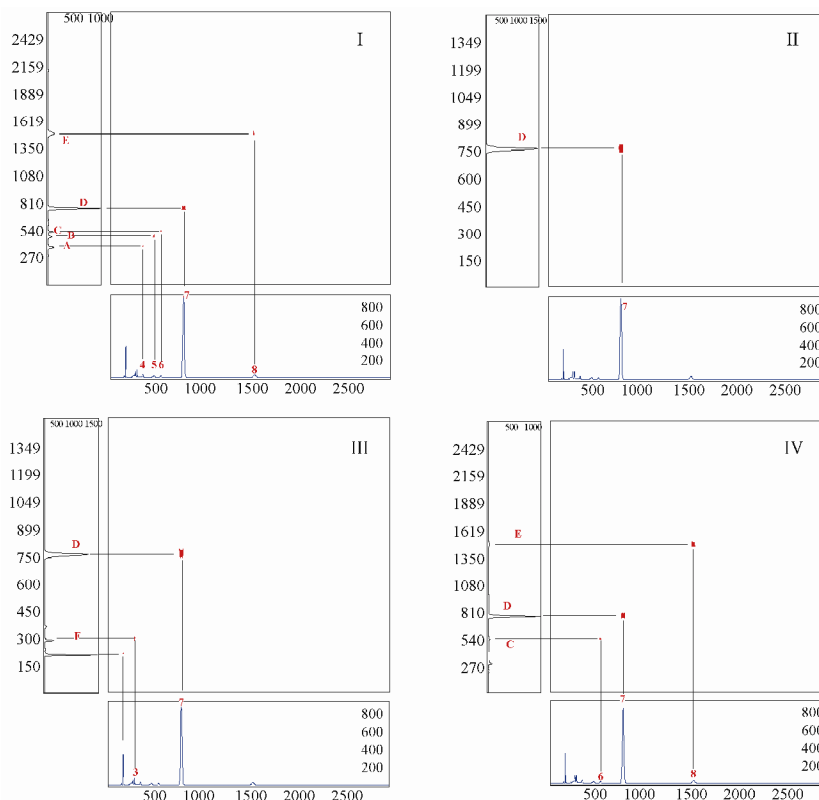


**Figure 4** 2D chromatographic spectral correlative map of degradation samples analyzed in HPLC and LC-MS methods. I: Alkaline; II: Acid; III: Hydrogen peroxide; IV: Hydrolysis

推测为准分子离子峰的 7 位侧链上的 C-C 键断裂进一步脱去一分子的 CO<sub>2</sub> 产生的。美国药典<sup>[16]</sup>报道了 M<sub>r</sub> 395 的杂质, 根据相对保留时间推测杂质 A 为头孢地尼的反式异构体。

把各降解溶液的三维色谱图数据与混合降解杂质标准色谱-UV 光谱库进行二维相关分析, 其中混合降解杂质标准色谱图 (Chp2010) 中的色谱峰 1、3、4、10 和 14 与 LC-MS 方法的色谱峰 B、C、D、E 和 A 实现相互识别 (阈值为 0.999)。

## References

- [1] Görög S. The importance and the challenges of impurity profiling in modern pharmaceutical analysis [J]. *Trends Anal Chem*, 2006, 25: 755–757.
- [2] Hu CQ. Current situation and the trend in impurity control of chemical drugs [J]. *Sci Sin Chim (中国科学: 化学)*, 2010, 40: 679–687.
- [3] Lu CY, Feng CH. Identification of dimer impurities in ampicillin and amoxicillin by capillary LC and tandem mass spectrometry [J]. *Sep Sci*, 2007, 30: 329–332.
- [4] Bharathi C, Prasad CS, Bharathi DV, et al. Structural identification and characterization of impurities in ceftizoxime sodium [J]. *Pharm Biomed Anal*, 2007, 43: 733–740.
- [5] Rao KVVP, Rani A, Reddy AVR, et al. Isolation, structural elucidation and characterization of impurities in cefdinir [J]. *Pharm Biomed Anal*, 2007, 43: 1476–1482.
- [6] Grahek R, Zupancic-Kralj L. Identification of gentamicin impurities by liquid chromatography tandem mass spectrometry [J]. *Pharm Biomed Anal*, 2009, 50: 1037–1043.
- [7] Hu M, Hu CQ. Identification of the components and products of hydrolysis in acetyloucomycin by LC-MS [J]. *Acta Pharm Sin (药学报)*, 2006, 41: 476–480.
- [8] Loke ML, Jespersen S, Vreeken R, et al. Determination of oxytetracycline and its degradation products by high-performance liquid chromatography-tandem mass spectrometry in manure-containing anaerobic test systems [J]. *J Chromatogr B*, 2003, 783: 11–23.
- [9] Hu M, Hu CQ. Identification of the degradation compounds of cefathiamidine by liquid chromatography-tandem mass spectrometry [J]. *Acta Pharm Sin (药学报)*, 2006, 41: 1015–1019.
- [10] Li W, Hu CQ. Spectral correlation of high-performance liquid chromatography-diode array detection data from two independent chromatographic runs peak tracking in pharmaceutical impurity profiling [J]. *J Chromatogr A*, 2008, 1190: 141–149.
- [11] Li W, Hu CQ, Jin SH. Identification of related substances in rifampicin by HPLC-DAD spectroscopy correlation [J]. *Acta Pharm Sin (药学报)*, 2007, 42: 1292–1297.
- [12] State Pharmacopoeia Commission. Pharmacopoeia of the People's Republic of China (中华人民共和国药典) [S]. 2010 ed. Part II. Beijing: China Medical Science Press, 2010.
- [13] Li XS, Li ZA, Wang ZQ, et al. Application of accurate mass and elemental composition determination for pesticides identification using a unit mass resolution gas chromatography/mass spectrometry [J]. *Chem Chin Univ (高等学校化学学报)*, 2010, 31: 2383–2389.
- [14] Erve JCL, Gu M, Wang YD, et al. Spectral accuracy of molecular ions in an LTQ/Orbitrap mass spectrometer and implications for elemental composition determination [J]. *Am Soc Mass Spectrom*, 2009, 20: 2058–2069.
- [15] Qian JQ, Hu CQ. Rapid identification of the degradation products in cefuroxime aqueous solution by HPLC coupled with unit resolution single quadrupole mass spectrometer and calibrated lineshape isotope profile search (CLIPS) [J]. *Chin Pharm Anal (药物分析杂志)*: in press.
- [16] The United States Pharmacopoeial Convention. United States Pharmacopoeia / National Formulary [S]. 2011 ed. Vol. 2. Baltimore: United Book Press, 2011.

## 天然同位素信息在多级质谱裂解规律解析中的应用 ——以磺胺类化合物为例

张海燕<sup>1,2</sup>, 刘鑫<sup>2</sup>, 严华<sup>2</sup>, 李建辉<sup>2</sup>, 韩深<sup>2</sup>,  
张朝晖<sup>2</sup>, 王金花<sup>2</sup>, 许泓<sup>3</sup>, 叶晓霞<sup>1</sup>

(1. 温州医学院药学院, 浙江温州 325000;  
2. 北京出入境检验检疫局检验检疫技术中心食品实验室, 北京 100026;  
3. 天津出入境检验检疫局动植物食品中心, 天津 300000)

**摘要:** 为了更好的对多级质谱裂解信息进行解析, 本研究在多级质谱中应用同位素峰信息进行分子式确证。使用二级质谱中同位素峰丰度比例和峰形信息, 对化合物的质谱裂解碎片分子组成进行预测和推断。通过改变 LTQ Orbitrap XL 仪器的离子阱参数, 将 isolation width 设为 6 u, 使目标母离子的最轻同位素峰和两个较重同位素峰共同裂解, 报道了在二级质谱中获得目标化合物的同位素信息, 并使用这些信息对化合物裂解碎片进行推测。以磺胺甲基嘧啶为例, 通过同位素信息提供的丰度比和峰形信息, 对主要裂解碎片离子进行解析, 大多数结果与文献报道的裂解途径一致, 但对于磺胺甲基嘧啶二级质谱中  $m/z$  65 的碎片离子, 与已发表的文献报道不同, 通过高分辨质谱和同位素丰度比的佐证, 重新对其进行了解析, 证明这是一个不含硫元素的子离子。结果表明, 该方法能够有效减少分子式推测过程中产生的错误备选结果, 可以为多级质谱的解析提供更准确的依据。

**关键词:** ESI; 多级质谱; 同位素分布; 谱图准确度

**中图分类号:** O 657.63 **文献标志码:** A **文章编号:** 1004-2997(2013)05--

**doi:** 10.7538/zpxb.2013.34.05.00

## Elucidation Tandem Mass Fragment Pathway by Isotopic Ion Ratio and Accuracy Mass Measure——An Example in Sulfanilamide

ZHANG Hai-yan<sup>1,2</sup>, LIU Xin<sup>2</sup>, YAN Hua<sup>2</sup>, LI Jian-hui<sup>2</sup>,  
HAN Shen<sup>2</sup>, ZHANG Zhao-hui<sup>2</sup>, WANG Jin-hua<sup>2</sup>, XU Hong<sup>3</sup>, YE Xiao-xia<sup>1</sup>

(1. School of Pharmacy, Wenzhou Medical College, Wenzhou 325000, China;  
2. Food Laboratory of Beijing Inspection and Quarantine Testing Center, Beijing Entry-Exit Inspection  
and Quarantine Bureau, Beijing 100026, China;  
3. Tianjin Entry-Exit Inspection and Quarantine Bureau of Animal and Plant Food Center, Tianjin 300000, China)

**收稿日期:** 2013-02-28; **修回日期:** 2013-05-13

**基金项目:** “十二五”农村领域国家科技计划课题(2011BAD23B05), 质检公益性行业科研专项(201210029), 国家质检总局科研计划项目(2012JK145)资助

**作者简介:** 张海燕(1986~), 女(汉族), 温州人, 硕士研究生, 中药学专业。E-mail: 354751072@qq.com

**通信作者:** 叶晓霞(1969~), 女(汉族), 温州人, 教授, 有机化学专业。E-mail:

**Abstract:** MS/MS isotope ratio and accuracy mass measure were used to further confirm the elemental composition and structural information of molecular formula by performing on an LTQ/Orbitrap. The light and heavy isotopes of target parent ion were detected when setting the ion trap's isolation width at 6 u. We reported the MS/MS isotope ratio and accuracy mass measure were used to elucidate the fragments pathway. Sulfamerazine was used as an example, most of the fragmentations were analyzed by isotopic abundance ratio and peak shape information, the result is as same as literature reported. However, the fragment ion at  $m/z$  65 is different from previous report. According to its accuracy mass measure and isotope abundance ratio, there's no S atom in this ion. The result shows that the proposed isotope distribute fragmentation method is a powerful trick to provide large amounts of the necessary elemental composition to the fragment news of compounds.

**Key words:** ESI; tandem mass spectrometry (MS/MS); isotopic abundance ratio; spectral accuracy

质谱是对未知化合物分子进行定性和解析的重要工具<sup>[1-5]</sup>。通过质谱获得化合物的分子质量信息,可以为确定化合物的元素组成提供一定的帮助,但是要获得化合物的准确分子式仍有相当大的难度。现代的高分辨质谱仪(Orbitrap、Q-TOF 和 FTICR-MS)为未知化合物定性提供了更高的质量精度(质量误差小于  $5 \times 10^{-6}$ ),大大缩小了待选化合物分子式的范围,但对元素组成复杂的化合物,即使质量误差小于  $5 \times 10^{-6}$ ,仍有许多待选分子式<sup>[6]</sup>。为进一步确定化合物的分子组成,应用同位素信息对化合物的分子组成进行判断已成为重要的手段<sup>[7-9]</sup>。应用一级质谱获得同位素分布信息,从而确定化合物分子式的方法已在药物分子<sup>[10]</sup>及代谢产物的鉴定<sup>[6, 12-13]</sup>,环境与安全<sup>[14]</sup>,农药的定性分析<sup>[15]</sup>,非目标化合物扫描<sup>[16-17]</sup>以及天然产物研究<sup>[18]</sup>中得到广泛应用。目前,人们主要关注母离子的同位素分布信息,却很少有文献报道化合物子离子的同位素丰度和峰形信息。这是由于大部分实验都是选用目标化合物的最丰同位素母离子(most abundant isotopic peak)进行裂解,得到仅含有单同位素裂解信息的子离子(monoisotopic peak),这种实验方法忽略了对天然同位素信息的利用。Alon 等<sup>[19]</sup>使用超声波三重四极杆气质联用仪(supersonic GC/MS)对二级子离子的天然同位素丰度比进行研究,并用作者设计的 Tal-Aviv IAA 软件对 EI 源裂解的化合物碎片同位素信息进行分析,通过对离子碎片进行解析确定了最匹配的候选分子式。目前,还没有相

关文献报道在 ESI 源下利用高分辨质谱的精确质量数信息及同位素丰度信息对化合物子离子的多级质谱裂解规律进行分析。

对于高分辨质谱,通过精确质量过滤,可以很好的减少待选分子式,应用同位素信息,通过对质量轴、质谱峰形变异和随机噪声进行校正,可以进一步减少候选分子式的数量。质谱采集的同位素信息不仅包括同位素丰度比,还包括同位素峰的轮廓信息。应用同位素轮廓信息能够更准确的从质谱图得到质荷比推测分子式<sup>[20]</sup>。Gu 等<sup>[21]</sup>用 MassWorks 软件校正谱图,解析同位素轮廓信息,并提出了“谱图准确度”(spectral accuracy)的概念。李雪生等<sup>[15]</sup>运用“谱图准确度”方法在单位分辨质谱仪 GC/MS 上实现了目标农药分子式的准确识别。然而,现有“谱图准确度”的文献仅局限于一级质谱的分析,并未有在多级质谱中应用。

本研究采用 LTQ-Orbitrap XL 高分辨质谱仪,通过改变离子阱质谱中的重要参数 isolation width,建立在高分辨质谱仪上获得子离子同位素信息的方法,并根据同位素丰度比和同位素峰形进行子离子结构的解析。以磺胺甲基嘧啶(sulfamerazine)子离子的同位素峰信息为例,使用 Xcalibur 软件模拟子离子的同位素丰度比与实测值进行比较,通过同位素峰形信息确证子离子的元素组成。为进一步确证该法可行性,本研究运用 Massworks 软件对子离子碎片进行质谱轮廓分析。

## 1 试验部分

### 1.1 试剂与仪器

LTQ-Orbitrap XL 线性离子阱-轨道离子阱高分辨组合式质谱仪;美国 ThermoFisher Scientific 公司产品,配有电喷雾离子源(ESI 源)。

磺胺甲基嘧啶(纯度>98%);购于 Dr. Ehrenstorfer 公司;标准品用 50% 甲醇水溶液配制成 100  $\mu\text{g}/\text{L}$  溶液;其他试剂均为色谱纯;试验用水为 Milli-Q 超纯水。

### 1.2 质谱条件

质量分析器:Orbitrap;离子化方式:ESI+;喷雾电压:4.5 kV;管状透镜电压:115 V;鞘气(氮气)流速:25 arb;辅助气(氮气)流速:3.00 arb;毛细管温度:350  $^{\circ}\text{C}$ ;质量扫描范围: $m/z$  50~300;静电场轨道阱的高分辨扫描;分辨率  $R=30\,000$ ;高能诱导裂解(HCD 裂解),归一化能量:55%;isolation width:1 u 或 6 u。

### 1.3 试验方法

蠕动泵直接进样,流速 10  $\mu\text{L}/\text{min}$ 。按照 1.2 条件进行检测,记录总离子流图、质谱图和精确质量数。通过离子阱的二级质谱图和 Xcalibur 软件模拟质谱图对化合物进行确认,并用 MassWorks 软件对子离子碎片进一步确认。

## 2 结果与讨论

### 2.1 多级质谱同位素峰的理论分布

将化合物的同位素峰定义为 A、A+1、A+2、A+3 和 A+4(A+i 表示 i 个附加的中子),A 为轻同位素峰,A+1、A+2、A+3 和 A+4 为重同位素峰<sup>[8]</sup>,同位素峰度的比值以元素同位素的贡献率计算得出。以含有硫元素的化合物磺胺甲基嘧啶( $\text{C}_{11}\text{H}_{12}\text{N}_4\text{O}_2\text{S}$ )为例,其子离子可分为含硫和不含硫两类,示于图 1<sup>[22]</sup>。其子离子  $[\text{C}_6\text{H}_6\text{NSO}_2]^+$  的 A 峰是其轻同位素峰  $[\text{C}_6\text{H}_6^{14}\text{N}^{32}\text{S}^{16}\text{O}_2]^+$ ,将其丰度设定为 100%;A+1 峰由  $[\text{C}_6\text{H}_6^{13}\text{C}_2\text{C}_5\text{H}_6^{14}\text{N}^{32}\text{S}^{16}\text{O}_2]^+$  (6.48%)、 $[\text{C}_6\text{H}_6\text{D}_5^{14}\text{N}^{32}\text{S}^{16}\text{O}_2]^+$  (0.07%)、 $[\text{C}_6\text{H}_6^{15}\text{N}^{32}\text{S}^{16}\text{O}_2]^+$  (0.37%)、 $[\text{C}_6\text{H}_6^{14}\text{N}^{33}\text{S}^{16}\text{O}_2]^+$  (0.80%) 和  $[\text{C}_6\text{H}_6^{14}\text{N}^{32}\text{S}^{17}\text{O}^{16}\text{O}]^+$  (0.08%) 等组成,由于  $^{13}\text{C}$  的同位素丰度较  $^2\text{H}$ 、 $^{15}\text{N}$ 、 $^{17}\text{O}$  和  $^{33}\text{S}$  高,因此 A+1 峰的丰度和峰形主要由  $[\text{C}_6\text{H}_6^{13}\text{C}_2\text{C}_5\text{H}_6^{14}\text{N}^{32}\text{S}^{16}\text{O}_2]^+$  决定;同理,因  $^{34}\text{S}$  对 A+2 峰贡献最大,A+2 的丰度和峰形是由  $[\text{C}_6\text{H}_6^{14}\text{N}^{34}\text{S}^{16}\text{O}_2]^+$  (4.52%) 决定,  $[\text{C}_6\text{H}_6^{14}\text{N}^{32}\text{S}^{18}\text{O}^{16}\text{O}]^+$  (0.42%)、 $[\text{C}_6\text{H}_6^{13}\text{C}_2\text{C}_5\text{H}_6^{15}\text{N}^{32}\text{S}^{16}\text{O}_2]^+$  (0.02%) 等 10 个峰是 A+2 的次要组成部分。上述各峰共同组成了  $[\text{C}_6\text{H}_6\text{NSO}_2]^+$  的 A、A+1 和 A+2 同位素峰。

决定,  $[\text{C}_6\text{H}_6^{14}\text{N}^{32}\text{S}^{18}\text{O}^{16}\text{O}]^+$  (0.42%)、 $[\text{C}_6\text{H}_6^{13}\text{C}_2\text{C}_5\text{H}_6^{15}\text{N}^{32}\text{S}^{16}\text{O}_2]^+$  (0.02%) 等 10 个峰是 A+2 的次要组成部分。上述各峰共同组成了  $[\text{C}_6\text{H}_6\text{NSO}_2]^+$  的 A、A+1 和 A+2 同位素峰。

### 2.2 Isolation width 对质谱采集同位素峰的影响

离子阱的 isolation width 是获得多级质谱中重同位素信息的重要参数。当 isolation width 设为 1 u 时,母离子选择范围在  $[\text{M}+\text{H}]^+ \pm 0.5$  u 之间,子离子峰仅有  $m/z$  108.044 29,其重同位素没有被选中,而无相应的碎片同位素峰,示于图 2a-1。当 isolation width 设为 6 u 时,即母离子选择范围在  $[\text{M}+\text{H}]^+ \pm 3.0$  u 之间,除  $m/z$  108.044 30 峰产生外,还检测到  $m/z$  109.047 45 的重同位素峰,示于图 2a-2。同理,对于图 2 中列出的其他子离子,当 isolation width 设为 1 u 时,只产生  $m/z$  92.049 33 和  $m/z$  65.038 40;当 isolation width 设为 6 u 时,检测到相应的重同位素峰  $m/z$  93.052 57 和  $m/z$  66.041 67。这与仪器配套软件 Xcalibur 模拟的  $[\text{C}_6\text{H}_6\text{NO}]^+$  (图 2a-3)、 $[\text{C}_6\text{H}_6\text{N}]^+$  (图 2b-3) 和  $[\text{C}_5\text{H}_5]^+$  (图 2c-3) 相符。具体相对丰度比列于表 1。因此,在实验过程中,选择 isolation width 为 6 u 进行下一步实验。

### 2.3 多级质谱同位素峰推测化合物的分子组成

以磺胺甲基嘧啶为例,当子离子分子式由 C、H、O 和 N 元素组成时,对重同位素丰度比和峰形贡献较大的主要是 C,多级质谱的同位素峰应包含 A 和 A+1 峰;当化合物的分子组成含 S 时,其同位素峰主要由 C 和 S 的含量共同决定,多级质谱的同位素峰应包含 A、A+1 及 A+2 峰。通过以上规律,分析质谱采集到的同位素峰的组成,可以判断化合物的元素信息。

对于子离子  $m/z$  108.044 39、92.049 48 和 65.038 58,质谱只检测到相应的 A 和 A+1 峰,而无明显的 A+2 峰,可以判断这几个子离子是不含 S 的子离子。对于含 S 的子离子, $m/z$  156.011 38 在质谱上产生 A ( $m/z$  156.011 38, 100.00%)、A+1 ( $m/z$  157.014 91, 5.26%) 和 A+2 峰 ( $m/z$  158.007 13, 4.19%),其丰度比符合 S 元素的分布规律。这与 Xcalibur 软件模拟的  $[\text{C}_6\text{H}_6\text{NSO}_2]^+$  (图 2d-3) 相符。具体相对丰度比列于表 2。



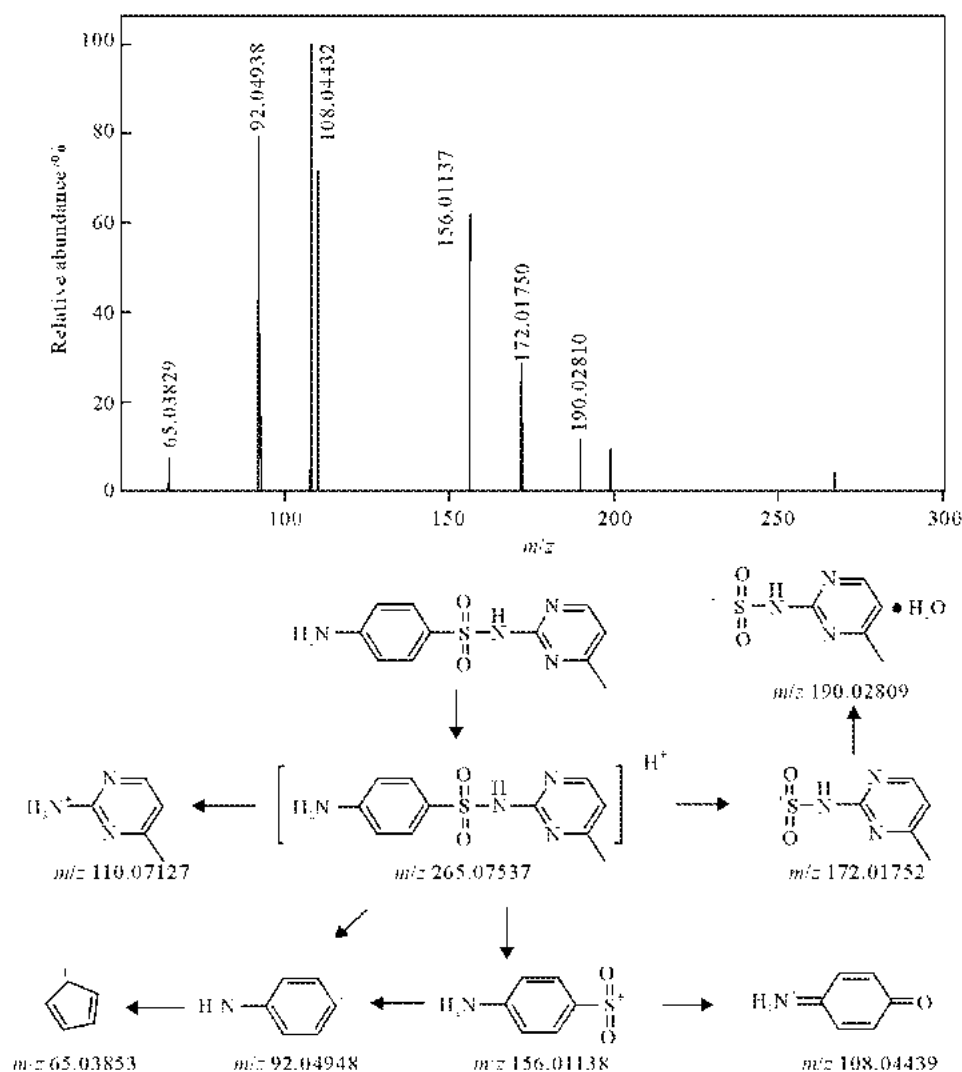


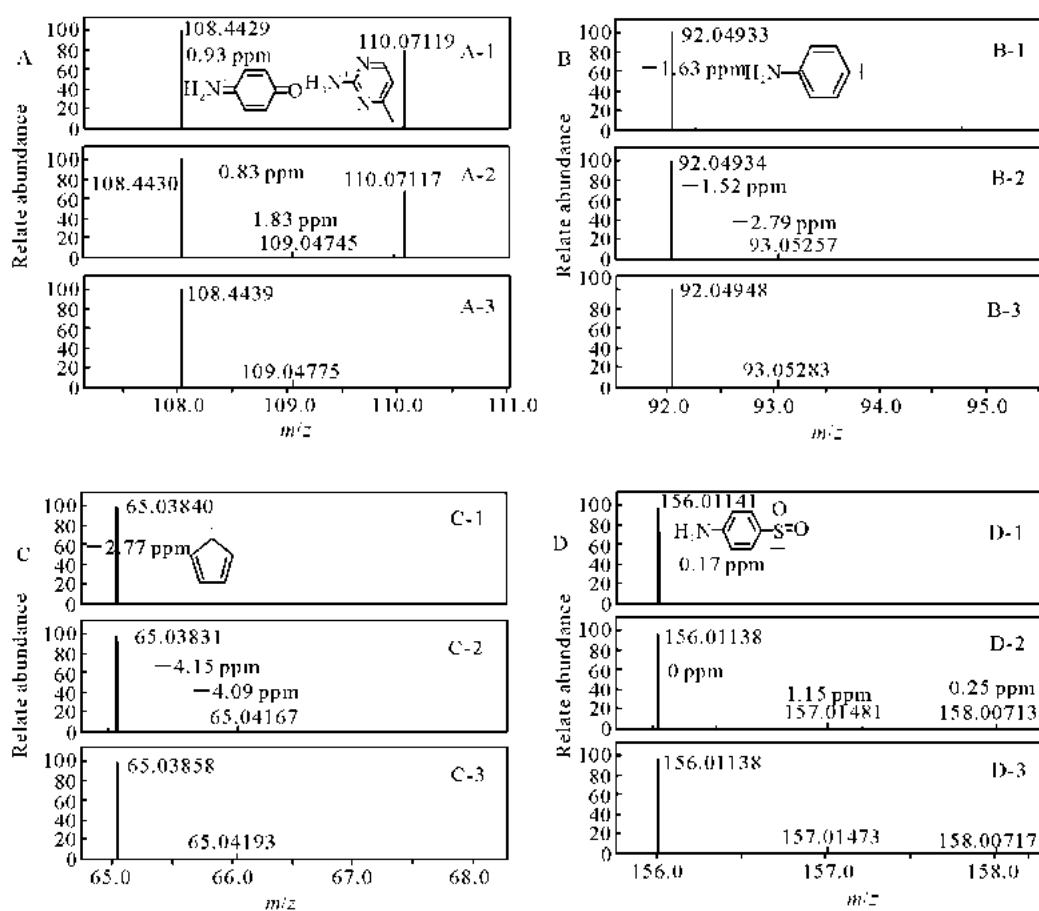
图 1 磺胺甲基嘧啶的结构式及 HCD 质谱裂解

Fig. 1 The structure and HCD fragmentation pathway of sulfamerazine

表 1 磺胺甲基嘧啶离子碎片理论同位素和实测同位素 (Isolation width=6 u) 分布信息

Table 1 Comparison of accurate mass acquired by Orbitrap (Isolation width=6 u) and the isotope pattern predicted by the Xcalibur software

分子式	理论值			实测值		
	A	A+1	A+2	A	A+1	A+2
$[\text{C}_6\text{H}_6\text{NSO}_2]^+$	156.01138 (100.00%)	157.01473 (6.49%)	158.00717 (4.52%)	156.01138 (100.00%)	157.01491 (5.26%)	158.00713 (4.19%)
$[\text{C}_6\text{H}_6\text{NO}]^+$	108.04429 (100.00%)	109.0474 (6.49%)	—	108.04439 (100.00%)	109.04775 (5.68%)	—
$[\text{C}_6\text{H}_6\text{N}]^+$	92.04948 (100.00%)	92.05283 (6.49%)	—	92.04934 (100.00%)	93.05257 (5.79%)	—
$[\text{C}_5\text{H}_5]^+$	65.03858 (100.00%)	66.04193 (5.40%)	—	65.03831 (100.00%)	66.04167 (4.62%)	—



注: a-1, b-1, c-1 和 d-1, isolation width=1 u; a-2, b-2, c-2 和 d-2, isolation width=6 u; a-3, b-3, c-3 和 d-3, Xcalibur 软件模拟图

图 2 在不同 isolation width 下磺胺甲基嘧啶子离子同位素丰度信息

Fig. 2 Tandem mass isotope pattern acquired by Orbitrap in different isolation width

表 2 子离子峰  $m/z$  156.011 38 和  $m/z$  65.038 58 的 MassWorks 检索结果

Table 2 Search result of fragment ion peaks ( $m/z$  156.011 38 and  $m/z$  65.038 58) by MassWorks

碎片离子 $m/z$	分子式	排序	理论值/ $u$	实测值/ $u$	质量误差/ $\times 10^{-6}$	谱图准确度/%
156.011 38	$[C_6H_6NSO_2]^+$	1	156.011 4	156.011 4	0	96.1
65.038 58	$[C_5H_5]^+$	1	65.038 6	65.038 3	-4.61	99.2

## 2.4 由同位素峰轮廓推测化合物的分子组成

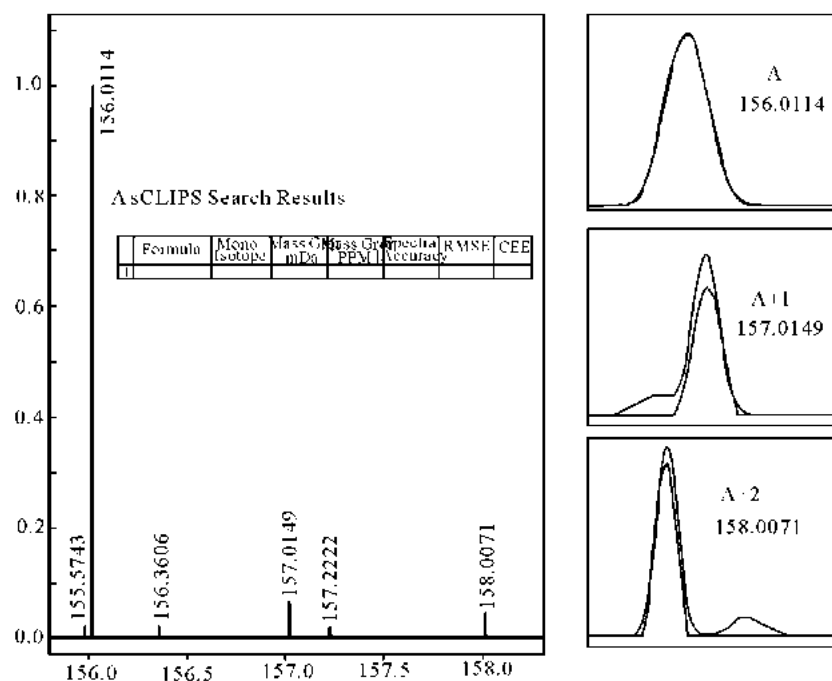
用 MassWorks 对磺胺甲基嘧啶子离子的精确分子质量及元素组成进行识别。选取精确分子质量 156.011 4 和 65.038 3, 以离子电荷数为 1, 质量误差为  $5 \times 10^{-6}$ , C、H、O、N 及 S 为可能含有的元素, 利用 MassWorks 同位素峰形校正检索技术 (sCLIPS), 通过同位素峰形轮廓匹配原则, 推测  $m/z$  156.011 38 和  $m/z$  65.038 31 的分子式, 分别示于图 3 和图 4。子离子  $m/z$  156.011 4 经软件检索只得到分子式

$[C_6H_6NSO_2]^+$ , 该分子式的理论值与仪器获得的  $m/z$  156.011 4, 质量误差为 0, A, A+1 和 A+2 同位素峰轮廓显示很好的匹配性, 匹配度达到 96.1%, 故推测该离子是  $[C_6H_6NSO_2]^+$ ; 子离子  $m/z$  65.0383 经软件检索只得到分子式  $[C_5H_5]^+$ , 该分子式的理论值与仪器获得的  $m/z$  65.038 6, 质量误差为  $-4.61 \times 10^{-6}$ , A, A+1 和 A+2 同位素峰轮廓显示很好的匹配性, 匹配度达到 99.2%, 故推测该离子是  $[C_5H_5]^+$ 。

据文献<sup>[23]</sup>报道, 磺胺甲基嘧啶在 EI 源上裂

解产生的子离子  $m/z$  65 的分子式为  $\text{HS}^+\text{O}_2$ 。本研究运用 ESI 源也产生质荷比为  $m/z$  65 的子离子,其精确质量数  $m/z$  65.038 31,与  $\text{HS}^+\text{O}_2$ (计算值  $m/z$  64.969 18)质量误差为  $1.06 \times$

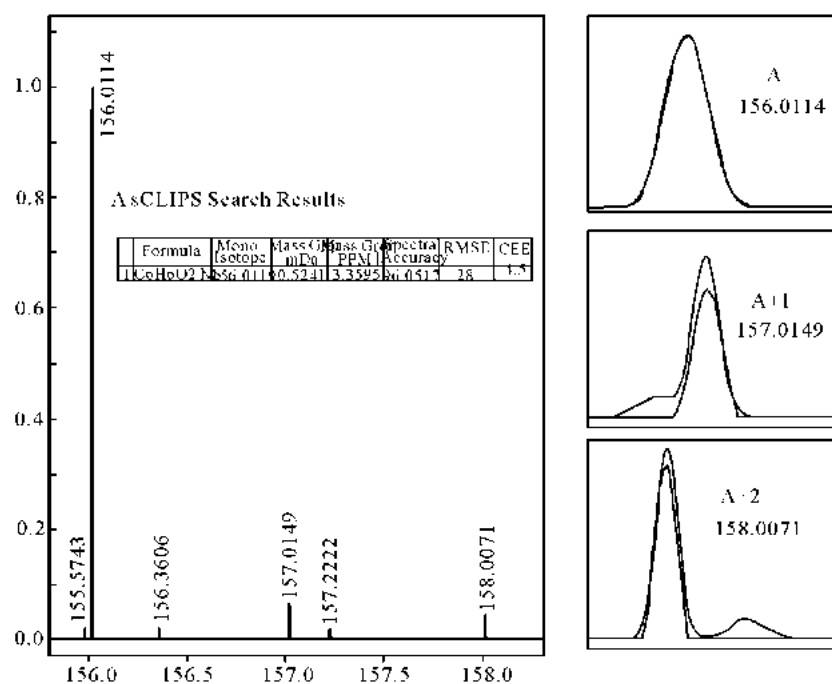
$10^{-4}$ ,推断该子离子的分子式不是  $\text{HS}^+\text{O}_2$ 。根据本研究的结果,证明了  $m/z$  65.038 31 对应的分子式是  $[\text{C}_5\text{H}_5]^+$ 。



注:绿色代表理论值,红色代表实测值

图 3 Mass Works 准确识别  $m/z$  156.011 4 分子式的结果

Fig. 3 The spectral accuracy and mass error of  $[\text{C}_4\text{H}_4\text{NSO}_2]^+$  ( $m/z$  156.011 4) with mono isotope value showed by MassWorks software



注:绿色代表理论值和红色代表实测值

图 4 Mass Works 准确识别  $m/z$  65.038 3 分子式的结果

## 2.5 方法验证

用磺胺对甲氧嘧啶对该方法进行验证,碎片离子  $m/z$  156.011 38 在质谱上产生 A( $m/z$  156.011 34, 100.00%)、A+1( $m/z$  157.014 51, 5.42%)和 A+2 峰( $m/z$  158.006 99, 3.01%),其丰度比符合 S 元素的分布规律,示于图 5。碎片离子  $m/z$  108.044 39, 质谱只检测到相应的 A( $m/z$  108.044 23, 100.00%),和 A+1 峰( $m/z$  109.047 53, 4.12%),而无明显的 A+2 峰,示于图 6。符合离子的天然同位素丰度比。

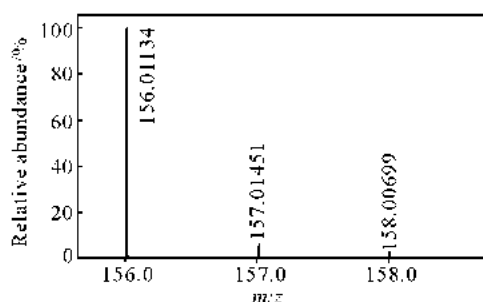


图 5 在 isolation width=6 u 下磺胺甲基嘧啶离子  $m/z$  156.011 34 的同位素丰度信息

Fig. 5

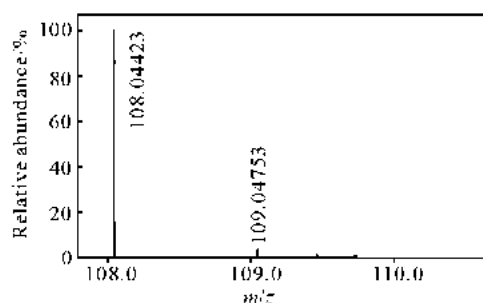


图 6 在 isolation width=6 u 下磺胺甲基嘧啶离子  $m/z$  108.044 23 的同位素丰度信息

Fig. 6

## 3 结论

本研究通过扩大 isolation width 进行多级质谱试验,得到磺胺甲基嘧啶的子离子同位素信息,根据子离子同位素丰度比和峰形产生的原理,分析子离子的分子组成,为磺胺类化合物的裂解机理提供了更丰富和准确的依据。在多级质谱实验中关注同位素丰度和峰形信息,可以快速排除绝大多数假阳性待选分子式,使结构解析更加快捷准确。

致谢:感谢北京绿绵科技有限公司李斌工程师为本研究进行数据处理工作。

## 参考文献:

- [1] 张鸿伟,简慧敏,林黎明,等. 液相色谱-四极杆/离子阱质谱快速测定蜂蜜中痕量硝基咪唑类药物及其代谢物残留[J]. 分析测试学报, 2012, 31(7): 763-770.  
ZHANG Hongwei, JIAN Yuimin, LIN Liming, et al. Rapid detection of trace amounts of nitroimidazoles and their metabolites in honey using liquid chromatography coupled with quadrupole/linear ion trap mass spectrometry[J]. J Instrum Anal, 2012, 31(7): 763-770(in Chinese).
- [2] 凌睿,胡文彦,乔玲,等. 高分辨快速液相色谱-串联质谱法测定肉制品中的刚果红[J]. 分析测试学报, 2012, 31(6): 730-733.  
LING Rui, HU Wenliao, QIAO Lin, et al. Determination of Congo red in meat products by rapid resolution liquid chromatography-tandem mass spectrometry[J]. J Instrum Anal, 2012, 31(6): 730-733(in Chinese).
- [3] LIU X, ZHOU Y, CHEN H B, et al. Detection of carbonyl groups in triterpenoids by hydroxylamine hydrochloride derivatization using electrospray ionization mass spectrometry[J]. Rapid Commun Mass Spectrom, 2008, 22(12): 1 981-1 992.
- [4] LIU X, LI S L, ZHOU Y, et al. Characterization of protostane triterpenoids in *Alisma orientalis* by ultra-performance liquid chromatography coupled with quadrupole time-of-flight mass spectrometry [J]. Rapid Commun Mass Spectrom, 2010, 24(11): 1 514-1 522.
- [5] PLUSKAL T, UEHARA T, YANAGIDA M, et al. Highly accurate chemical formula prediction tool utilizing high-resolution mass spectra, MS/MS fragmentation, heuristic rules, and isotope pattern matching[J]. Anal Chem, 2012, 84(10): 4 396-4 403.
- [6] ERVE J C L, GU M, WANG Y D, et al. Spectral accuracy of molecular ions in an LTQ/Orbitrap mass spectrometer and implications for elemental composition determination [J]. J Am Soc Mass Spectrom, 2009, 20(11): 2 058-2 069.
- [7] ALON T, AMIRAV A. Isotope abundance analysis methods and software for improved sample identification with supersonic gas chromatography/mass spectrometry [J]. Rapid Commun Mass

- Spectrum, 2006, 20(17): 2 579-2 588.
- [8] KIND T, FIEHN O. Seven golden rules for heuristic filtering of molecular formulas obtained by accurate mass spectrometry[J]. *Bmc Bioinformatics*, 2007, (8): 105.
- [9] KIND T, FIEHN O. Metabolomic database annotations via query of elemental compositions: Mass accuracy is insufficient even at less than 1 ppm[J]. *Bmc Bioinformatics*, 2006, (7): 234.
- [10] 周 围,李卫建. Massworks 结合单位分辨质谱识别喹诺酮类药物分子式[J]. *质谱学报*, 2009, 30(增刊): 126-128.  
ZHOU Wei, LI Weijian. Identification quinolones drug' formulas by MassWorks combination of unit-resolved mass spectrometry[J]. *Journal of Chinese Mass Spectrometry Society*, 2009, 30 (Suppl): 126-128(in Chinese).
- [11] BOCKER S, LETZEL M C, LIPTAK Z, et al. SIRIUS: Decomposing isotope patterns for metabolite identification[J]. *Bioinformatics*, 2009, 25(2): 218-224.
- [12] ZHU P J, TONG W, ALTON K, et al. An accurate-mass-based spectral-averaging isotope-pattern-filtering algorithm for extraction of drug metabolites possessing a distinct isotope pattern from LC-MS data[J]. *Anal Chem*, 2009, 81 (14): 5 910-5 917.
- [13] GU M, WANG Y D, ZHAO X G, et al. Accurate mass filtering of ion chromatograms for metabolite identification using a unit mass resolution liquid chromatography/mass spectrometry system [J]. *Rapid Commun Mass Spectrom*, 2006, 20 (5): 764-770.
- [14] CHEN J P, GU M, WANG Y D, et al. Improving the confidence of unknown compound identification by first responder mobile GC-MS laboratories in time-critical environmental and homeland security incidents [J]. *LC-GC North America*, 2008, 26(9): 938-945.
- [15] 李雪生,李子昂,王正全,等. 精确质量数在单四极杆质谱定性分析农药中的应用[J]. *高等学校化学学报*, 2010, 31(12): 2 383-2 389.  
LI Xuesheng, LI Zi'ang, WANG Zhengquan. Application of accurate mass and elemental composition determination for pesticides identification using a unit mass resolution gas chromatography/mass spectrometry[J]. *Chemical Journal of Chinese Universities*, 2010, 31(12): 2 383-2 389(in Chinese).
- [16] JIANG W, ERVE J C L. Spectral accuracy of a new hybrid quadrupole time-of-flight mass spectrometer: application to ranking small molecule elemental compositions[J]. *Rapid Commun Mass Spectrom*, 2012, 26(9): 1 014-1 022.
- [17] 张 喆,李卫建,袁有荣. 使用 MassWorks 快速筛查药品中非法添加物[J]. *质谱学报*, 2010, 31 (增刊): 224-226.  
ZHANG Zhe, LI Weijian, YUAN Yourong. Rapid identification of chemical drug mixed illegally by MassWorks[J]. *Journal of Chinese Mass Spectrometry Society*, 2010, 31(Suppl): 224-226 (in Chinese).
- [18] 周 围,张雅珩,周小平. 中国苦水玫瑰精油中部分天然产物的质谱分析与元素组成的确定[J]. *检验检疫学刊*, 2010, 20(5): 226-233.  
ZHOU Wei, ZHANG Yaheng, ZHOU Xiaoping. Mass spectrum analysis and elemental composition of partial natural products in essential oil of Chinese Kushui rose [J]. *Journal of inspection and quarantine*, 2010, 20(5): 226-233 (in Chinese).
- [19] ALON T, AMIRAV A. Isotope abundance analysis for improved sample identification with tandem mass spectrometry[J]. *Rapid Commun Mass Spectrom*, 2009, 23(23): 3 668-3 672.
- [20] 刘 可,马 彬,王永东,等. 一种新软件方法用于单位分辨质谱仪上药物相对分子质量的准确测定[J]. *药学报*, 2007, 42(10): 1 112-1 114.  
LIU Ke, MA Bin, WANG Yongdong, et al. A new software method for accurate mass measurements of drugs on unit mass resolution mass spectrometer [J]. *Acta Pharmaceutica Sinica*, 2007, 42(10): 1 112-1 114(in Chinese).
- [21] WANG Y D, GU M. The concept of spectral accuracy for MS[J]. *Anal Chem*, 2010, 82(17): 7 055-7 062.
- [22] KLAGKOU K, PULLEN F, HARRISON M, et al. Fragmentation pathways of sulphonamides under electrospray tandem mass spectrometric conditions[J]. *Rapid Commun Mass Spectrom*, 2003, 17(21): 2 373-2 379.
- [23] 彭 涛. 电喷雾串联质谱裂解规律及其在残留分析中的应用研究[D]. 北京: 中国农业大学, 2007.



# 酸枣仁微量生物碱成分的筛查方法研究

胡彦周, 丁轲\*, 韩涛, 陈湘宁

北京农学院食品科学与工程学院 食品质量与安全北京实验室  
农产品有害微生物及农残安全检测与控制北京市重点实验室 北京 102206

**摘要:** 为了准确、迅速地筛查并确定酸枣仁中微量生物碱成分, 运用含氮有机物(生物碱)分析包中的色谱柱建立酸枣仁生物碱成分的高效液相色谱在线分离方法, 然后利用 MassWorks 分子识别软件和 LC-ESI-MS/MS 对在线分离的生物碱成分进行确认, 共筛查到 3 种阿朴芬类生物碱: 酸枣仁碱 K ( $C_{17}H_{19}NO_3$ )、山矾碱 ( $C_{17}H_{17}NO_2$ ) 和 N-甲基巴婆碱 ( $C_{18}H_{19}NO_2$ ); 2 种环肽类生物碱: 酸枣仁碱 F ( $C_{31}H_{42}N_4O_5$ ) 和酸枣仁碱 A ( $C_{31}H_{42}N_4O_4$ ); 还有一对同分异构体阿朴芬生物碱: 木兰花碱和酸李碱 ( $C_{20}H_{24}NO_4$ ) 有待进一步确定。

**关键词:** 酸枣仁; 生物碱; MassWorks; LC-ESI-MS/MS

中图分类号: O657.63; R284.1

文献标识码: A

DOI: 10.16333/j.1001-6880.2017.7.015

## Screening Methods of Trace Alkaloids Components from *Semen Zizyphi spinosae*

HU Yan-zhou, DING Ke\*, HAN Tao, CHEN Xiang-ning

College of Food Science and Engineering, Beijing University of Agriculture, Beijing Food Quality and Safety Laboratory; Microbiological and Safety Inspection and Control of Pesticide Residues in Agricultural Products Harmful Beijing Key Laboratory, Beijing 102206, China

**Abstract:** To accurately and quickly screen and identify trace alkaloids components from *Semen Zizyphi spinosae*, a HPLC online separation method of alkaloids components was developed using the columns which belong to the nitrogen-containing organic compounds (alkaloids) analysis kit. Then the alkaloids components separated on line were identified with the help of MassWorks molecular recognition software and LC-ESI-MS/MS. Three compounds: sanjoinine K ( $C_{17}H_{19}NO_3$ ), caaverine ( $C_{17}H_{17}NO_2$ ) and N-methylasimilobine ( $C_{18}H_{19}NO_2$ ), belong to aporphine alkaloids and two compounds: sanjoinine F ( $C_{31}H_{42}N_4O_5$ ) and sanjoinine A ( $C_{31}H_{42}N_4O_4$ ), belong to cyclopeptide alkaloids were screened and identified. In addition, there was a pair of isomeric compounds: magnoflorine and zizyphusine ( $C_{20}H_{24}NO_4$ ), which belong to aporphine alkaloids to be further identified. A rapid and efficient screening method for alkaloids from Chinese medicine was established in this study.

**Key words:** *Semen Zizyphi spinosae*; alkaloid; MassWorks; LC-ESI-MS/MS

酸枣仁 (*Semen Zizyphi spinosae*) 为鼠李科植物酸枣的种子, 具有改善睡眠等<sup>[1, 2]</sup>功能。有研究表明酸枣仁皂苷和黄酮具有改善睡眠的功能, 并进一步确定了改善睡眠的具体成分为酸枣仁皂苷 A、B<sup>[3]</sup>和黄酮斯皮诺素、阿魏酰斯皮诺素<sup>[4, 5]</sup>。然而, 酸枣仁中还有一大类成分——生物碱, 有学者发现

酸枣仁生物碱也具有改善睡眠的功能<sup>[6]</sup>, 但具体功能成分还有待进一步确定。由于市场上没有酸枣仁生物碱的标准品, 要对酸枣仁生物碱改善睡眠具体成分进行确定, 首先要筛查、分离得到生物碱的具体成分。

本实验首先用含氮有机物分析包中的  $C_{18}$  柱和  $C_{18}$ 、IEX 混合色谱柱建立酸枣仁生物碱的液相分析分离方法, 然后通过 MassWorks 分子识别软件与三重四级杆质谱的结合使用对分离后的酸枣仁生物碱进行筛查、识别。

## 1 材料与仪器

### 1.1 材料与试剂

中药材酸枣仁 (*Semen Zizyphi spinosae*) 购于河

收稿日期: 2016-11-21 接受日期: 2017-04-12

基金项目: 北京市属高等学校高层次人才引进与培养计划 (CIT&T CD20154045); 北京农学院青年基金——实验技术体系研发基金项目 (SXST201604); 北京市自然科学基金委员会——北京市教育委员会联合资助项目 (KZ201710020014); 2016 年北京农学院学位与研究生教育改革与发展项目 (2016YJS051)

\* 通信作者 E-mail: dingk@tom.com

北安国中药材市场。

石油醚、甲醇、乙醚、浓盐酸、氨水、三氯甲烷(分析纯):北京化工厂;乙腈(色谱纯):韩国 DUK-SAN 药品工业;甲酸、甲酸铵(色谱纯):上海阿拉丁试剂有限公司;荷叶碱标准品( $C_{19}H_{21}NO_2$ , HPLC  $\geq 98\%$ )、木兰花碱标准品( $C_{20}H_{24}NO_4$ , HPLC  $\geq 98\%$ ):上海顺勃生物工程技术有限公司。

## 1.2 仪器与设备

日本 SHIMADZU 公司 LC-20AD 型高效液相色谱仪,具体配置为:LC-20AD 型高压双泵;SIL-20A 自动进样器;CTO-20A 柱温箱;SPD-M20A 二极管阵列检测器;SCL-10A 岛津液相系统控制器;CLASS-VP 色谱数据工作站。北京泰克美高新技术有限公司含氮有机物(生物碱)分析专用工具包:分析柱 1(极低金属不纯物的  $C_{18}$  柱, TechMate  $C_{18}$ -ST A.  $6 \times 150$  mm,  $5 \mu\text{m}$ );分析柱 2(填料经特殊工艺处理的键合  $C_{18}$  和 IEX 的硅胶柱, TechMate CR(1:5)-ST,  $2.0 \times 150$  mm,  $5 \mu\text{m}$ )。美国 Agilent 公司 1200-6410B 液相色谱-三重四级杆质谱联用仪,具体配置为:Agilent 1200 系列真空脱气机;Agilent 1200 系列 SL 型二元泵;Agilent 1200 系列 SL 型高效自动进样器;Agilent 1200 系列柱温箱;带电喷雾离子源(Electrospray Ionization, ESI)的 Agilent 6410B 三重串联四级杆系统;Agilent MassHunter 工作站软件。

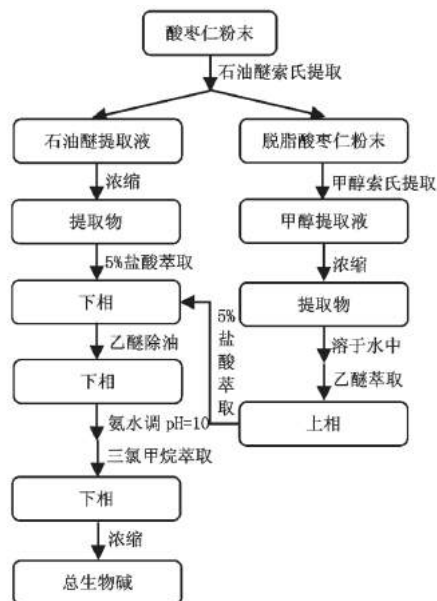


图 1 酸枣仁生物碱提取流程

Fig. 1 Extraction process of alkaloids from *Semen Zizyphi Spinosae*

## 2 实验方法

### 2.1 酸枣仁生物碱的提取

酸枣仁生物碱的提取流程如图 1 所示<sup>[7]</sup>。

### 2.2 酸枣仁生物碱成分的分析分离

本实验应用生物碱分析包对酸枣仁提取物中的生物碱成分进行分离,该方法主要基于以下原理:生物碱在酸性环境下会成盐,分子极性增大,在反相色谱体系中不保留或保留时间较短,先通过  $C_{18}$  柱对提取物进行初步分离,收集其中不保留或者保留较差的成分。再将这些成分通过  $C_{18}$  和 IEX 的混合色谱柱分离,因为静电力的存在生物碱有较好的保留,可以通过改变洗脱剂的盐浓度和 pH 值对生物碱进行进一步的分离。

#### 2.2.1 反相色谱柱分析条件

反相色谱柱 TechMate  $C_{18}$ -ST( $4.6 \times 150$  mm,  $5 \mu\text{m}$ ) 的流动相 A 相选用 0.1% 的甲酸水溶液, B 相选用乙腈,总流速为 1 mL/min,采用梯度洗脱,洗脱梯度:0~5 min, 30% B; 5~25 min, 30%~60% B; 25~27 min, 60%~100% B; 27~45 min, 100% B。柱温选用 40 °C,进样量 20  $\mu\text{L}$ ,检测器采用二极管阵列检测器,波长 254 nm。

#### 2.2.2 混合色谱柱分析条件

由于混合色谱柱对生物碱的分离和生物碱成分的筛查是同时进行的,所以混合色谱柱分析条件同 2.3.1 的色谱条件。

### 2.3 酸枣仁生物碱成分的筛查

#### 2.3.1 色谱条件

色谱柱选用  $C_{18}$  和 IEX 的混合色谱 TechMate CR(1:5)-ST( $2.0 \times 150$  mm,  $5 \mu\text{m}$ )。A 流动相选用甲酸水溶液(pH=3)和乙腈,比例 70:30; B 流动相选用 50 mmol/L 甲酸铵水溶液(甲酸调 pH=3)和乙腈,比例 70:30。总流速 0.2 mL/min,柱温 40 °C,进样量 5  $\mu\text{L}$ 。经反相色谱柱收集的第一部分(0~5 min 部分)的洗脱梯度:0~5 min, 0% B; 5~30 min, 0%~100% B; 30~60 min, 100% B。第二部分(5~25 min 部分)的洗脱梯度:0~10 min, 0% B; 10~50 min, 0%~100% B; 50~80 min, 100% B。

#### 2.3.2 质谱条件

质谱选择 MS2 Scan 模式,步长(Step size) 0.1 amu,在 profile 模式下采集化合物信息,离子源为 ESI,质量扫描范围  $m/z$  100~800 amu,碎裂电压为 135 V,正离子模式。雾化气压力为 20 psig,干燥气

流速为 10 L/min,干燥气温度 350 °C,  $V_{cap}$  毛细管电压 4000 V。

### 2.3.3 校正函数的建立

为了能通过 MassWorks 分子识别软件在低分辨质谱上获得精确的质量数,需要一个包含有质量漂移和峰形失真的校正函数<sup>[8-11]</sup>,所以,首先要利用已知标样建立一个校正函数,当相对质量误差的绝对值小于 2 ppm,且 Spectral Accuracy 值大于 98% 时,校正函数可用<sup>[12,13]</sup>。本实验选用荷叶碱 ( $C_{19}H_{21}NO_2$ ) 和木兰花碱 ( $C_{20}H_{24}NO_4$ ) 建立校正函数。

### 2.3.4 生物碱成分的筛查

先将提取得到的总生物碱在液相上经过反相色谱柱(分析柱 1)进行初步分离,分别收集 0~5 min、5~25 min 洗出液,多次收集,在旋转蒸发仪上浓缩,然后在液质上通过混合色谱柱(分析柱 2)进一步分离,同时在 2.3.2 的质谱条件下进行检测。

在 MassWorks 分子识别软件上,用建立好的校正函数对总离子流图中特定峰对应的质谱图进行质量漂移以及峰形失真的校正,从而在低分辨质谱上获得精确质量数<sup>[14]</sup>。利用 MassWorks 的同位素峰形校正检索功能(Calibrated Lineshape Isotope Profile Search, CLIPS)<sup>[15]</sup>对质谱图中的准分子离子峰的化学式进行检索,根据检索结果确定总离子流图中特定峰对应的物质,再根据质谱图中的碎片离子信息以及已知的化合物信息(包括分子式、结构式)进行验证。

## 3 结果与分析

### 3.1 阿朴芬类生物碱的筛查结果

酸枣仁碱 K,也即右旋衡州乌药碱(sanjoinine K 或 coclaurine,  $C_{17}H_{19}NO_3$ ),在酸枣仁生物碱提取物经过分析柱 1 后收集的第一部分(0~5 min 部分)通过分析柱 2 时洗脱到第 30.6 min 时出现(见图 2, 峰 1),质谱图见图 3。 $m/z$  286.1427 的峰为准分子离子峰。对准分子离子进行同位素峰形校正检索,在给定的质量误差范围( $\pm 0.01$  Da)内得到的结果根据谱图准确度排名前三位见表 1,排在第一位的即为该准分子离子的化学式  $C_{17}H_{20}NO_3 [M+H]^+$ ,相应的分子式为  $C_{17}H_{19}NO_3$ ,推测为酸枣仁碱 K。它的质谱图中含有  $m/z$  269.1246 的碎片离子峰,比准分子离子的质荷比小了 17,是由准分子离子失去一个羟基(-OH)或氨基(-NH<sub>3</sub>)得到,酸枣仁碱 K 的结构式如图 4 所示<sup>[16]</sup>,含有羟基,符合条件。

山矾碱(caaverine,  $C_{17}H_{17}NO_2$ ) 在生物碱提取物经过分析柱 1 后收集的第一部分(0~5 min 部分)通过分析柱 2 时洗脱到第 43.0 min 时出现(见图 2, 峰 3),质谱图见图 3。 $m/z$  268.1344 的峰为准分子离子峰。对此准分子离子的化学式在  $\pm 0.01$  Da 的质量误差范围内进行检索,得到的结果中根据谱图准确度排名前三位见表 1,排在第一位的为该准分子离子的化学式  $C_{17}H_{18}NO_2 [M+H]^+$ ,相应的分子式为  $C_{17}H_{17}NO_2$ ,推测为山矾碱。它的质谱图中存在  $m/z$  251.1051 的碎片离子峰,是由准分子离子失去一个羟基(-OH)或氨基(-NH<sub>3</sub>)得到,酸枣仁碱 K 的结构式如图 4 所示<sup>[16]</sup>,含有羟基,符合条件。

N-甲基巴婆碱(N-methylasimilobine,  $C_{18}H_{19}NO_2$ ) 在生物碱提取物经过分析柱 1 后收集的第一部分(0~5 min 部分)通过分析柱 2 时洗脱到第 53.5 min 时出现(见图 2, 峰 4),质谱图见图 3。 $m/z$  282.1489 的峰为准分子离子峰,对此峰进行检索,结果前三位见表 1,准分子离子的化学式为  $C_{18}H_{20}NO_2 [M+H]^+$ ,相应的分子式为  $C_{18}H_{19}NO_2$ ,推测为 N-甲基巴婆碱或酸枣仁碱 Ia(去甲荷叶碱),两者为同分异构体,结构式如图 4 所示<sup>[16]</sup>。从它的质谱图可以看到  $m/z$  265.1197 和 251.0985 的离子碎片,比准分子离子的质荷比分别小了 17 和 31,所以  $m/z$  265.1197 的碎片离子是由准分子离子失去一个羟基(-OH)或氨基(-NH<sub>3</sub>)得到,  $m/z$  251.0985 的碎片离子是由准分子离子失去一个甲氧基(-OCH<sub>3</sub>)或羟甲基(-CH<sub>2</sub>OH)得到。从 N-甲基巴婆碱和酸枣仁碱 Ia 结构式可以看到, N-甲基巴婆碱同时含有羟基和甲氧基,而酸枣仁碱 Ia 只含有羟甲基,没有羟基或氨基,所以目标物推测为 N-甲基巴婆碱。进一步分析,目标物是否同时存在两种同分异构体,若存在酸枣仁碱 Ia,就会出现同时失去两个甲氧基的碎片离子  $m/z$  220,显然,质谱图中不存在  $m/z$  220 的碎片离子,所以不含有酸枣仁碱 Ia。质谱图中  $m/z$  234.0780 的碎片离子是由准分子离子同时失去一个羟基和一个甲氧基后得到,  $m/z$  219.0826 的碎片离子是由准分子离子同时失去一个羟基、一个甲氧基和一个甲基后得到。

木兰花碱(magnoflorine,  $C_{20}H_{24}NO_4$ )、酸李碱(zizyphusine,  $C_{20}H_{24}NO_4$ ) 在第一部分(0~5 min 部分)通过分析柱 2 时洗脱到第 35.4 min 时出现(见图 2, 峰 2),质谱图见图 3。对  $m/z$  342.1690 的准分子离子进行检索,检索结果根据谱图准确度排名前

三位见表 1 排在第一位的化学式为  $C_{20}H_{24}NO_4$ 。木兰花碱和酸李碱属于同分异构体,结构式如图 4 所示<sup>[16]</sup>,由于它们以离子形式存在,本身带一个单位的正电荷,所以质谱图中的离子为  $M^+$  ( $C_{20}H_{24}NO_4^+$ ) 而不是  $[M+H]^+$ ,推测相应的成分是木兰花碱或酸李碱。用木兰花碱和酸李碱标准品试验发现它们通过色谱柱的保留时间相同,通过 ESI-LC-MS/MS 得到的质谱图中均没有明显的碎片离子,并且它们的母离子和子离子均相同,所以无法通过 Mass-Works 和 LC-ESI-MS/MS 对其进行区分,要想进一

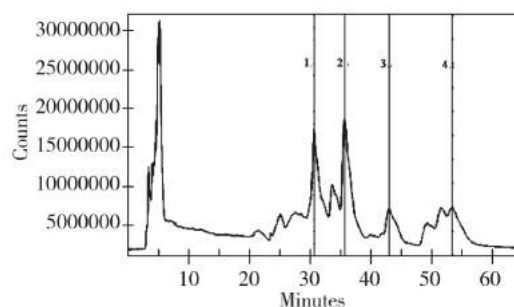


图 2 第一部分总离子流图

Fig. 2 Total ions chromatogram of part one

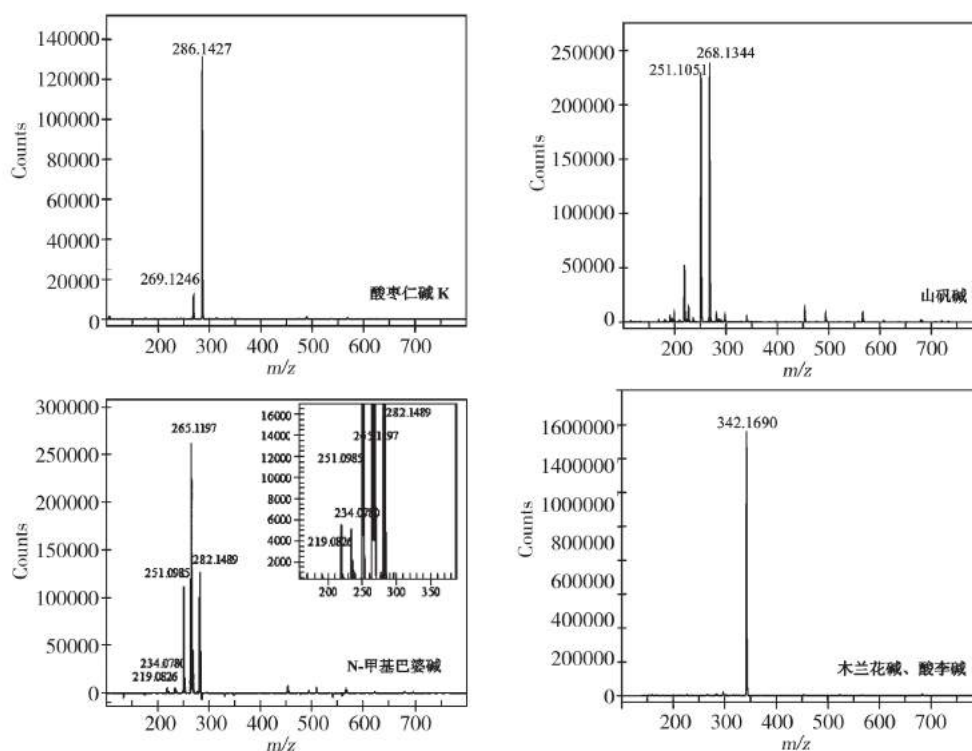


图 3 阿朴芬类生物碱质谱图

Fig. 3 Mass spectra of aporphine alkaloids

表 1 阿朴芬类生物检索结果

Table 1 CLIPS search results of aporphine alkaloids

名称 Name	排序 Order	化学式 Formula	理论质量 Theoretical mass	绝对质量误差 Absolute error (mDa)	相对质量误差 Relative error (ppm)	谱图准确度 Accuracy (%)	环加双键数 Unsaturation degree
酸枣仁碱 KSanjoinine K	1	$C_{17}H_{20}O_3N$	286.1438	-1.0699	-3.7392	98.5330	8.5
	2	$C_{13}H_{16}ON_7$	286.1411	1.6154	5.6455	98.4629	9.5
	3	$C_{12}H_{16}N_9$	286.1523	-9.6180	-33.6125	98.4165	9.5
山矾碱 Caaverine	1	$C_{17}H_{18}O_2N$	268.1332	1.1948	4.4558	98.1075	9.5
	2	$C_{13}H_{14}N_7$	268.1305	3.8801	14.4707	97.9755	10.5
N-甲基巴婆碱 N-Methylasimilobine	3	$C_{12}H_{18}O_4N_3$	268.1292	5.2175	19.4585	97.5049	5.5
	1	$C_{18}H_{20}O_2N$	282.1489	0.0447	0.1584	98.4007	9.5



名称 Name	排序 Order	化学式 Formula	理论质量 Theoretical mass	绝对质量误差 Absolute error (mDa)	相对质量误差 Relative error (ppm)	谱图准确度 Accuracy (%)	环加双键数 Unsaturation degree
木兰花碱、酸李碱 Magnoflorine and Zizyphusine	2	C <sub>14</sub> H <sub>16</sub> N <sub>7</sub>	282.1462	2.7300	9.6758	98.3709	10.5
	3	C <sub>13</sub> H <sub>20</sub> O <sub>4</sub> N <sub>3</sub>	282.1448	4.0674	14.4159	97.9040	5.5
	1	C <sub>20</sub> H <sub>24</sub> O <sub>4</sub> N	342.1700	-0.9847	-2.8778	98.9620	9.5
	2	C <sub>16</sub> H <sub>20</sub> O <sub>2</sub> N <sub>7</sub>	342.1673	1.7007	4.9702	98.6823	10.5
	3	C <sub>15</sub> H <sub>20</sub> ON <sub>9</sub>	342.1785	-9.5327	-27.8597	98.5707	10.5

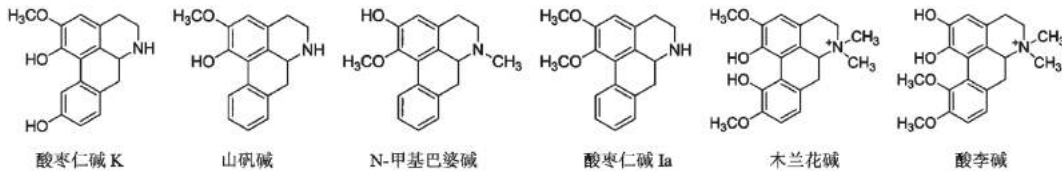


图4 阿朴芬类生物碱结构式

Fig. 4 Chemical structure of aporphine alkaloids

步鉴定,需要借助红外光谱(IR)、核磁共振谱(NMR)<sup>[17-18]</sup>等其他手段。

### 3.2 环肽类生物碱的筛查结果

酸枣仁碱 F (sanjoinine F, C<sub>31</sub>H<sub>42</sub>N<sub>4</sub>O<sub>5</sub>) 在经过分析柱 1 后收集的第二部分(5~25 min 部分)通过分析柱 2 时洗脱到第 45.8 min 出现(见图 5 峰 1),相应的质谱图见图 6,  $m/z$  551.3190 的峰为准分子离子峰,对此峰进行检索,根据谱图准确度排名前三位见表 2, C<sub>31</sub>H<sub>43</sub>N<sub>4</sub>O<sub>5</sub> [M+H]<sup>+</sup> 为准分子离子的化学式,相应的分子式为 C<sub>31</sub>H<sub>42</sub>N<sub>4</sub>O<sub>5</sub>, 推测为酸枣仁碱 F。

酸枣仁碱 A, 也即欧鼠李叶碱 (sanjoinine A 或 frangufoline, C<sub>31</sub>H<sub>42</sub>N<sub>4</sub>O<sub>4</sub>) 在经过分析柱 1 后收集的第二部分(5~25 min 部分)通过分析柱 2 时洗脱到第 58.0 min 出现(见图 5 峰 2),它的质谱图见图 6,  $m/z$  535.3211 的峰为准分子离子峰,对此峰进行检索,根据谱图准确度排名前三位见表 2, C<sub>31</sub>H<sub>43</sub>N<sub>4</sub>O<sub>4</sub>

为该准分子离子的化学式,相应的分子式为 C<sub>31</sub>H<sub>42</sub>N<sub>4</sub>O<sub>4</sub>, 推测为酸枣仁碱 A。

## 4 结论

实验结果表明含氮有机物分析包中的 C<sub>18</sub> 色谱柱和 C<sub>18</sub>-IEX 混合硅胶柱结合使用对生物碱的分离

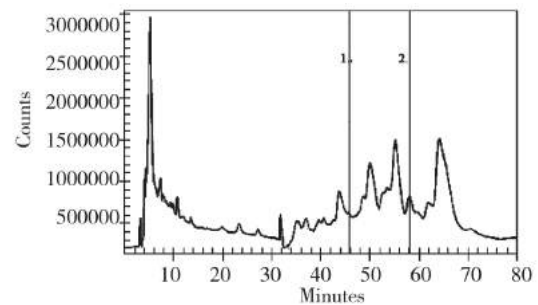


图5 第二部分总离子流图

Fig. 5 Total ions chromatogram of part two

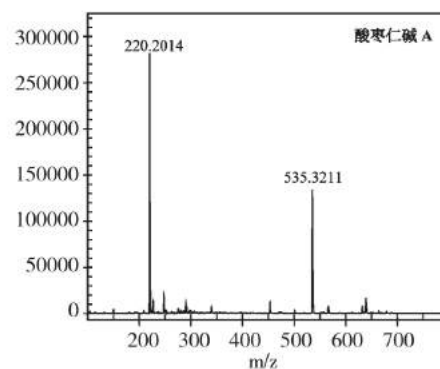
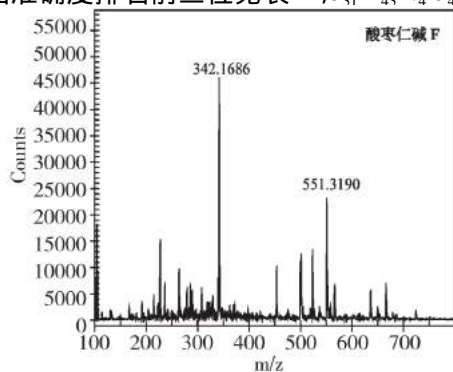


图6 环肽类生物碱质谱图

Fig. 6 Mass spectra of cyclopeptide alkaloids

表2 环肽类生物碱检索结果  
Table 2 CLIPS search results of cyclopeptide alkaloids

名称 Name	排序 Order	化学式 Formula	理论质量 Theoretical mass	绝对质量误差 Absolute error (mDa)	相对质量误差 Relative error (ppm)	谱图准确度 Accuracy (%)	环加双键数 Unsaturation degree
酸枣仁碱 FSanjoinine F	1	C <sub>31</sub> H <sub>43</sub> O <sub>5</sub> N <sub>4</sub>	551.3228	-3.7969	-6.8870	98.9025	12.5
	2	C <sub>32</sub> H <sub>43</sub> O <sub>6</sub> N <sub>2</sub>	551.3116	7.4365	13.4885	98.8459	12.5
	3	C <sub>30</sub> H <sub>47</sub> O <sub>9</sub>	551.3215	-2.4595	-4.4612	98.7754	7.5
酸枣仁碱 ASanjoinine A	1	C <sub>31</sub> H <sub>43</sub> O <sub>4</sub> N <sub>4</sub>	535.3279	-6.7823	-12.6696	98.8227	12.5
	2	C <sub>32</sub> H <sub>43</sub> O <sub>5</sub> N <sub>2</sub>	535.3166	4.4511	8.3148	98.7594	12.5
	3	C <sub>28</sub> H <sub>39</sub> O <sub>3</sub> N <sub>8</sub>	535.3140	7.1364	13.3311	98.7344	12.5

具有较好的效果,对生物碱的筛查具有一定帮助。MassWorks 分子识别软件结合低分辨质谱使用对已发现并报道但没有标准品的中药活性成分的快速筛查具有重要意义,可对中药中已发现的微量活性成分进行快速筛查、识别,找到目标成分,为后续的分

#### 参考文献

- Zhao LH (赵连红), Qiao W (乔卫), Xu L (许岚). Experimental study on anti-convulsion effect of alkaloids from *Semen zizyphi spinosae*. *Tianjin Pharm (天津药学)* 2007, 19(4):4-5.
- Zhu TL (朱铁梁), Hu ZS (胡占嵩), Li L (李璐) *et al.* Study on the antidepressant effect of active fraction from *Semen Zizyphi Spinosae*. *Acta Coll Med. CPAF (武警医学院学报)* 2009, 18:420-425.
- Cao JX, Zhang QY, Cui SY *et al.* Hypnotic effect of jujubosides from *Semen Zizyphi Spinosae*. *J Ethnopharmacol* 2010, 130:163-166.
- Niu CY, Wu CS, Sheng YX *et al.* Identification and characterization of flavonoids from *Semen Zizyphi Spinosae* by high performance liquid chromatography/linear ion trap FTICR hybrid mass spectrometry. *J Asian Nat Prod Res* 2010, 12:300-312.
- Wang LE, Bai YJ, Shi XR *et al.* Spinosin, a C-glycoside flavonoid from *Semen Zizyphi Spinosae*, potentiated pentobarbital-induced sleep via the sero-tonergic system. *Pharmacol Biochem Behav* 2008, 90:399-403.
- Han BH, Park MH. Alkaloids are the sedative principles of the seeds of *Zizyphus vulgaris* var. *spinosus*. *Arch. Pharmacol Res* 1987, 10:203-207.
- Han BH, Park MH, Han YN. Cyclic peptide and peptide alkaloids from seeds of *Zizyphus vulgaris*. *Phytochemistry*, 1990, 29:3315-3319.
- Wang YD, Prest H. Accurate mass measurement on real chromatographic time scale with a single quadrupole mass spectrometer. *Chromatography* 2006, 27:135-140.
- Gu M, Wang YD, Zhao XG *et al.* Accurate mass filtering of ion chromatograms for metabolite identification using a unit mass resolution liquid chromatography/mass spectrometry system. *Rapid Commun. Mass Spectrom.* 2006, 20:764-770.
- Wang YN (王亚男), Wang CH (汪聪慧), Li WJ (李卫建). A new technology for accurate identify pesticide residues—Massworks. *J Agric Sci Tech China (中国农业科技导报)* 2009, 11(S1):39-42.
- Ho HP, Lee RJ, Chen CY *et al.* Identification of new minor metabolites of penicillin G in human serum by multiple-stage tandem mass spectrometry. *Rapid Commun Mass Spectrom*, 2011, 25(1):25-32.
- Liu K, Ma B, Wang YD *et al.* A new software method for accurate mass measurements of drugs on unit mass resolution mass spectrometer. *Acta Pharm Sin* 2007, 42:1112-1114.
- Wang YD, Gu M. The concept of spectral accuracy for MS. *Anal Chem* 2010, 82:7055-7062.
- Li WJ (李卫建), Yuan YR (袁有荣), Ouyang WM (欧阳伟民) *et al.* Application of MassWorks™ molecular recognition technology in mass spectrometry. *Mod Instrum (现代仪器)* 2010, 16(5):11-19.
- Zhou W, Zhang YH, Xu HL *et al.* Determination of elemental composition of volatile organic compounds from Chinese rose oil by spectral accuracy and mass accuracy. *Rapid Commun Mass Spectrom* 2011, 25:3097-3102.
- Han BH, Park MH, Park JH. Chemical and pharmacological studies on sedative cyclopeptide alkaloids in some Rhamnaceae plants. *Pure Appl Chem* 1989, 61:443-448.
- Kind T, Fiehn O. Metabolomic database annotations via query of elemental compositions: Mass accuracy is insufficient even at less than 1 ppm. *Bmc Bioinform* 2006, 7(6):1-10.
- Erve JC, Gu M, Wang YD *et al.* Spectral accuracy of molecular ions in an LTQ/Orbitrap mass spectrometer and implications for elemental composition determination. *J Am Soc Mass Spectrom.* 2009, 20:2058-2069.

# TD/GC-MS 法分析燃放烟花爆竹产生的大气有机污染物

魏荣霞<sup>1</sup>, 周 围<sup>\* 1 2</sup>, 解迎双<sup>2</sup>, 张雅珩<sup>2</sup>, 吴岳华<sup>3</sup>

(1. 西北师范大学地理与环境科学学院, 兰州 730070; 2. 甘肃出入境检验检疫局综合技术中心, 兰州 730320;  
3. 甘肃农业大学食品科学与工程学院, 兰州 730070)

**摘 要:** 利用热脱附/气相色谱-质谱(TD/GC-MS)联用技术初步分析了实验室燃放烟花爆竹产生的大气有机污染物。将烟花爆竹在密闭的实验室里进行燃放,用装有 Tenax-TA 吸附剂的不锈钢采样管以 200 mL/min 流量富集,连接热脱附装置进行解吸,最后通过气质联用技术结合 massworks 软件综合定性,结果表明爆竹类鞭炮燃放过程中会产生 3 种大气污染物,分别是二氧化硫、二硫化碳和糠醛。烟雾型烟花燃放产生 24 种有毒大气污染物,分属于呋喃、醛酮、芳烃、醇酯和酚 4 类。

**关键词:** 烟花爆竹; 大气污染物; 热脱附气质联用

中图分类号: O657.63 文献标识码: A 文章编号: 1000-0720(2013)03-098-05

目前关于烟花爆竹对环境的影响研究主要集中在烟花爆竹燃放后所产生的环境噪声、颗粒物、SO<sub>2</sub>、氮氧化物、气溶胶等方面。文献[1-2]采用甲苯、甲醇吸收的方法对燃放烟花可能产生的致癌物质如多氯代二苯并-对-二噁英(PCDDs)和多氯代二苯并呋喃(PCDFs)进行了气相色谱质谱联用的研究。文献[3-4]研究了产生的源挥发性污染物。

对空气中挥发性有机物(VOCs)的研究方法主要有溶剂解析法、固相微萃取法、热解吸法 3 种。热解吸法已成为国内外分析 VOCs 的主要方法。本研究采用热脱附(TD)/气相色谱(GC)-质谱(MS)联用技术对满堂红鞭炮和 colorball 烟花燃放后的产物进行分析,该法具有直接溯源、快速全面等优点,通过 massworks 软件和标准物质的综合定性得到结果,定性方法准确可靠。

## 1 实验部分

### 1.1 仪器与试剂

7890A-5975C 气相色谱质谱仪(美国安捷伦公司);自动热脱附解吸仪;低流量采样泵;不锈钢吸附管(管长 90 mm,内径 6.4 mm),Tenax-TA 吸附剂;色谱柱:SE-54 80 m × 200 μm i. d × 0.25 μm 弹性石英毛细管柱。

丙酮(95%)、苯(95%)、甲苯(98%)、乙苯

(100%)、对二甲苯(100%)、3-甲基己烷(95%)、2-甲基呋喃(99%)。Massworks 软件。

### 1.2 样品来源

A: 市售浏阳满堂红鞭炮(2 万响),由浏阳市大瑶友爱花炮厂生产。产品级别 C 级,单个含药量 0.05g,属于氯酸盐类爆竹。

B: 市售 Color ball 烟雾型烟花。由浏阳市澄潭江镇龙潭鞭炮厂生产。单个含药量约 2.3g,产生紫黄蓝 3 种烟雾。3 种色彩的烟雾球各燃放 3 个。

### 1.3 吸附管的制备

不锈钢空吸附管规格为 90 mm × 6.4 mm,内填充 150 mg Tenax-TA 吸附剂(使用前在 300℃ 下活化 1h),采样前用 30 mL/min 的高纯氮气在 300℃ 下吹扫 30 min 进行老化。

### 1.4 采集方式

在一个密闭的实验室内对烟花爆竹燃放前后的空气分别进行采集。SKC 低流量采样泵连接 3 个 Tenax-TA 吸附管,设置泵流量为 200 mL/min 进行 3 管平行采样,采样时间为 3h,采样完毕后盖上采样管帽子封口备用。

### 1.5 仪器参数

(1) 热脱附参数:一级解析时间为 7 min,二级解析时间为 5 min,一级解析温度为 260℃,二级

收稿日期:2012-10-15

E-mail: wrongxia2006@163.com

解析温度为 200℃,六通阀温度为 180℃,传输线温度为 200℃,冷阱吸附温度为 -30℃,载气压力 280kpa,进样时间:45s。

(2) 气相色谱参数:进样口温度为 250℃,分流进样,分流比为 1:1,采用程序压力控制模式:初压为 74.7 kPa 保持 0.5 min 以 68.85 kPa/min 升至 0.281 MPa 保持 60 min,升温程序:50℃ 保持 1 min 然后以 4℃/min 升至 280℃ 保持 1.5 min,载气采用高纯 He。

(3) 质谱参数:采用电子轰击离子源(EI),离子源温度为 230℃,四极杆温度为 150℃,辅助加热区温度为 250℃,扫描质量数范围为 30 Da-600 Da。

## 2 结果和讨论

### 2.1 采样时间的确定

本研究以 Colourball 样品为例,进行了不同时间采样量的实验。优化结果比较 1、2 和 3h 不同采样时间的色谱图发现,当采样时间为 3h 时,小分子的轻物质含量变少,但重组分出现的多了,所以选择 3 h 采样。

### 2.2 质谱解析

为了提高质谱解析的准确度,本研究使用美国 Cerno Bioscience 公司研发的 MassWorks 软件,该软件通过建立校正函数方程,并将同位素效应、仪器噪音过滤及峰形补偿等纳入函数方程中,获得目标化合物的精确分子质量数值。其 MSIntegrity 技术可以使四极杆质谱仪器质量精度提高 100 倍,精度达到  $\times 10^{-6}$  级<sup>[5-7]</sup>。与此同时本研究选用了 7 种标准品对本实验的质谱解析结果进行验证,正确率达 100%,NIST 谱库在一些化合物进行检索时,得

到的匹配度要低于 90,例如 7.555 min 的化合物,谱库检索的匹配度仅为 65,分子式为 C<sub>3</sub>H<sub>6</sub>O,这样的匹配度用来确定化合物是远远不够的,将会使定性结果不准确,利用 Massworks 分析该化合物,得到精确分子量为 58.0419 Da,设置 CLIPs 的检索的质量误差为 20 m Da 后。其中排在第一位的是 C<sub>3</sub>H<sub>6</sub>O,谱图准确度为 98.1054,因此就可以确定该化合物的分子式为 C<sub>3</sub>H<sub>6</sub>O,再利用标准品进行了验证,从而确定该物质为丙酮。结果表明本研究使用 massworks 软件和 NIST08 谱库综合定性准确可靠。本研究还对部分 NIST 谱库定性匹配度较低的物质利用该软件进行了定性分析。

表 1 中羟基丙酮(C<sub>3</sub>H<sub>6</sub>O<sub>2</sub>) m/z 43 的碎片是连于叔碳上的甲氧基 CH<sub>3</sub>O 丢失而形成的;1,3-二甲基环戊烷(C<sub>7</sub>H<sub>14</sub>) m/z 81 的碎片是环戊烷上丢失一个 CH<sub>3</sub> 而形成的;2-环戊烯酮(C<sub>5</sub>H<sub>6</sub>O<sub>2</sub>) 环戊烯上  $\pi$  键的电离能比 CO 键的电离能低,因此 2-环戊烯酮分子被电离是时优先失去  $\pi$  电子而形成游离基和电荷中心。在游离基中心的诱导下发生 a 断裂反应,造成环的断裂,接着再发生  $\delta$  断裂反应(丢失 CH<sub>3</sub>) 和 i 断裂反应生成 m/z 54 的碎片离子;2(3H)-呋喃酮(C<sub>5</sub>H<sub>6</sub>O<sub>2</sub>) m/z 70 的碎片离子是呋喃环丢失 CO 而形成的;2-乙酰基呋喃(C<sub>6</sub>H<sub>6</sub>O<sub>2</sub>) 中乙酰基失去甲基形成稳定的中性丢失,产生较高的 m/z 95 的碎片;2(5H)-呋喃酮(C<sub>6</sub>H<sub>8</sub>O<sub>2</sub>) m/z 55 的碎片是呋喃环经过开环丢失 CHO 和 CO 而形成的;3-环戊烯-1-酮(C<sub>5</sub>H<sub>4</sub>O<sub>2</sub>) 是环戊烯经过 a 断裂反应失去乙烯基 C<sub>2</sub>H<sub>4</sub> 而形成 m/z 70 的碎片离子。

表 1 NIST 谱库匹配度较低物质的碎片 massworks 检索表

Tab. 1 Fragmentation's massworks retrieve table for lower Matching degree materials in NIST library

分子式	保留时间 t/min	碎片检索	精确质量数 (Da) / (g/mol)	光谱精度 (排序)
C <sub>3</sub> H <sub>6</sub> O <sub>2</sub>	11.146	C <sub>2</sub> H <sub>3</sub> O	43.0029	98.7456(1)
C <sub>7</sub> H <sub>14</sub>	13.680	C <sub>6</sub> H <sub>11</sub>	81.0340	98.8383(1)
C <sub>5</sub> H <sub>6</sub> O <sub>2</sub>	18.649	C <sub>3</sub> H <sub>2</sub> O	54.0106	99.0945(1)
C <sub>5</sub> H <sub>6</sub> O <sub>2</sub>	20.297	C <sub>4</sub> H <sub>6</sub> O	70.0419	98.7027(1)
C <sub>6</sub> H <sub>6</sub> O <sub>2</sub>	22.456	C <sub>5</sub> H <sub>3</sub> O <sub>2</sub>	94.9980	99.2181(1)
C <sub>6</sub> H <sub>8</sub> O <sub>2</sub>	22.551	C <sub>5</sub> H <sub>7</sub> O	55.0425	99.2284(1)
C <sub>5</sub> H <sub>6</sub> O <sub>2</sub>	23.026	C <sub>3</sub> H <sub>2</sub> O <sub>2</sub>	70.0419	98.4363(1)



### 2.3 实验结果

实验结果见图 1, 2。浏阳满堂红鞭炮(2 万响) 燃放所产生的大气污染物和 Colour ball 烟雾型烟花燃放产生的大气污染物见表 2, 3。通过对浏

阳满堂红鞭炮燃放后的产物进行分析, 检测到了  $\text{SO}_2$ 、 $\text{CS}_2$  和糠醛 3 种源污染物质, 分别占了总量的 1.24%、0.36%、0.81%。

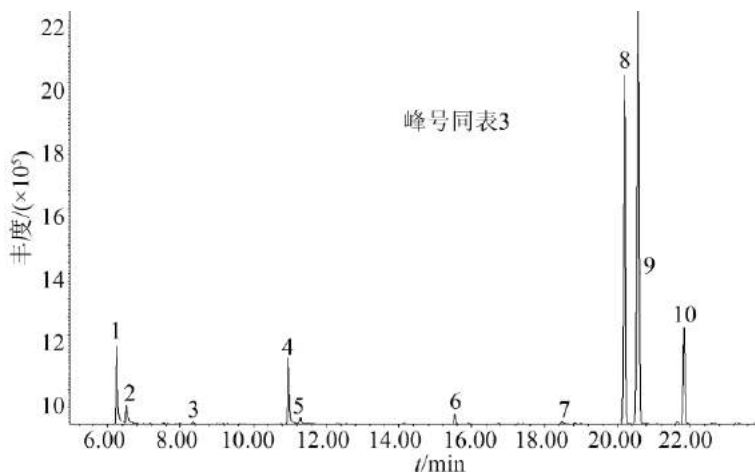


图 1 满堂红鞭炮燃放后产生的物质总离子流色谱图(TIC)

Fig. 1. Total ion chromatogram (TIC) of components from setting off fireworks

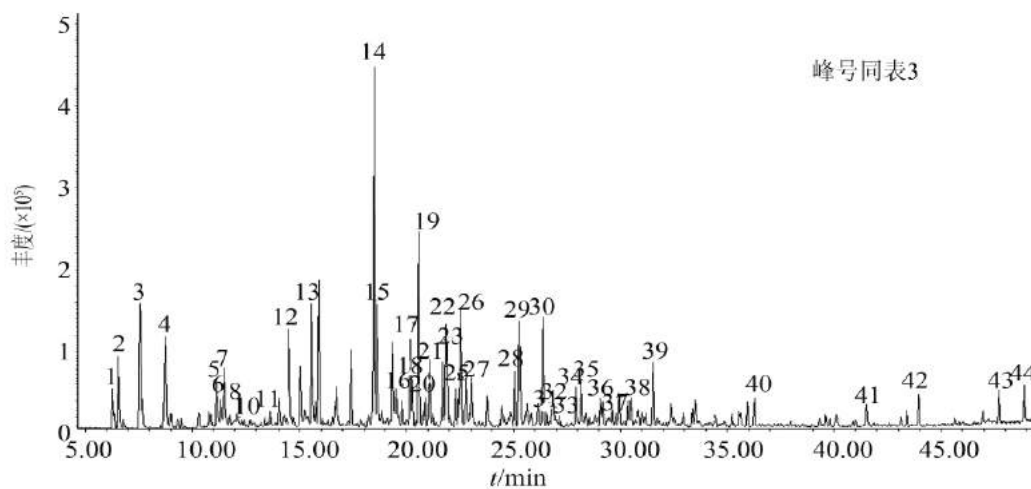


图 2 Colour ball 烟花燃放时的物质总离子流图(TIC)

Fig. 2 Total ion chromatogram (TIC) of components from setting off Colour ball fireworks

表 2 浏阳满堂红鞭炮(2 万响) 燃放产生的大气污染物成分解析

Tab. 2 Atmospheric organic pollutants of setting off Liuyang firecrackers (20000 ring)

峰号	中文名称	分子式	保留时间 t/min	Massworks 软件分析		NIST08 分析 匹配度 (排序)	标准品 确证
				精确 质量数	光谱精度 (排序)		
1	二氧化碳*	$\text{CO}_2$	6.254	44.0098	99.0702(1)	3(1)	
2	二氧化硫	$\text{SO}_2$	6.543	63.9819	98.9336(1)	90(1)	
3	二硫化碳	$\text{CS}_2$	8.336	75.9491	98.6913(1)	83(3)	
4	正丁醇*	$\text{C}_4\text{H}_{10}\text{O}$	10.296	74.0732	98.2398(1)	90(1)	

续表 2(Continued Tab. 2)

峰号	中文名称	分子式	保留时间 t/min	Massworks 软件分析		NIST08 分析 匹配度 (排序)	标准品 确证
				精确 质量数	光谱精度 (排序)		
5	苯*	C <sub>6</sub> H <sub>6</sub>	10.97	78.0469	99.1202(1)	90(1)	苯
6	甲苯*	C <sub>7</sub> H <sub>8</sub>	15.538	92.0826	98.4301(1)	80(1)	甲苯
7	糠醛	C <sub>5</sub> H <sub>4</sub> O <sub>2</sub>	18.476	96.0214	98.5139(1)	91(1)	
8	乙苯*	C <sub>8</sub> H <sub>10</sub>	20.189	106.0783	99.2674(1)	95(1)	乙苯
9	对二甲苯*	C <sub>8</sub> H <sub>10</sub>	20.562	106.0783	99.5229(1)	97(1)	对二甲苯
10	间二甲苯*	C <sub>8</sub> H <sub>10</sub>	21.838	106.0783	98.5139(1)	97(1)	

注 “\*”表示该化合物为本底中大气内已含有的物质

表 3 Colour ball 烟花在燃放时所产生的大气污染污染物成分解析

Tab. 3 Identification of atmospheric organic pollutants of setting off color ball fireworks

峰号	中文名称	分子式	保留时间 t/min	Massworks 软件分析		NIST08 分析 匹配度 (排序)	标准品 确证
				精确 质量数	光谱精度 (排序)		
1	二氧化碳*	CO <sub>2</sub>	6.252	44.0098	99.0702(1)	3(1)	
2	二氧化硫*	SO <sub>2</sub>	6.528	63.9819	98.9336(1)	90(1)	
3	丙酮*	C <sub>3</sub> H <sub>6</sub> O	7.555	58.0419	98.1054(1)	65(1)	丙酮
4	巴豆醛*	C <sub>4</sub> H <sub>6</sub> O	10.773	70.0419	98.2253(1)	90(1)	
5	羟基丙酮	C <sub>3</sub> H <sub>6</sub> O <sub>2</sub>	11.146	74.0368	98.1458(1)	80(2)	
6	苯*	C <sub>6</sub> H <sub>6</sub>	11.33	100.1252	96.3639(1)	91(1)	苯
7	3-甲基己烷*	C <sub>7</sub> H <sub>16</sub>	11.499	100.1252	98.0093(1)	90(1)	3-甲基己烷
8	顺-1,3-二甲基环戊烷*	C <sub>7</sub> H <sub>14</sub>	12.127	98.1095	98.8507(1)	78(2)	
9	1,2-二甲基环戊烷*	C <sub>7</sub> H <sub>14</sub>	12.225	98.1095	98.1772(1)	91(1)	
10	正庚烷*	C <sub>7</sub> H <sub>16</sub>	12.397	100.1252	99.1022(1)	91(1)	
11	甲基环戊烷*	C <sub>7</sub> H <sub>14</sub>	13.68	98.1095	98.3584(1)	90(1)	
12	2-甲基呋喃	C <sub>5</sub> H <sub>6</sub> O	14.534	82.0419	98.5004(1)	94(1)	2-甲基呋喃
13	甲苯*	C <sub>7</sub> H <sub>8</sub>	15.572	92.0625	98.5044(1)	94(1)	甲苯
14	呋喃甲醛	C <sub>5</sub> H <sub>4</sub> O <sub>2</sub>	18.505	96.0211	98.6598(1)	97(1)	
15	2-环戊烯酮	C <sub>5</sub> H <sub>6</sub> O	18.649	82.0419	98.4523(1)	91(1)	
16	2-呋喃醇	C <sub>5</sub> H <sub>6</sub> O <sub>2</sub>	19.333	98.0368	97.0327(1)	98(1)	
17	乙苯*	C <sub>8</sub> H <sub>10</sub>	20.207	106.0788	97.5458(1)	93(1)	乙苯
18	2(3H)-呋喃酮	C <sub>5</sub> H <sub>6</sub> O <sub>2</sub>	20.297	98.0368	98.974(1)	90(2)	
19	对二甲苯*	C <sub>8</sub> H <sub>10</sub>	20.596	106.0788	96.0368(1)	97(1)	对二甲苯
20	苯乙炔 <sup>e</sup>	C <sub>8</sub> H <sub>6</sub>	20.888	102.047	98.5621(1)	93(2)	
21	2-环戊烯-1,4-二酮	C <sub>5</sub> H <sub>4</sub> O <sub>2</sub>	21.092	96.0211	98.8668(1)	91(1)	
22	邻二甲苯*	C <sub>8</sub> H <sub>10</sub>	21.863	106.0788	98.8149(1)	97(1)	
23	甲酸糠酯	C <sub>6</sub> H <sub>6</sub> O <sub>3</sub>	21.961	126.0317	99.2181(1)	86(1)	
24	2-甲基-2-环戊烯-1-酮	C <sub>6</sub> H <sub>8</sub> O	22.314	96.0575	98.2712(1)	91(1)	
25	2-乙酰基呋喃	C <sub>6</sub> H <sub>6</sub> O <sub>2</sub>	22.456	110.0368	99.0663(1)	90(3)	
26	2(5H)-呋喃酮	C <sub>4</sub> H <sub>4</sub> O <sub>2</sub>	22.551	84.0211	98.3695(1)	72(1)	
27	3-环戊烯-1-酮	C <sub>5</sub> H <sub>6</sub> O <sub>2</sub>	23.026	98.0368	98.5279(1)	80(1)	
28	5-甲基呋喃醛	C <sub>6</sub> H <sub>6</sub> O <sub>2</sub>	25.049	110.0368	99.348(1)	95(1)	
29	苯甲醛*	C <sub>7</sub> H <sub>6</sub> O	25.23	106.0788	98.8149(1)	95(2)	
30	苯甲腈	C <sub>7</sub> H <sub>5</sub> N	26.38	103.0423	99.214(1)	95(3)	
31	癸烷*	C <sub>10</sub> H <sub>22</sub>	26.57	142.1722	98.1411(1)	92(1)	

续表 3(Continued Tab. 3)

峰号	中文名称	分子式	保留时间 t/min	Massworks 软件分析		NIST08 分析 匹配度 (排序)	标准品 确证
				精确 质量数	光谱精度 (排序)		
32	1,2,3-三甲苯*	C <sub>9</sub> H <sub>12</sub>	26.866	120.0939	97.9927(1)	91(1)	
33	苯并呋喃	C <sub>8</sub> H <sub>6</sub> O	27.181	118.0419	98.7682(1)	93(3)	
34	1,4-二氯苯*	C <sub>6</sub> H <sub>4</sub> Cl <sub>2</sub>	27.944	145.989	98.1075(1)	97(1)	
35	3-甲基环戊烷-1,2-二酮	C <sub>6</sub> H <sub>8</sub> O <sub>2</sub>	28.165	112.0524	98.6419(1)	93(1)	
36	对甲基苯酚	C <sub>7</sub> H <sub>8</sub> O	29.068	108.0675	98.118(1)	98(1)	
37	茚	C <sub>9</sub> H <sub>8</sub>	29.632	116.0616	99.261(1)	95(1)	
38	苯乙酮	C <sub>8</sub> H <sub>8</sub> O	30.348	120.0575	98.7219(1)	91(2)	
39	N,N-二甲基苯胺	C <sub>8</sub> H <sub>11</sub> N	31.546	121.0891	98.3029(1)	94(1)	
40	萘*	C <sub>10</sub> H <sub>8</sub>	36.298	128.0625	98.6991(1)	93(1)	
41	间苯二甲腈	C <sub>8</sub> H <sub>4</sub> N <sub>2</sub>	41.492	128.0374	98.7346(1)	94(1)	
42	联苯*	C <sub>12</sub> H <sub>10</sub>	43.969	154.0783	98.0581(1)	93(1)	
43	2,4-二叔丁基苯酚*	C <sub>14</sub> H <sub>22</sub> O	47.728	206.1671	91.2075(1)	97(1)	
44	邻苯基苯酚	C <sub>12</sub> H <sub>10</sub> O	48.891	170.0732	99.1631(1)	96(1)	

注：“\*”表示该化合物为本底中大气内已含有的物质，“#”表示进一步进行 massworks 碎片检索的物质见表 1

通过对 Colour ball 烟花在燃放后的产物进行分析,得出 24 种源污染物质,其中主要物质是呋喃甲醛,共计五类。第一类是呋喃类(3 种)占了所有物质总量的 4.33%。第二类是醛酮类(11 种),占了物质总量的 25.64%。第三类是芳烃类(6 种)。第四类是酯醇类(2 种),占了物质总量的 3.9%。第五类是酚类(2 种),占了总量的 1.83%。

#### 参考文献

[1] Fleischer O, W ichmann H, Lorenz W. *Chemosphere*, 1999, 39 (6) : 191

- [2] PDyke, PColeman, Ray James. *Chemosphere*, 1997, 34(1) : 191
- [3] 张宁,张翔,袁悦. *安全与环境学报*, 2010, (6) : 307
- [4] 戴斐,高翔. *分析试验室* 2010 29(2) : 56
- [5] Wang Y, Prest H. *Chromatography*, 2006, 27(3) : 135
- [6] Gu M, Wang Y D, Zhao XG, *et al.* *Rapid Commun Mass Spectrom*, 2008, 20 (5) : 764
- [7] Erve J C L, Gu M, Wang Y D, *et al.* *J Am Soc Mass Spectrom*, 2009, 20 (11) : 2058

### TD/GC-MS analysis of atmospheric organic pollutants from setting off fireworks and firecrackers

WEI Rong-xia<sup>1</sup>, ZHOU Wei<sup>\*1,2</sup>, XIE Ying-shuang<sup>2</sup>, ZHANG Ya-heng<sup>2</sup> and WU Yue-hua<sup>3</sup> (1. College of Geography and Environment Science, Northwest Normal University, Lanzhou 730070; 2. Central Laboratory of Technical Center of Gansu Entry-Exit Inspection and Quarantine Bureau, Lanzhou 730020; 3. College of Food Science and Engineering, Gansu Agricultural University, Lanzhou 730070), *Fenxi Shiyanshi* 2013 32(03) : 98 ~ 102

**Abstract:** The air organic pollutants of setting off fireworks and firecrackers in laboratory were analyzed preliminarily by thermal desorption-gas chromatography/mass spectrometry (TD/GC-MS) hyphenated technique. This study set off fireworks and firecrackers in closed chambers and the stainless steel sampling tube filled with Tenax-TA adsorbent at a flow rate of 200 mL/min to enrich and connected to the thermal desorption device for desorption, finally GC-MS technique combined with the massworks software to identify the components. It was concluded that setting off firecrackers generated 3 kinds of atmospheric pollutants such as Sulfur dioxide, carbon disulfide and furfural. And the Smoke-type fireworks generated 23 kinds of atmospheric pollutants, including five categories, furans, aldehydes and ketones, aromatic hydrocarbons, esters and phenols.

**Keywords:** Fireworks and firecrackers; Atmospheric organic pollutions; Thermal desorption-gas chromatography/mass spectrometry

## KNAUER (诺尔) K-7400S冰点渗透压仪

KNAUER公司是渗透测量领域的先驱之一,以其可靠和用户友好的仪器闻名50多年。



最新K-7400S冰点渗透压仪,不仅可以简单快速测定各种水溶液的冰点,还可以测量这些样品的冰点下降度。经过验证的冰点测定技术与该装置的稳健智能设计相结合,可以进行快速和可重复的测量。K-7400S冰点渗透压仪符合欧洲药典(2.2.35, 01/2012), 2015版《中国药典》, 美国药典, K-7400S冰点渗透压仪可提供IQ、OQ服务。

## LUMTECH ECO<sup>PLUS</sup> GPC 全自动凝胶净化系统

采用电子压力脉动抑制设计的串联双柱塞溶剂输送泵(流速50ml/min),保证流速的稳定可靠性。适合各规格净化柱,内置过滤系统,外置金属套,使用周期更长,确保安全。创新的电子多通道转换阀设计,最大实现15个不同样品量的自动净化、收集,真正实现样品的无人值守自动净化处理。独立的通道避免样品之间、收集的组份之间交叉污染。符合最新的国标 GB 23200.113-2018 植物源性食品中208种农药及其代谢物残留量的测定气相色谱-质谱联用法中 GPC部分。主要应用:部分弱极性兽药、持久性有机污染物。



## KNAUER (诺尔) AZURA系列分析型液相色谱系统

最新的分析半制备AZURA®HPLC Plus通用性和可靠性强,能够满足实验室每天的挑战。可选等度、二元梯度或四元低压梯度泵;泵头可用10ml/min或流速,实现分析半制备切换;自动进样器0.1ul-10ml进样量;集成温度控制的超高灵敏度二极管阵列检测器;多种流通池方案,支持光纤远程流。



## F-DGSi 氮气/氢气/空气发生器

F-DGSi(法德赛)气体工厂是全球专业实验室气源供应商,具有十五年以上的发生气体专业经验。专为LC-MS设计,确保长期提供压力、流速稳定,纯度高的氮气流,且完全兼容市售液质APCI及ESI接口。维护简单、快捷,直接从前面板进行维护;



## LUMTECH Sin-QuEChERS 一步净化多残留方法包

——适用于动物源性食品、植物源食品中多残留分析

LUMTECH Sin-QuEChERS改良QuEChERS方法,采用特定的纳米结构填料(MWCNTs)与PSA等固相吸附材料结合,能够非常有效去除色素、糖类、甾醇类、油脂类、蜡、酶、茶多酚,去除有机酸等酸性物质、去除生物碱性干扰物及甙类等,完全脱水。符合AOAC 2007.01、EN 15662、NY/T 1380 2007、SN/T 4138-2015、2015《中国药典》四部及最新国标 GB 23200.113-2018 植物源性食品中208种农药及其代谢物残留量的测定气相色谱-质谱联用法。



## LUMTECH m-PFC 快速滤过型多残留试剂盒

——非常适合快速检测、第三方检测、大批量样品检测等

LUMTECH m-PFC(multiplug filtration clean-up),采用特定的纳米(Nano)结构填料(MWCNTs)与PSA等固相材料结合,能够去除基质中各种干扰。15分钟轻松完成样品净化,获得较好的净化效果,不用特殊的SPE装置,实验员无需特殊的培训就能很好的完成。



北京绿绵科技有限公司 ( Lumiere Tech. Ltd. ) (简称:绿绵科技)成立于2001年。成立初期为Thermo Fisher公司的色谱质谱产品(原Finnigan产品线)中国区总代理。十六年,绿绵以体现客户服务最高价值为宗旨,以专业精神和技能为广大实验室分析工作者提供样品前处理、样品制备、样品分析、实验室气源、质谱数据精确分析和实验室管理的全面解决方案,协助客户提高分析检测的效率和水平。公司在杭州、郑州设有办事处和技术中心,在东北、华南、西南、西北地区均有长期稳定的合作伙伴。

绿绵科技通过ISO9001质量管理体系认证,用户可以得到标准化的安装、调试、维护、保养。全国服务电话 400-810-8267

绿绵科技产品已广泛应用于食品安全、环境保护、新药研发、生命科学、能源化工、材料等领域。绿绵科技作为分析测试行业前沿技术的传播者,视客户的需求为企业发展的源动力。绿绵科技希望同越来越多的分析检测行业工作者成为合作伙伴,共同走向成功。



关于绿绵微信公众号

北京绿绵科技有限公司  
北京市海淀区北四环西路68号左岸工社806室, 100080  
Tel : 010-82676061/2/3/4/5/6/7  
Fax : 010-82676068  
E-mail : info@lumtech.com.cn

[www.lumtech.com.cn](http://www.lumtech.com.cn)